AD-A075 968 ARMY MISSILE COMMAND REDSTONE ARSENAL AL HIGH ENERG--ETC F/G 20/5
NUCLEAR STUDIES OF A URANIUM METAL-METAL EXCIMER NUCLEAR LASER/--ETC(U)
JUL 78 D R WOMACK, B MCDANIEL, T G MILLER
UNCLASSIFIED DRSMI-H-78-8 NL

1 OF 1
AD A075968

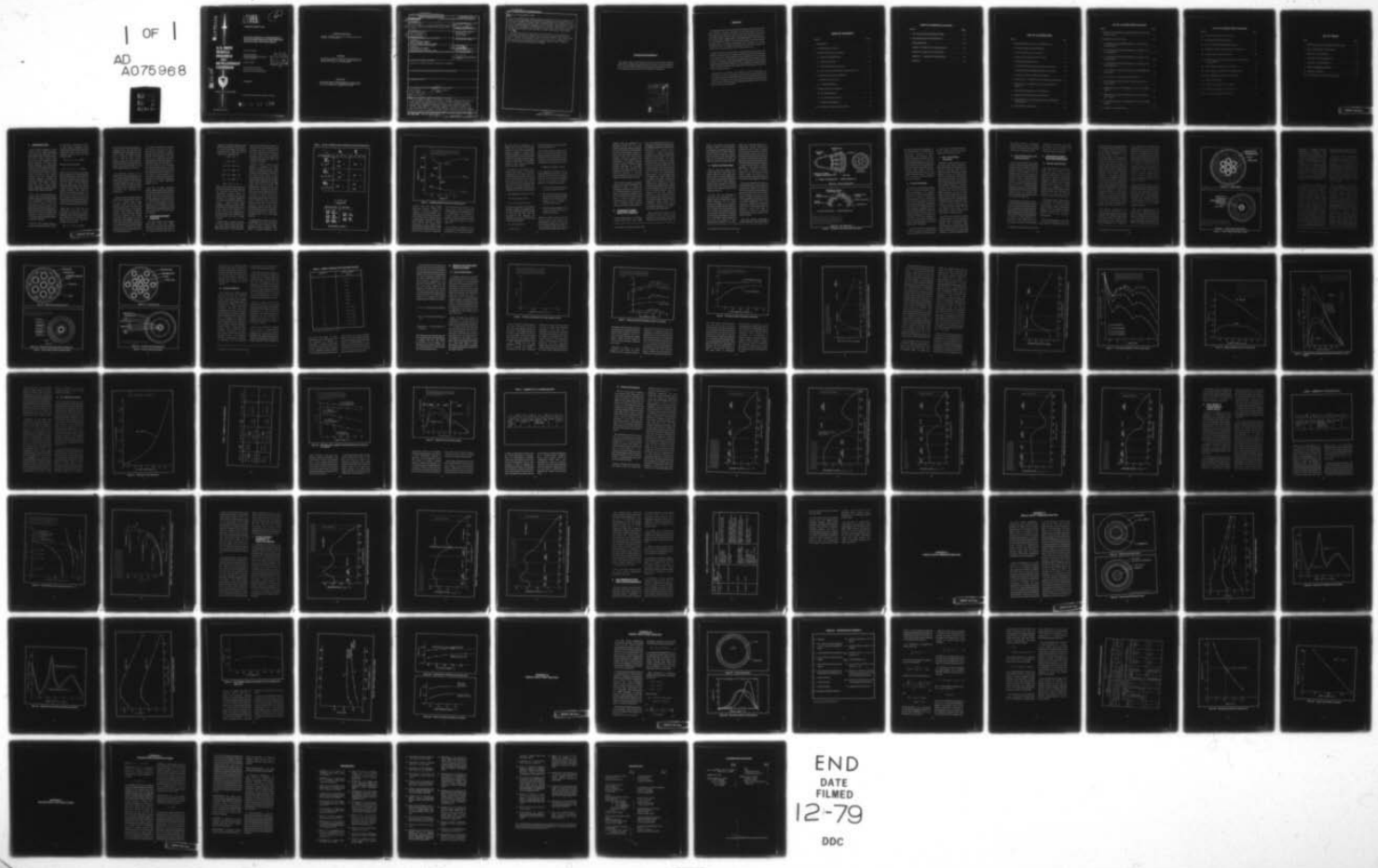

END
DATE FILMED
12-79
DDC

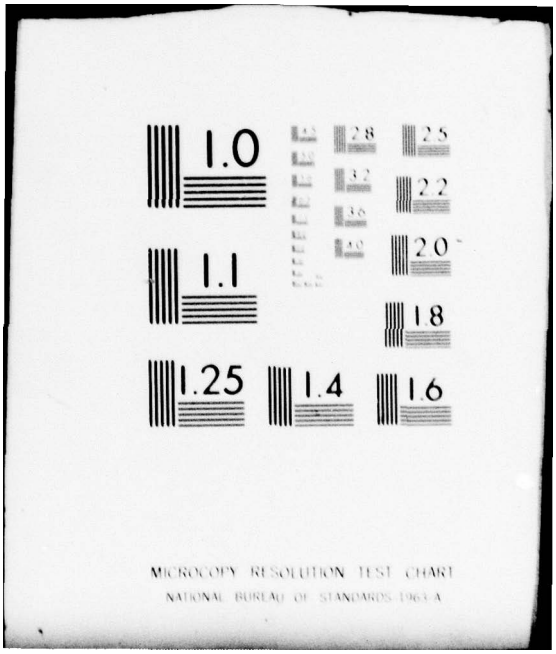
1.0
1.1
1.25
1.4
1.6
2.8
3.2
3.6
4.0
2.5
2.2
2.0
1.8
MICROCOPY RESOLUTION TEST CHART
NATIONAL BUREAU OF STANDARDS 1963-A

LEVEL II

TECHNICAL REPORT H-78-8

NUCLEAR STUDIES OF A URANIUM METAL—METAL EXCIMER NUCLEAR LASER/REACTOR WITH NUCLEAR LIGHT BULB DESIGN

Dennis R. Womack*

Bonnie G. McDaniel
Systems Development Corporation
Huntsville, Alabama

Thomas G. Miller*

*Laser Science Directorate
High Energy Laser Laboratory
Redstone Arsenal, Alabama 35809

U.S. ARMY MISSILE RESEARCH AND DEVELOPMENT COMMAND

Redstone Arsenal, Alabama 35809

17 July 1978

DMI FORM 1000, 1 APR 77

DISPOSITION INSTRUCTIONS

DESTROY THIS REPORT WHEN IT IS NO LONGER NEEDED. DO NOT RETURN IT TO THE ORIGINATOR.

DISCLAIMER

THE FINDINGS IN THIS REPORT ARE NOT TO BE CONSTRUED AS AN OFFICIAL DEPARTMENT OF THE ARMY POSITION UNLESS SO DESIGNATED BY OTHER AUTHORIZED DOCUMENTS.

TRADE NAMES

USE OF TRADE NAMES OR MANUFACTURERS IN THIS REPORT DOES NOT CONSTITUTE AN OFFICIAL INDORSEMENT OR APPROVAL OF THE USE OF SUCH COMMERCIAL HARDWARE OR SOFTWARE.

Unclassified

SECURITY CLASSIFICATION OF THIS PAGE (When Data Entered)

REPORT DOCUMENTATION PAGE		READ INSTRUCTIONS BEFORE COMPLETING FORM
(14) DRSMI-H-78-8	2. GOVT ACCESSION NO.	3. RECIPIENT'S CATALOG NUMBER
4. TITLE (and Subtitle) (6) Nuclear Studies of a Uranium Metal-Metal Excimer Nuclear Laser/Reactor With Nuclear Light Bulb Design.		5. TYPE OF REPORT & PERIOD COVERED (9) Technical Report. 6. PERFORMING ORG. REPORT NUMBER
7. AUTHOR(s) (10) Dennis R. Womack, Bonnie McDaniel Thomas G. Miller		8. CONTRACT OR GRANT NUMBER(s) 000000-00-00-7110 612303.214911
9. PERFORMING ORGANIZATION NAME AND ADDRESS Commander US Army Missile Command ATTN: DRSMI-HS (R&D) Redstone Arsenal, Alabama 35809		10. PROGRAM ELEMENT, PROJECT, TASK AREA & WORK UNIT NUMBERS
11. CONTROLLING OFFICE NAME AND ADDRESS Commander US Army Missile Command ATTN: DRSMI-TI (R&D) Redstone Arsenal, Alabama 35809		(11) 12. REPORT DATE 17 July 1978 13. NUMBER OF PAGES 91 (12) 88
14. MONITORING AGENCY NAME & ADDRESS (if different from Controlling Office)		15. SECURITY CLASS. (of this report) Unclassified 15a. DECLASSIFICATION/DOWNGRADING SCHEDULE

16. DISTRIBUTION STATEMENT (of this Report)

Approved for Public Release; Distribution Unlimited.

17. DISTRIBUTION STATEMENT (of the abstract entered in Block 20, if different from Report)

18. SUPPLEMENTARY NOTES

19. KEY WORDS (Continue on reverse side if necessary and identify by block number)

Metal Excimer
Nuclear Pumped Laser
Nuclear Light Bulb
High Power Laser
Uranium Plasma
ANISN

20. ABSTRACT (Continue on reverse side if necessary and identify by block number)

Uranium metal may have the potential of forming a metal excimer with zinc, cadmium or mercury. Excimers are the most efficient electronic transition lasers known, and metal excimers have spectra in the visible wavelength regions. Metal excimers of interest are InZn (5308, 5626 A°), InCd (5544, 5760 A°), InHg (5226 A°), TlZn (4680, 6200 A°), TlCd (4872, 6400 A°), and TlHg (4590, 6560 A°). A laser is proposed where uranium is both the pumping source, via fission fragments, and the lasant, via excimer formation (UZn, UCd, UHg) with output in the visible wavelengths. The metal excimers mentioned

DD FORM 1 JAN 73 1473 EDITION OF 1 NOV 65 IS OBSOLETE

41012 7

Unclassified

SECURITY CLASSIFICATION OF THIS PAGE (When Data Entered)

have not yet been made to lase.

In this initial study, reactor physics calculations with the computer code ANISN, a multi-geometrym, one-dimensional Boltzmann neutron transport code, were made to examine different reactor configurations. The uranium is required to be in a vapor state, and therefore reactor design is based heavily on the Nuclear Light Bulb Engine. Dependent upon the density requirements (of uranium and mercury, for example) for transmitting laser light, the reactor options include lasers that are self-critical to lasers that require criticality drivers.

Self-critical reactor-lasers and criticality driven reactor-lasers are investigated. Curves are presented for the reactor options depicting the ratio of fission source in laser cells to fission source of the total system given a specific U-235 density in the laser cells. It is not know what fuel density can be employed before seriously degrading laser light, nor were and laser physics calculations attemped.

ACKNOWLEDGEMENTS

The authors wish to acknowledge the timely assistance given by Henry Smith, Science Applications, Incorporated, on the use of neutron transport codes. One of the authors (DRW) wishes to express gratitude for the patience and cooperation shown by System Development Corporation.

PREFACE

Uranium metal may have the potential of forming a metal excimer with zinc, cadmium or mercury. Excimers are the most efficient electronic transition lasers known, and metal excimers have spectra in the visible wavelength regions. Metal excimers of interest are InZn (5308, 5625 A°), InCd (5544, 5760 A°), InHg (5226 A°), TlZn (4680, 6200 A°), TlCd (4872, 6400 A°), and TlHg (4590, 6560 A°). A laser is proposed where uranium is both the pumping source, via fission fragments, and the lasant, via excimer formation (UZn, UCd, UHg) with output in the visible wavelengths. The metal excimers mentioned have not yet been made to lase.

In this initial study, reactor physics calculations with the computer code ANISN, a multi-geometry, one-dimensional Boltzmann neutron transport code, were made to examine different reactor configurations. The uranium is required to be in a vapor state, and therefore reactor design is based heavily on the Nuclear Light Bulb Engine. Dependent upon the density requirements (of uranium and mercury, for example) for transmitting laser light, the reactor options include lasers that are self-critical to lasers that require criticality drivers.

Self-critical reactor-lasers and criticality driven reactor-lasers are investigated. Curves are presented for the reactor options depicting the ratio of fission source in laser cells to fission source of the total system given a specific U-235 density in the laser cells. It is not known what fuel density can be employed before seriously degrading laser light, nor were any laser physics calculations attempted.

TABLE OF CONTENTS

TABLE OF CONTENTS (Concluded)

LIST OF ILLUSTRATIONS

LIST OF ILLUSTRATIONS (Continued)

LIST OF ILLUSTRATIONS (Concluded)

LIST OF TABLES

1. INTRODUCTION

Direct nuclear pumping of lasers promises to have many advantages over present day electrically excited high energy lasers. Nuclear fission is the most compact energy source known, with the potential for high power deposition to lasant gases. Nuclear pumping also holds great promise for overall higher efficiencies, by-passing the conversion of energy-to-heat-to-energy by directly exciting lasant materials with fission fragments and the accompanying electrons. Simplicity of design over electrically excited lasers is another possibility with nuclear pumped lasers. The high voltage power supply technology required for high energy electric lasers is avoided.

Since 1975, several groups have demonstrated nuclear pumped lasing. [1-6] The principle of nuclear pumping is the absorption of a neutron by a fissionable nucleus, and the subsequent release of energy in the fission process which is then used to pump the laser gas. The experiments of References (1-7) have used either wall coatings of boron-10 or uranium-235, or volumetric pumping using helium-3 to pump the laser gas.

With the wall coating method, a neutron is absorbed in a layer of B-10 or U-235 that is coated on the inside of a tube. Fission fragments escape from the wall coating and enter the gas region where they, and the electrons produced, excite the gas. The B-10 reaction yields:

$$^{10}B + n \rightarrow \alpha + {}^{7}Li + 2.3 \text{ Mev.}$$

The U-235 reaction yields:

$$^{235}U + n \rightarrow F_h + F_l + \sim 170 \text{ Mev,}$$

where F_h and F_l are heavy and light fission fragments. A main disadvantage of wall coatings is that much of the fission energy is deposited in the wall, the range of fission fragments being so small that only fissions occurring at the surface of the coating escape to the gas. With the optimum coating thickness only about 50 percent of the fission fragments, and only about 20 percent of the total fission energy, escape to the gas. [8] Gas pressures are extremely important to the range of the fragments to obtain uniform energy deposition in the gas.

With He-3 as a laser gas, the fissionable material is mixed uniformly with lasant gases. Fission fragments are created throughout the gas uniformly with very little fission energy lost to the walls. The He-3 volumetric source yields:

$$^{3}He + n \rightarrow p + {}^{3}H + 0.76 \text{ Mev.}$$

He-3 has two main disadvantages as a pumping source. As with the B-10 coating, He-3 cannot support a nuclear chain reaction, and therefore must have a neutron source (nuclear reactor). Also, the He-3 reaction produces relatively little energy per neutron absorbed, and would therefore require high neutron fluxes to yield large energy deposition to the gas.

An important method for the simulation of nuclear pumping is to use a charged particle accelerator for optimization studies [7].This method is being pursued by using a proton accelerator and an electron accelerator to simulate fission fragments while searching for optimum gas mixtures [9].

Optimum nuclear pumping of lasers in the future will require the use of U-235 as a volume source mixed uniformly with the lasant. Two possible forms the U-235 could take would be enriched UF_6 or an enriched uranium metal plasma. Volumetric uranium sources promise uniform laser gas excitation, large energy deposition, little energy lost to the walls, and the possibility of being a self-critical system. This method may be the ultimate goal of nuclear pumped laser research — the direct conversion of fission energy into light energy in a self-sustaining system.

The idea of using UF_6 in a gaseous core reactor is an old one, but is receiving new emphasis in nuclear pumped laser and space propulsion research [10-12]. However, UF_6 has proven to be chemically aggressive and unstable at high temperatures. A uranium plasma would consist of U-235 metal heated by the fissioning process to its plasma state (or at least to a vapor state). It would not contain the contaminants that a dissociating UF_6 would. Current emphasis is on UF_6 since it is readily in gaseous form, and does not propose the confinement problems of a high temperature plasma [11,13].

One type of highly promising nuclear pumped laser system that has been generally ignored is a self-critical excimer laser system [13,14]. Such a concept could use free flourine from UF_6 decomposition to generate the Ar-F or Kr-F excimer reaction. Another concept is one proposed in a patent application by T. G. Miller [15], using uranium for both pumping energy and as one of the metals in a metal excimer laser system.

2. URANIUM-EXCIMER CONCEPT

The term excimer (also exciplex, dissociation, bound free) applies generally to molecules that are bound only in an excited state, and radiate to an unbound ground state [16]. An

example of excimer formation is the KrF* molecule, which, for the case of an electrical discharge and Penning ionization with a buffer gas (Ar), is formed by the following [17]:

$$e + AR \rightarrow Ar^* + e$$

$$e + Kr \rightarrow Kr^* + e$$

$$Ar^* + Kr \rightarrow Kr^* + Ar$$

$$Ar^* + F_2 \rightarrow ArF^* + F$$

$$ArF^* + Kr \rightarrow KrF^* + Ar$$

$$Kr^* + F_2 \rightarrow KrF^* + F$$

$$KrF^* \rightarrow Kr + F + h\upsilon$$

When the excited molecule radiates to the ground state the atoms repel and the molecule dissociates to its constituent elements. Thus, for excimers, any excited molecule formed represents an automatic population inversion [16]. The KrF* molecule is a rare-gas — halide excimer. Other examples of this type are XeF*, ArF*, and XeBr*. It is possible that UF_6 could be the donor of free fluorine in a nuclear excimer laser, supplying the pumping energy and contributing to the formation of rare-gas — halide excimers.

Another type of excimer formation can occur between alkali and noble-gas atoms, which include NaX, KX, RbX, and CsX (X = Ar, Kr, Xe) [18]. A type of excited molecule consisting of one element, an excited dimer, are the noble-gas excimers, represented by Xe_2^*, and metal excimers, represented by Hg_2^*. Other types of excimers involving metals are metal-noble-gas excimers, represented by TlXe*, and metal-metal excimers.

Metal excimers exhibit great promise as candidates for highly efficient, moderate pressure visible laser systems [19]. The metal excimers of interest to this study have spectra in the visible regions (*Table 1*): these include InZn (5308, 5625 Å) [20], InCd (5544, 5760 Å), InHg (5226 Å) [21], TlZn (6200 Å), TlCd (4872 Å) [22], and TlHg (4590, 6560 Å) [19]. Indium and thallium have one electron in the outer subshell; zinc, cadmium and mercury have a closed outer subshell. If Zn, Cd, or Hg has an electron excited, they may form an excited molecule by combining with the outer electron of Tl or In. A potential well of sufficient binding energy exists for the excited molecule, but the ground state possesses a repulsive potential and the molecule flies apart upon radiating to the ground state. *Figure 1* depicts the potential energy curves of the TlHg molecule.

Drummond [19] reports the potential of TlHg* to be about four times as deep as those of other excimer systems involving noble-gases. This leads to stronger bonding in the

TABLE 1. METAL-EXCIMER LASER CANDIDATES AND THEIR SPECTRA.

EXCITED METAL	I_N $5s^2\ 4d^{10}\ 5p^1$	T_L $6s^2\ 4f^{14}\ 5d^{10}\ 6p^1$
Z_N $4s^2\ 3d^{10}$	5308 Å 5625	6200 Å
C_D $4p^6\ 5s^2\ 4d^{10}$	5544 Å 5760	4872 Å
H_G $6s^2\ 4f^{14}\ 5d^{10}$	5226 Å	4590 Å 6560

U: $7s^2\ 5f^3\ 6d^1$

CANDIDATES

METAL EXCITED	U EXCITED
$U-C_D$ $U-Z_N$ $U-H_G$	$U-I_N$ $U-T_L$

WAVELENGTH-VISIBLE?

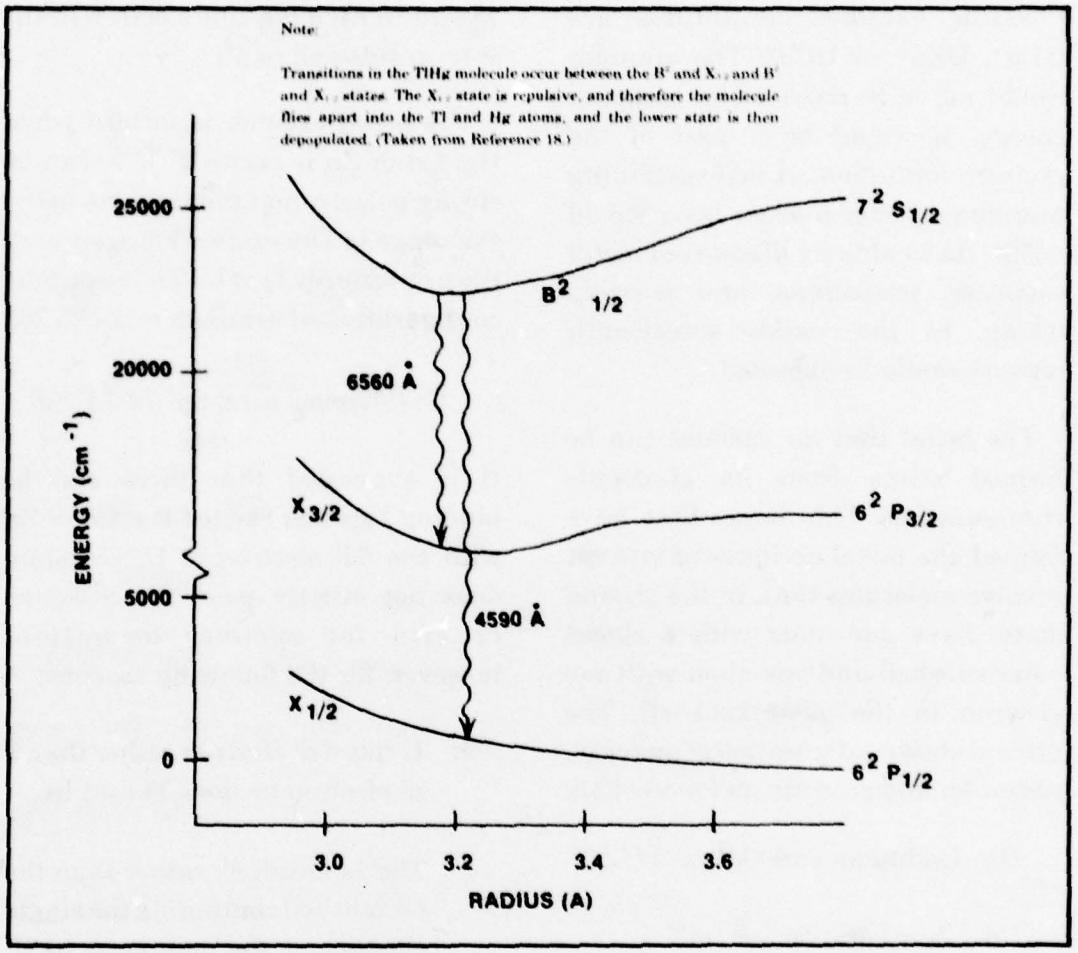

Figure 1. Possible potential curves for the TlHg molecule.

excimer state and more intense molecular emission. Noble-gases require 8 eV energy or higher for excitation to the metastable state, whereas mercury requires only about 5 eV, giving rise to more efficient energy transfer, and in a more direct manner than noble-gas excimers, to metals radiating in the visible [19]. Drummond also reports that the TlHg system can be efficiently run at less than one atm. pressure, eliminating many inhomogeneity problems that arise in other excimer systems that require high pressures. High pressures are additionally less desirable in excimer systems involving noble-gases due to decreased electron density and increased formation of triplet states [22].

It is proposed by Miller [15] that uranium can be substituted for one of the metals in the excimer formation.

Possible excimer candidates are UHg*, UZn*, or UCd*. The uranium would not only provide the pumping energy, it would be a part of the excimer formation. A self-sustaining uranium-excimer nuclear laser would result. As in already discovered metal excimers, transitions, and possibly lasing, in the visible wavelength regions would be expected.

The belief that an excimer can be formed stems from its electronic configuration. The atoms that have formed the metal excimers of interest involve molecules that, in the ground state, have one atom with a closed outer subshell and one atom with one electron in the outer subshell. The ground state configuration of mercury, cadmium and zinc are as follows [24]:

Hg: (Cadmium core)$5p^6\ 6s^2\ 4f^{14}\ 5d^{10}$

Cd: (Zinc core) $4p^6\ 5s^2\ 4d^{10}$

Zn: $1s^2\ 2s^2\ 2p^6\ 3s^2\ 3p^6\ 4s^2\ 3d^{10}$

Each has closed outer $d^{10}s^2$ subshells, and Hg also fills the 4f subshell (noble-gases are obtained when the p subshell is outermost and full, with the exception of He). Thallium and indium, however, have one electron in the outer subshell [25]:

Tl: $6s^2\ 4f^{14}\ 5d^{10}\ 6p^1$

In: $5s^2\ 4d^{10}\ 5p^1$

Tl and In each has one electron in the outer p subshell (s^2p^1).

The metal excimer is formed when Hg, Cd or Zn is excited. There can be strong polarization binding due to the exchange of the excited electron with the p electron of Tl or In. The electronic configuration of uranium is [24,25,26]:

U: (Mercury core) $6p^6\ 7s^2\ 5f^6\ 6d^1$

It is suggested that there can be binding between excited Hg, Cd or Zn with the $6d^1$ electron of U. Uranium does not strictly meet the assumed criteria for excimer formation, however, for the following reasons:

1. U has a d^1 electron rather than a p^1 electron as does Tl and In.

2. The 7s subshell, rather than the 6d subshell containing the single electron, is the outermost in U, whereas the p subshell is outermost in Tl and In.

3. All the previous subshells of Tl and In are filled, but U has an unfilled 5f subshell.

Because of reason 2 above, if U can form excimers with metals the probability is high that Pu, or any of the actinides having one electron in the 6d subshell, could also form an excimer. The shielding effect of the $7s^2$

subshell causes the actinides to be chemically similar [27]. It is not certain at this time whether uranium will or will not form an excimer. More research on the uranium-excimer, as well as the other metal excimers, is required. Until the other metal excimers are better understood, the possibility of forming uranium-excimers cannot be decided, except through experiment. It is possible uranium may form excimers with metals other than Hg, Cd or Zn. The attractive features a uranium-excimer proposes are too great to be dismissed without further research.

The reactor concept for a uranium-excimer laser will be described in the following section. It should be mentioned at this time, however, that for a uranium-excimer to form, free U atoms or molecules are required. UF_6, UF_5 or UF_4 will not form with another metal to create an excimer. For a uranium-excimer to become a reality, "pure" uranium vapors will be required for the fuel/lasant mixtures.

3. URANIUM PLASMA REACTOR CONCEPT

In this initial study of a uranium-excimer nuclear laser, only steady-state and simplified geometries are considered for criticality† calculations, investigating densities, materials and dimensions of a laser/reactor. Extensive research has been conducted by United Technologies Research Center (UTRC) and by the National Aeronautics and Space Administration (NASA) in uranium plasma rocket engines. Many of their concepts of plasma confinement and reactor housing can be directly applied to a laser housing containing uranium fuel in a vapor state. Technological achievements and breakthroughs accomplished by UTRC, NASA and Los Alamos Scientific Laboratories (LASL) can be applied to provide a complete and comprehensive system demonstrating engineering feasibility of the uranium-excimer laser. Except for low uranium densities that are projected for the fuel, additional metals for excimer formation in the fuel, geometrical variations and size, care has been taken not to deviate from established design criteria of the particular plasma rocket engine investigated intensively by UTRC — the nuclear light bulb engine.

Since much of the success of the uranium-excimer nuclear laser depends on the success of the laser housing, the nuclear light bulb, the

†See Appendix C for description of nuclear terms.

design of the engine will be briefly described. Much of the theoretical investigations and design concepts are being performed by UTRC (formerly United Aircraft Research Laboratories) with much of the experimental efforts to be provided by LASL, all under the auspices of NASA. [28,29]

A. Nuclear Light Bulb Design.

Figure 2 shows the design of the nuclear light bulb engine [30]. The engine consists of seven separate fuel cells housed in a moderator-pressure vessel. Newer designs have eliminated the central fuel cell, often adding a thorium region to exploit the Th-U233 *breeding cycle* [31], but the proposed design of the uranium-excimer will retain the fuel cell.

The fuel cells are embedded in moderator and surrounded by a pressure shell. A working fluid, such as seeded hydrogen gas, is flowed around the outside of the cells. The seeded gas absorbs thermal radiation from a fissioning uranium plasma in the fuel cells, and expands through nozzles. *Figure 2b* depicts a single fuel cell. The fuel is physically contained by an internally cooled transparent wall, but the plasma is fluid mechanically confined by an argon buffer gas [30,31]. The buffer gas is tangentially injected through the transparent wall to form a swirling vortex around the plasma in order to avoid plasma contact with the wall. Thermal radiation passes through the transparent wall and into silica tubes through which the working fluid flows. The working fluid (typically hydrogen) is seeded with particles to enhance absorption of the thermal radiation. The vortex volume is normally assumed to be one-half of the total cavity volume, the radius of the confined plasma being 85 percent of the radius to the transparent wall [30].

Laser cavity potential of the fuel cell will depend heavily on the transparent wall and the ability of the vortex to confine the fuel. Since laser light must pass out the end of the cell, to a mirror and eventually out of the reactor, common moderator materials would not be compatible with laser operation. A possible transparent wall would consist of single-crystal beryllium-oxide. BeO is a strong moderator and reflector,† would allow light to transmit to a mirror, but would not allow excessive loss of neutrons at the ends of the cell.

The most pressing technological problem with the nuclear light bulb is

†See Appendix C for a description of nuclear terms.

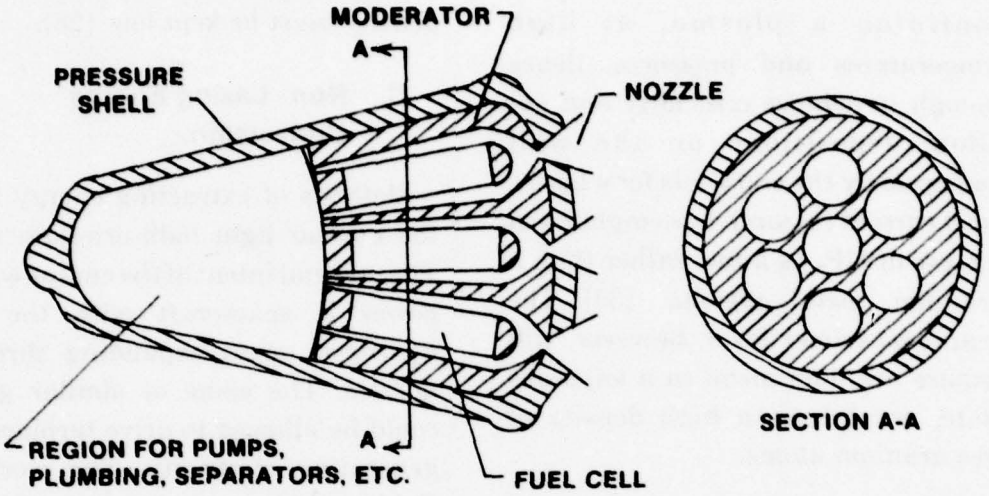

A) OVERALL CONFIGURATION. (TAKEN FROM REF. 28)

Figure 2a. Overall configuration.

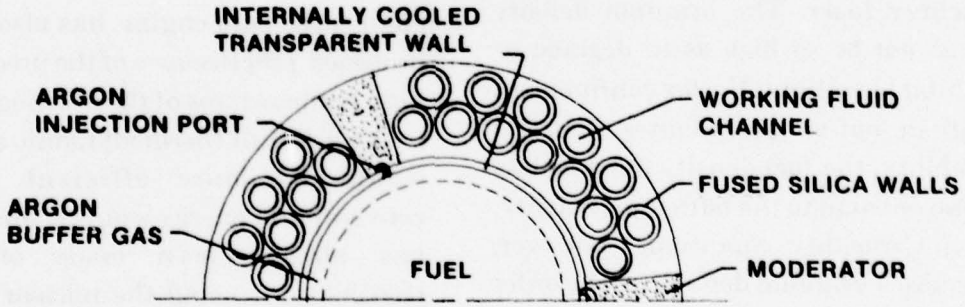

B) UNIT CAVITY (CELL). (TAKEN FROM REF. 29)

Note:

2a) depicts the overall configuration of the Nuclear Light Bulb engine. It consists of seven unit cavities embedded in moderator. 2b) shows one of the unit cavities. The uranium plasma is confined by a swirling vortex flow of argon gas. Thermal radiation is absorbed by a working fluid, and the high temperature working fluid is allowed to expand through nozzles.

Figure 2b. Unit cavity (cell).

Figure 2. Principle of the nuclear light bulb engine.

the fluid mechanical confinement of the fuel. Because of the difficulty of confining a plasma, at high temperatures and pressures, dense enough to achieve criticality and not allow depositions on the wall (particularly the end walls for a laser), most current research has emphasized the use of UF_6 as a fuel rather than a uranium metal plasma [33]. The uranium-excimer laser, however, will require uranium metal in a vaporous state, or at least a high density of free uranium atoms.

B. Critical Fuel Density.

Fuel density considerations in laser cells were of prime importance in this initial investigation of a uranium-excimer laser. The uranium density must not be so high as to degrade or inhibit laser light. Vortex confinement with a buffer gas dictates that, for stability, the fuel density must be less than or equal to the buffer gas density. [34] Criticality conditions, however, require a uranium density on the order of the molecular density of gases at standard conditions [11]. These two conditions leave little latitude in choice of fuel density (for a self-critical system), and that density may be too high for laser operations.

Criticality drivers may be employed to drive the reactor critical, at the expense of efficiency. Fuel plates, pins or rods could be arranged within the reactor should it prove the uranium density must be kept low [28].

C. Non-Lasing Energy Conversion.

Methods of extracting energy from the nuclear light bulb are numerous. The original intent of the engine was to power a spacecraft with the hot hydrogen gases expanding through nozzles. The same or similar gases could be allowed to drive turbines for generating electricity. The working fluid would be not only hot, but highly ionized after flowing over the fuel cells, and efficient electrical conversion could be achieved by allowing the gas to expand into ducts and through MHD generators. A type of piston engine, the Otto engine, has also been proposed [28]. Because of the predicted high temperatures of the working fluid ($> 5000°K$), all thermodynamic cycles would be more efficient than conventional energy sources. Mention has already been made of the possibility of using the nuclear light bulb engine in a breeder mode.

Should it prove necessary to employ criticality drivers in the reactor the fuel plates, pins or rods would require cooling, and conventional steam generating cycles could be used. Heat pipes could be used to cool the fuel clusters, and electric conversion using thermionic devices in conjunction with

heat pipes could be accomplished [35,36]. Another means of extracting energy from the light bulb is laser light, described in the following section.

D. Laser Potentials Other Than Uranium-Excimers.

It has been proposed that lasing could be achieved by using the thermal radiation from the plasma to optically pump gas mixtures [27,32]. The gas mixture could substitute for the working fluid and/or the buffer gas. Neutrons from the fissioning plasma could be used to pump He-3 gas mixtures, if neutron poison† effects can be overcome. A uranium plasma may not be in thermodynamic equillibrium and, thus, may possibly be optically thin. The electromagnetic radiations from an optically thin plasma could be used to optically pump gas mixtures [37,29,33,34].

With emphasis on the use of UF_6 as fuel rather than a metal plasma, lasing may be achieved in UF_6-gas mixtures directly pumped by fission fragments. Free fluorine from dissociating UF_6 might be utilized in excimer systems, such as KrF*. Excursions in fuel radius, density inhomogeneities, inefficiency, high temperatures and pressures, neutron poisoning, undesirable wavelengths, and suitable gas mixtures are all problems that plague the above potentials for extracting energy as laser light.

4. URANIUM-EXCIMER NUCLEAR MODELING

A. Physical Characteristics.

This report makes no attempt to model the laser physics of the uranium-excimer system. Only nuclear considerations on geometry, dimensions, materials and lasant density are explored in an effort to establish a reference laser housing design. Metal excimers are in their infancy in comparison to other excimer systems, with little theoretical studies having been performed. In addition, no data on excimer formation involving uranium exists.

To retain generality, insofar as fuel is concerned, all uranium density considerations are for 100 percent U-235. Oxygen, carbon, nitrogen and fluorine was not added to lasant mixtures to simulate UO_2, U_3O_8, UC, UN or UF_6 in the computer investigation.

The most limiting factor as regards the nuclear modeling was the

†See Appendix C for description of nuclear terms.

requirement for low uranium density. To avoid absorption of light created in the proposed excimer reaction, a design criteria established for the uranium density was 1×10^{7} atoms/barn-cm† (1×10^{17} atoms/cm^3) [38]. It was because of low density requirements predicted for the uranium fuel that the multiple cell design concept of UTRC was adopted. UTRC chose the use of multiple cells primarily to increase the total surface radiating area yielding thermal radiation to a hydrogen propellant [39]. The use of multiple, small cells over fewer, large cells or a single, large cavity allows a lower critical number density of fuel [40].Other reasons for a multiple cell configuration, separating fuel and moderator, is that outer moderator-reflector can also provide shielding of neutron and gamma radiation, and that the fission density distribution can be made more nearly flat [41]. This results in lower system weight, and more uniform energy deposition in prospective laser cells.

The density requirements for uranium are a critical issue to be resolved. High densities favor excimer formation but degrade light. More important, however, is the effect on the laser pumping source—fissions. Since fission fragments are to pump the laser, a high density of uranium would be preferred, to not only increase the number of fissions but also to insure the fission fragment range remains short so as to deposit maximum energy in the lasant mixture. Laser design will be based on a uranium density of 1×10^{7} atoms/b-cm, and then excursions in the density in the cell, and the resultant increase in fission density, will be explored. Copper was chosen to simulate the other excimer metal because of readily available neutron cross sections for copper and its isotopes, and was given the same atom density as uranium.

Since the reactor/laser is to be a self-critical system, whether internal criticality drivers are required or not, reflector and moderator materials were limited to those with low neutron absorption cross sections. Materials considered were beryllium, graphite (carbon) and BeO. Uranium was input as 100 percent U-235 to simplify computer operations.

Three main configurations of the reactor were considered (with two other configurations discussed in the appendices). The first, shown in *Figure 3a*, is essentially the same as the nuclear light bulb design proposed by UTRC. It consists of seven fuel cells

†See Appendix C for a description of nuclear terms.

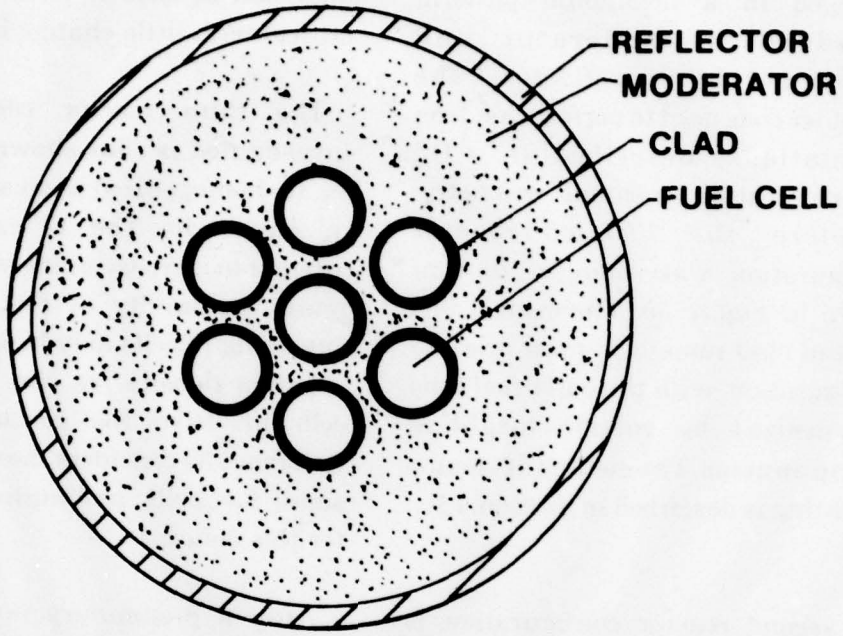

Figure 3a. 7-celled reactor.

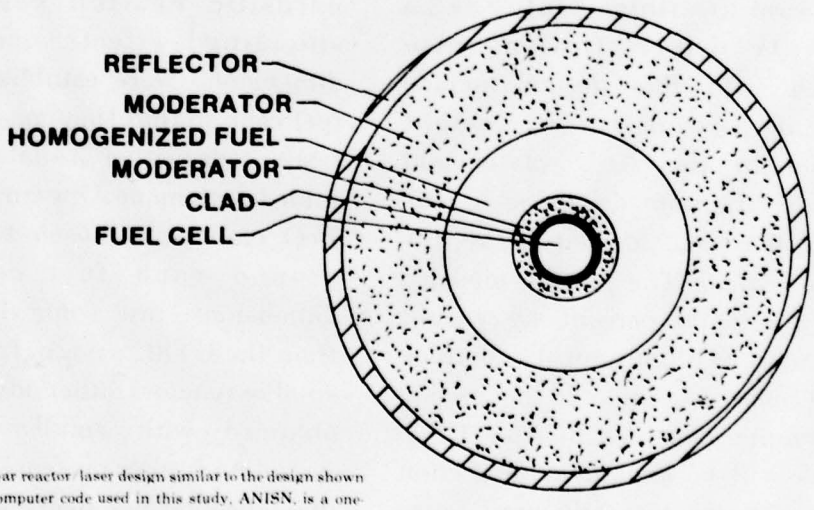

Note:

3a) depicts a nuclear reactor laser design similar to the design shown in Figure 2. The computer code used in this study, ANISN, is a one-dimensional code, and, therefore, the reactor is homogenized into concentric zones which can be solved in one-dimensional cylindrical geometry, shown in 3b).

Figure 3b. 7-celled reactor homogenized.

Figure 3. Seven-celled reactor/laser concept.

arranged in a hexagonal pattern, imbedded in moderator and surrounded by a reflector. The computer code used to perform neutron calculations, described in 4.B., requires one-dimensional geometry; therefore, the 7-Celled reactor configuration was changed to that shown in *Figure 3b*. The central fuel cell and clad remain in their original configuration, with the outer fuel cells homogenized by volume weighting into an annulus. The method of volume weighting is described in Section 4.B.

A second reactor configuration is that depicted in *Figure 4a*, with its homogenized equivalent shown in *Figure 4b*. This reactor employs aluminum-uranium plate as a criticality driver. Options also explored with this design include different percentages by weight uranium in the Al-U plate, and different uranium densities in the central fuel cell to help drive the reactor critical. The plating modeled was 10 and 20 percent by weight uranium in 2S aluminum, 0.5 cm thick and 20 cm across, similar to that used in the Argonne Research Reactor, CP-5 [42]. As will be explained in section 5.B., the computer code used is so general that methods other than Al-U plate can be used to drive the reactor critical with little change in results.

The third reactor configuration investigated is that shown in *Figure 5a*, its homogenized equivalent shown in *Figure 5b*. The 13 cells are an attempt to increase uranium mass, but retain uniformity of fuel cells. The outer ring of cells may be increased in uranium density, as can the central cell, to drive the reactor critical. Reference 39 considers the use of many small fuel cells, and outlines reasons for this concept.

After a preliminary investigation, the fuel cell dimensions were set at 30 cm diameter and 500 cm long. Although somewhat arbitrary until parasitic neutron capture self-shielding† effects occur, these dimensions were established for all fuel cells so that they may be used as laser cells either isolated or in a folded-path mode. One cm thickness of BeO clad was chosen to be placed around each fuel cell. These dimensions are somewhat smaller than the UTRC design. In addition to smaller reactors, other advantages are obtained with smaller fuel cells, including higher pressure allowances [39]. The thermal neutron flux shape was the means by which moderator

†See Appendix C for a description of nuclear terms.

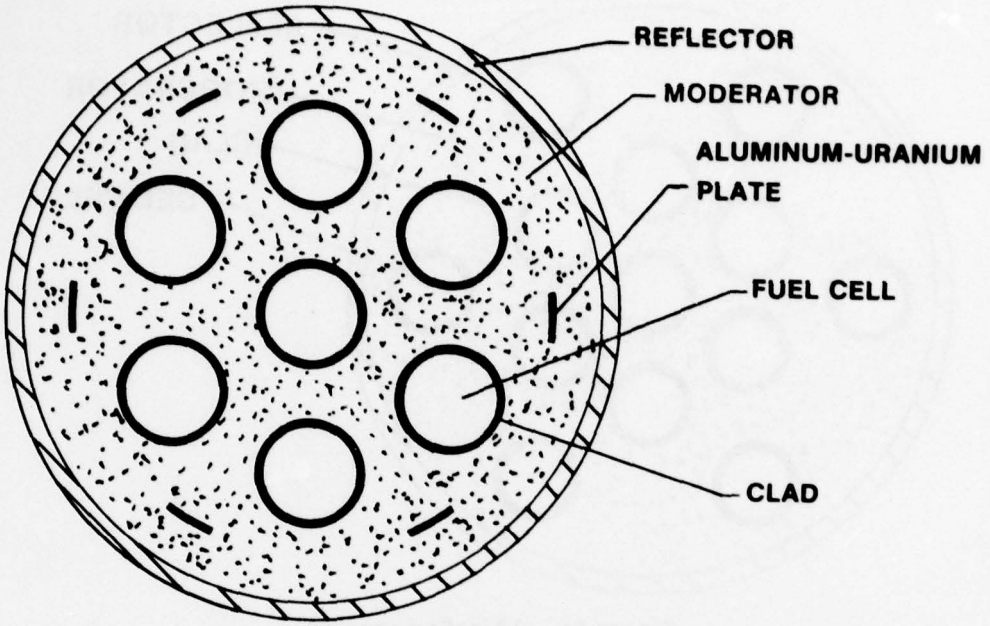

Figure 4a. Aluminum-uranium plate driver.

Note:

4a) depicts a design similar to Figure 3 but Al-U alloy has been positioned around the outside of the unit cavities to add reactivity to the assembly. 4b) is the homogenized equivalent of 4a).

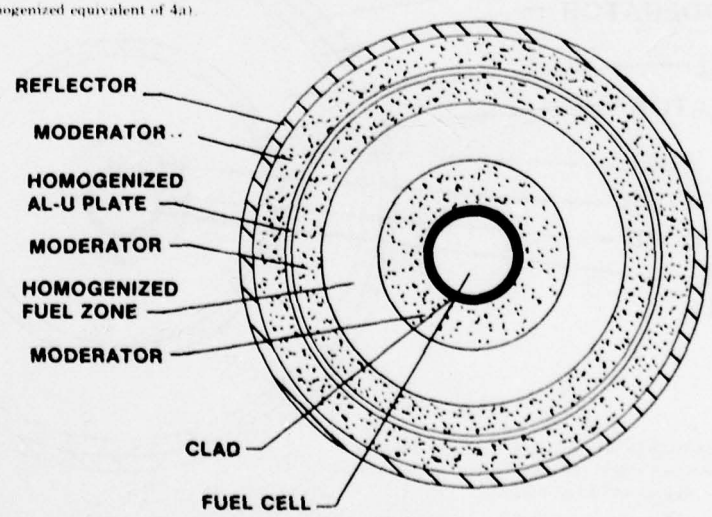

Figure 4b. Aluminum-uranium plate driver homogenized.

Figure 4. Reactor/laser concept using Al-U plate.

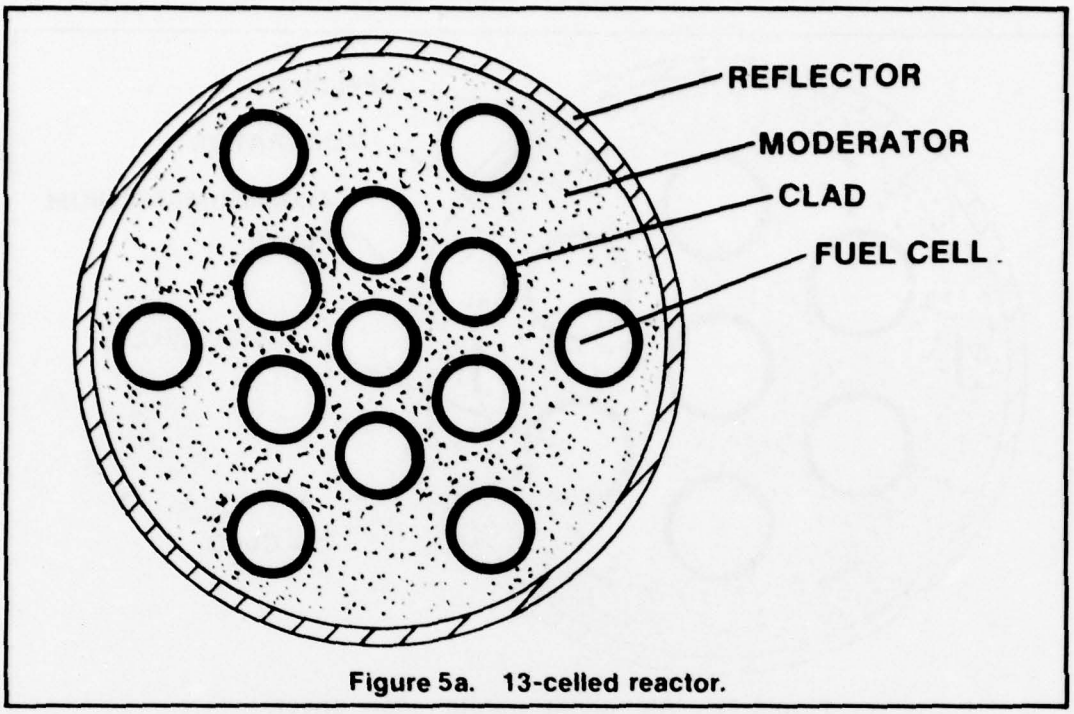

Figure 5a. 13-celled reactor.

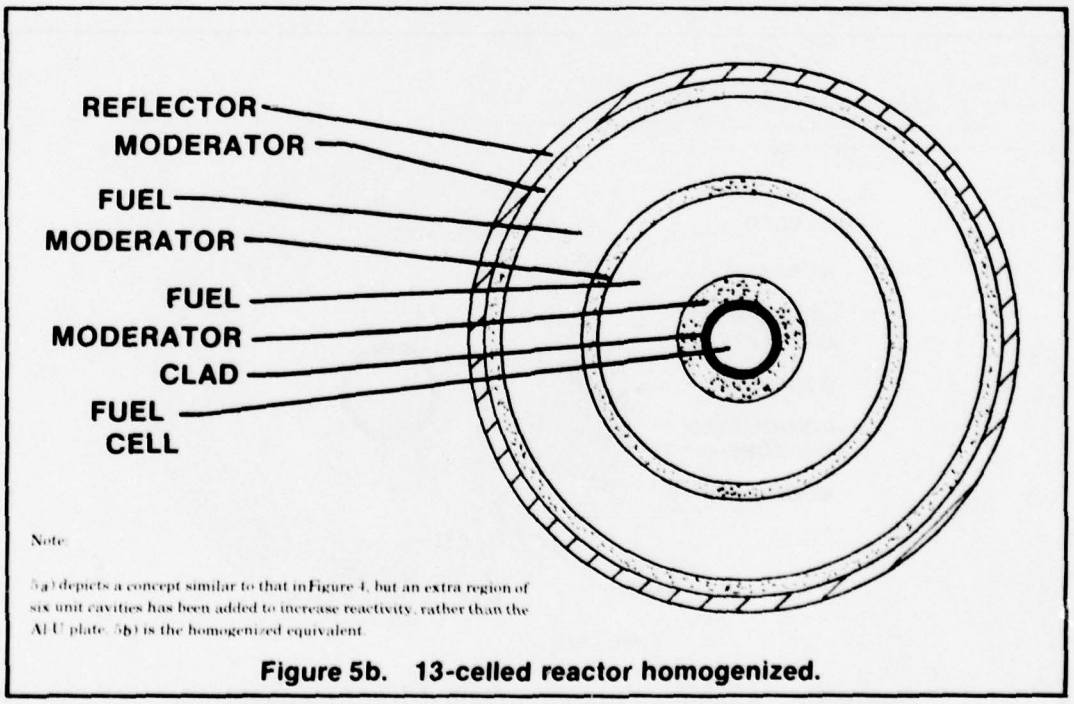

Note:

5a) depicts a concept similar to that in Figure 4, but an extra region of six unit cavities has been added to increase reactivity, rather than the Al-U plate. 5b) is the homogenized equivalent.

Figure 5b. 13-celled reactor homogenized.

Figure 5. Thirteen-celled reactor/laser.

thicknesses were judged. More important than effect on keffective,† moderator thicknesses were chosen to yield relatively flat flux shapes across the laser cells (those fuel cells having low uranium density), resulting in uniform fuel burn-up and nearly uniform fission density across the laser cell.

B. Computer Modeling.

The nuclear reactor computer model used to investigate the simplified homogenized equivalents of the reactor configurations was ANISN, obtained from Oak Ridge National Laboratories (ORNL) and made operational on a CDC 7600 series computer. ANISN solves the one-dimensional, energy dependent, linear Boltzmann transport equation with general anisotropic scattering for slab, cylindrical or spherical geometries. ANISN solves forward or adjoint, homogeneous or inhomogeneous problems. Vacuum, reflective, periodic, white or albedo boundary conditions may be specified. Time absorption calculations, concentration searches, outer radius searches, buckling searches, zone thickness searches, or eigenvalue calculations (i.e. keffective) may be performed. Cross sections may be input from a library tape and/or from cards.

The method of solution employed is the discrete ordinates or Carlson's S_n method using a diamond difference solution technique.[43] The solution in the code will approach the exact solution of the Boltzmann equation with increasing orders of approximation as the space, angle, and energy mesh approaches differential size.[43] An S_4 quadrature set was found sufficient as in Reference 44, and a P_3 scattering approximation was used.

Neutron cross sections were obtained from DLC-2, a 100 group neutron cross section data set obtained from ORNL. The 100 fine groups were collapsed into 14 coarse groups and weighted by the neutron flux energy distribution in fuel, moderator or reflector regions prior to input to ANISN. The 14-group energy intervals are shown in Table 2.

Some error is inherent in ANISN since it solves a one-dimensional configuration. Neutron leakage corrections are made axially with a buckling† term, supplied in the input as the reactor length. Fuel cells are not located spatially as they would be in

†See Appendix C for a description of nuclear terms.

TABLE 2. ENERGY INTERVALS FOR FOURTEEN GROUPS.

GROUP #	UPPER ENERGY (MeV)
1	14.92
2	3.67
3	2.23
4	1.35
5	0.498
6	0.183
7	0.067
8	0.025
9	3.35×10^{-3}
10	4.54×10^{-4}
11	6.14×10^{-5}
12	8.32×10^{-6}
13	2.38×10^{-6}
14*	5.31×10^{-7}

*The lower energy bound is zero.

the reactor, but appear as zones homogenized with surrounding clad and moderator. In addition, no temperature or pressure broadening corrections were made to neutron cross sections. Because of these inherent errors in ANISN, a keffective (keff) of 1.2 was chosen as criticality criteria to compensate for any overly optimistic results. The keff calculation option was used to establish reference designs having a uranium density of 1×10^{7} atoms/b-cm in the laser cells, and the concentration search option was used when investigating increasing uranium density in the fuel cells.

Outer fuel cells (or A1-U plate) were homogenized with clad and moderator into annular zones for compatibility with the cylindrical geometry option of ANISN. The zones were homogenized by volume weighting uranium (plus the other excimer metal, copper), clad and moderator appearing in the annulus circumscribed by the inner and outer radius defined by the diameter of the fuel cells. If R_a is the radius of the fuel cell, R_b the radius of fuel cell plus clad, R_i the inner radius of the annular fuel zone, and R_o the outer radius of the annulus, the volume weighting was performed as follows:

$$\% \text{ U+Cu} = [(\# \text{ fuel cells}) \cdot R_a^2]/[R_o^2 - R_i^2]$$

$$\% \textit{ Clad} = [(\# \text{ fuel cells}) \cdot (R_b^2 - R_a^2)]/[R_o^2 - R_i^2]$$

$$\% \textit{ Moderator} = 1 - \{[(\# \text{ fuel cells}) \cdot R_b^2]/[R_o^2 - R_i^2]\}$$

The thickness of the annular zone, R_o-R_i, is always equal to the diameter of a complete fuel cell, $2R_b$. These percentages would multiply the desired material number density and the adjusted density would be input into the homogenized zone.

5. RESULTS OF NUCLEAR CALCULATIONS

A. Seven-Celled Reactor.

Considered important in establishing a design basis, the 7-celled reactor, shown in *Figure 3*, was investigated thoroughly. The design criteria of a U-235 density in the fuel cells of 1×10^{-7} atoms/b-cm proved too low to yield meaningful results, keff being small. Initial investigations were directed at using the central fuel cell as a criticality driver by increasing its uranium density, resulting in higher values of keff and permitting useful results on material dimensions to be obtained. From initial work described in Appendix A, the reflector for all investigations of the 7-celled reactor was 10 cm of Be.

Figure 6 shows the results of increasing the U-235 density in the central fuel cell, hereafter termed the driver, while maintaining a density of 1×10^{-7} atoms/b-cm in the outer fuel cells, hereafter termed the laser cells. The inner moderator was 44 cm of carbon for the results shown in *Figure 6*. A density of 1×10^{-4} atoms/b-cm (1×10^{20} atoms/cm^3) was chosen as an upper limit for maintaining uranium in a vapor state. *Figure 6* clearly demonstrates that merely increasing the vaporous fuel density will not drive the reactor critical.

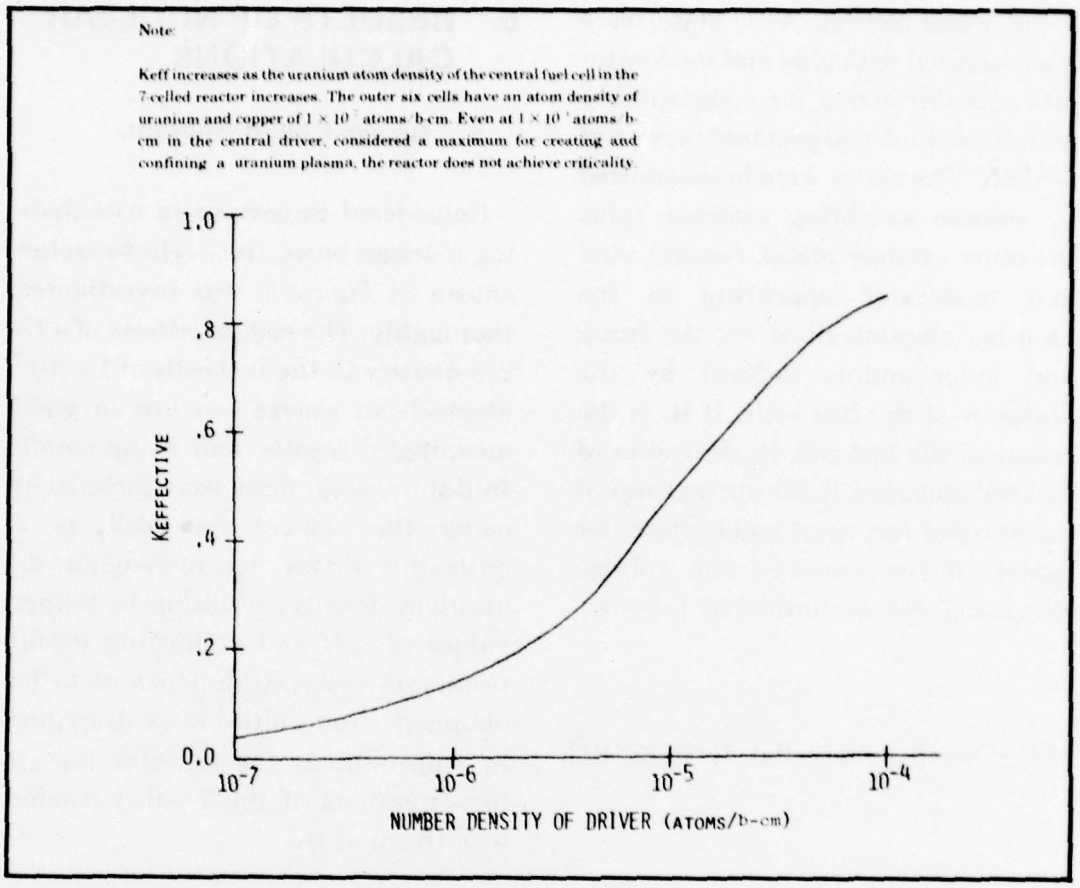

Figure 6. Criticality not attained with a vapor density in driver.

Figure 7 shows how keff varies as the inner moderator thickness increases, with different densities in the driver. At the higher densities in the driver, large thicknesses of inner carbon moderator increase the keff of the reactor, but not enough to attain criticality. The results of *Figures 6* and *7* were obtained with an outer moderator of 100 cm of graphite. *Figure 8* depicts the results of investigating the outer moderator thickness. It can be seen that the effect on keff is slight with moderator thicknesses greater than 60 cm. Hereafter, outer moderator thickness was maintained at 60 cm, with 10 cm of Be reflector surrounding the entire reactor. In *Figure 8*, extra moderator refers to the thickness of the inner moderator. No extra moderator implies the fuel cells are embedded in carbon moderator but have their walls in contact. Extra moderator refers to

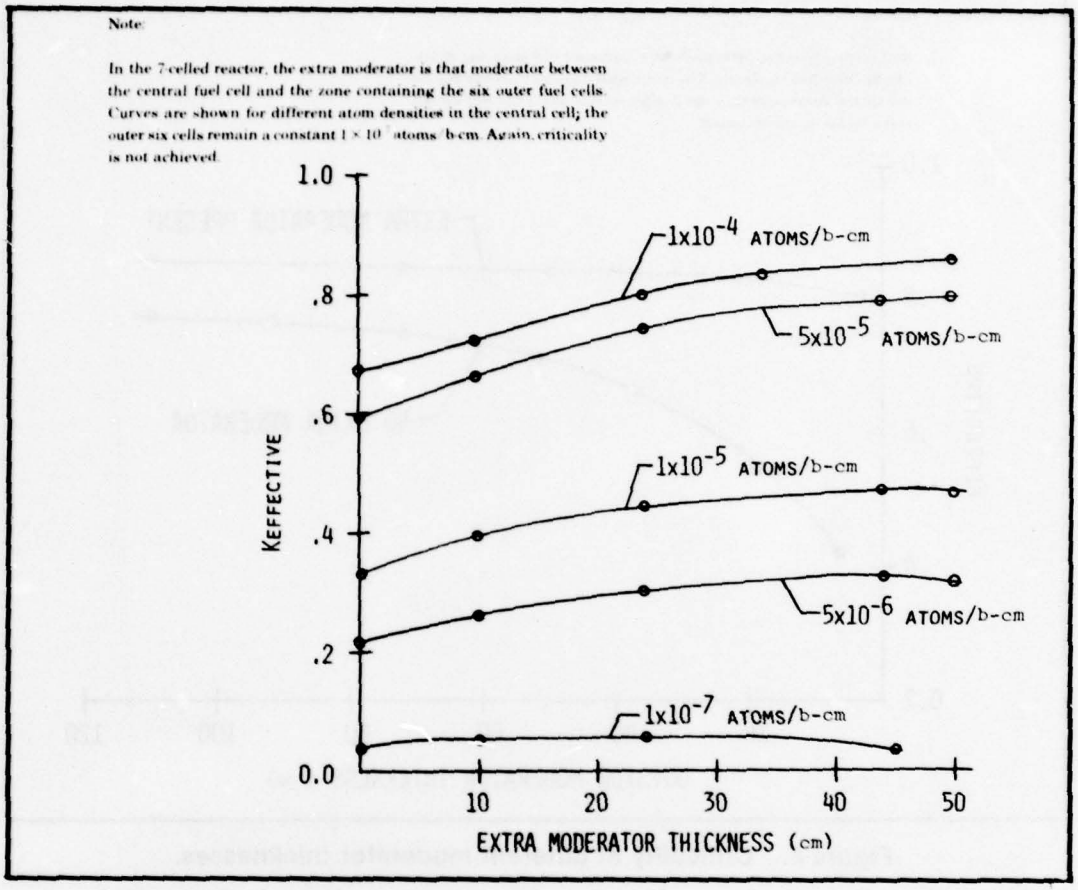

Figure 7. Uranium density and moderator effects on criticality.

the radius to the centerline of the laser cells having been increased with the resultant gap occupied by moderator. Extra inner moderator (44 cm in *Figure 8*) again demonstrates higher values of keff, and also makes the choice of outer moderator thickness less critical.

Referring to *Figure 7*, at low densities in the driver too much moderator had a damaging effect on keff. It was felt this effect might be attributed to thermal neutron flux suppression at high inner moderator thicknesses. *Figure 9* exhibits a plot of thermal neutron flux in a reactor with 44 cm of inner moderator and a density of 1×10^{-4} atoms/b-cm in the driver. It can be seen that the flux peaks early in the moderator, and is affected little in the low density laser cells. The flux shape is similar to that calculated in Reference 46, except that the flux in the

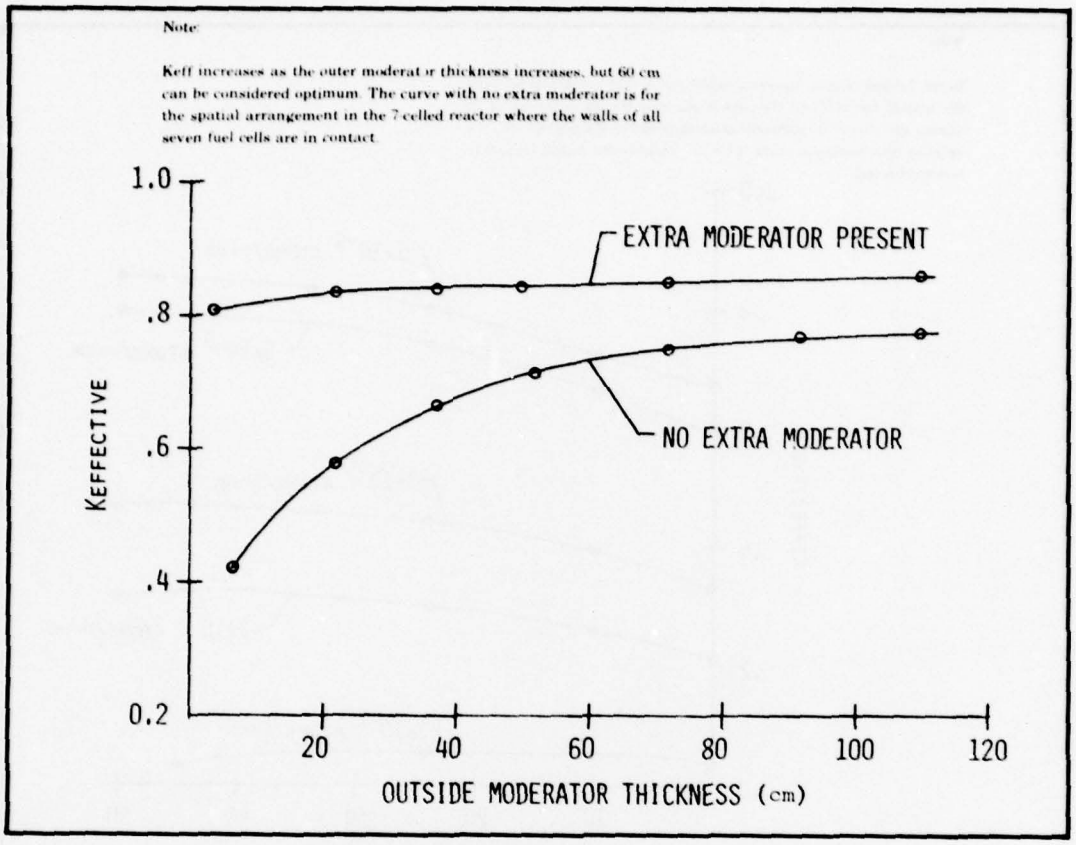

Figure 8. Criticality at different moderator thicknesses.

laser cells of *Figure 9* is higher than in the central driver, due to relatively little absorption of thermal neutrons in the low density cells. Plots of thermal flux in Reference 46 also exhibit a flux depression in fuel cells as does the driver of *Figure 9*. This was attributed to an "apparent self shielding" due to the large scattering cross section of hot gases included in the calculations of Reference 45. The results shown in *Figure 9*, however, are without any hot gases, buffer or propellant. Experiments performed at the National Reactor Testing Station [40] also found the self-shielding effect in fuel cells in tests with and without simulated gases. Reference 40 attributes the self-shielding to uranium density, indicating neutron capture without fission in higher densities of uranium. Flux peaking in the moderator regions is a typical phenomena of thermal neutron build-up, and is reported in both References 45 and 40.

Note:

Figures 9 and 10 show plots of the thermal neutron flux throughout the reactor, starting from the center of the 7-celled reactor. The flux can be seen to peak in the inner moderator, and then decrease steadily throughout the remainder of the reactor.

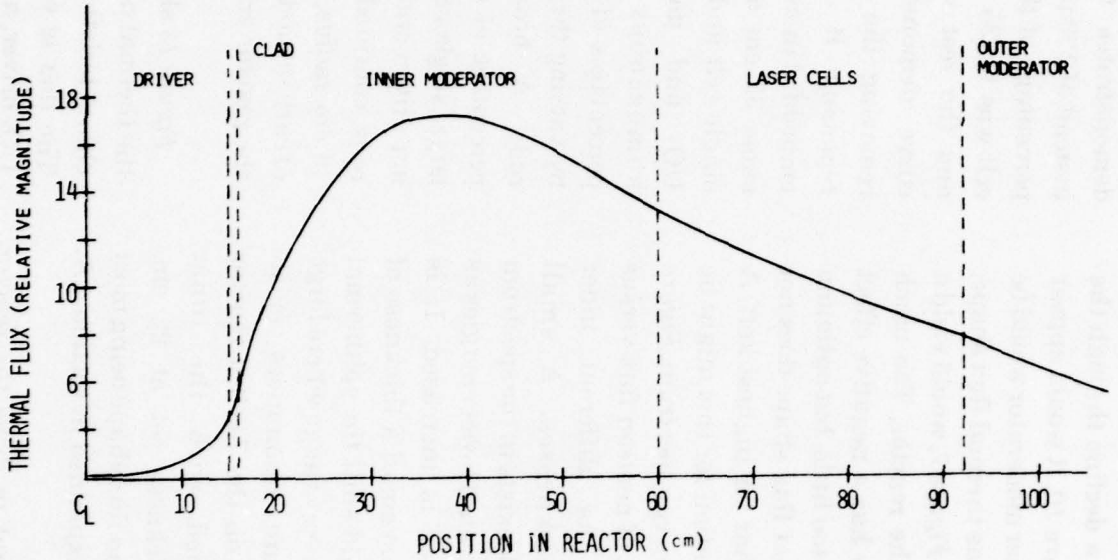

Figure 9. Spatial flux for 7-celled reactor with thick inner moderator.

The thermal flux peaked at about 22 cm of inner moderator in *Figure 9*, and *Figure 10* was generated with this thickness. The flux peaks as it enters the laser cell region, and does not exhibit as steep a decline through the laser. From *Figure 10*, it would appear that 18 cm of inner moderator would be optimum as far as thermal flux shape, but, referring to *Figure 7*, would yield a lower keff for the reactor. Too much inner moderator has a negative effect on keff, as does too little, but optimum thickness for best flux shape does not coincide with that for highest keff. A possible explanation for this might lie in the neutron energy spectrum. *Figure 11* shows a plot of neutron flux versus energy group for different inner moderator thicknesses. A small epithermal peak exists in the spectrum that is shifted toward lower energies as inner moderator is increased. It is possible that too small a thickness of moderator would shift the epithermal peak into an energy range where large neutron capture resonances exist. Further study on the 7-celled reactor was performed with the inner moderator thickness set at 22 cm, thermal neutron flux shape being most important as explained in section 4.A.

In an attempt to drive the reactor critical, the addition of moderator to the driver and replacement of the driver with solid fuel rods was investigated. *Figure 12* depicts the results of replacing some uranium vapor with carbon moderator, and replacing the vapor with solid fuel with varying amounts of moderator. The bottom curve of *Figure 12* demonstrates the effect on keff if, instead of 100 percent U-235, a certain percentage of the volume of the driver cell was U-235 at 1×10^{-4} atoms/b-cm and the rest was graphite. The top curve demonstrates the results of removing the large, single cell and replacing it with UO_2 fuel rods embedded in moderator. Retaining the same 32 cm diameter region as the single cell and volume weighting the UO_2 and moderator to create a homogenous zone, the varying percentages of moderator are obtained by varying the number (or size) of fuel rods. A broad range of optimum percentage of moderator exists for the large, single cell, but the reactor still is not driven critical. The use of UO_2 fuel rods, confined in the central region of 16 cm radius, with small percentages of carbon moderator would easily drive the reactor critical.

Figure 13 shows the spatial shape of the thermal neutron flux for the driver characteristics examined in *Figure 12*. The flux is severely depressed in the UO_2 driver, and higher percentages of moderator in the driver yields higher thermal fluxes. Note also that higher percentages of moderator in the driver results in earlier flux peaking in the

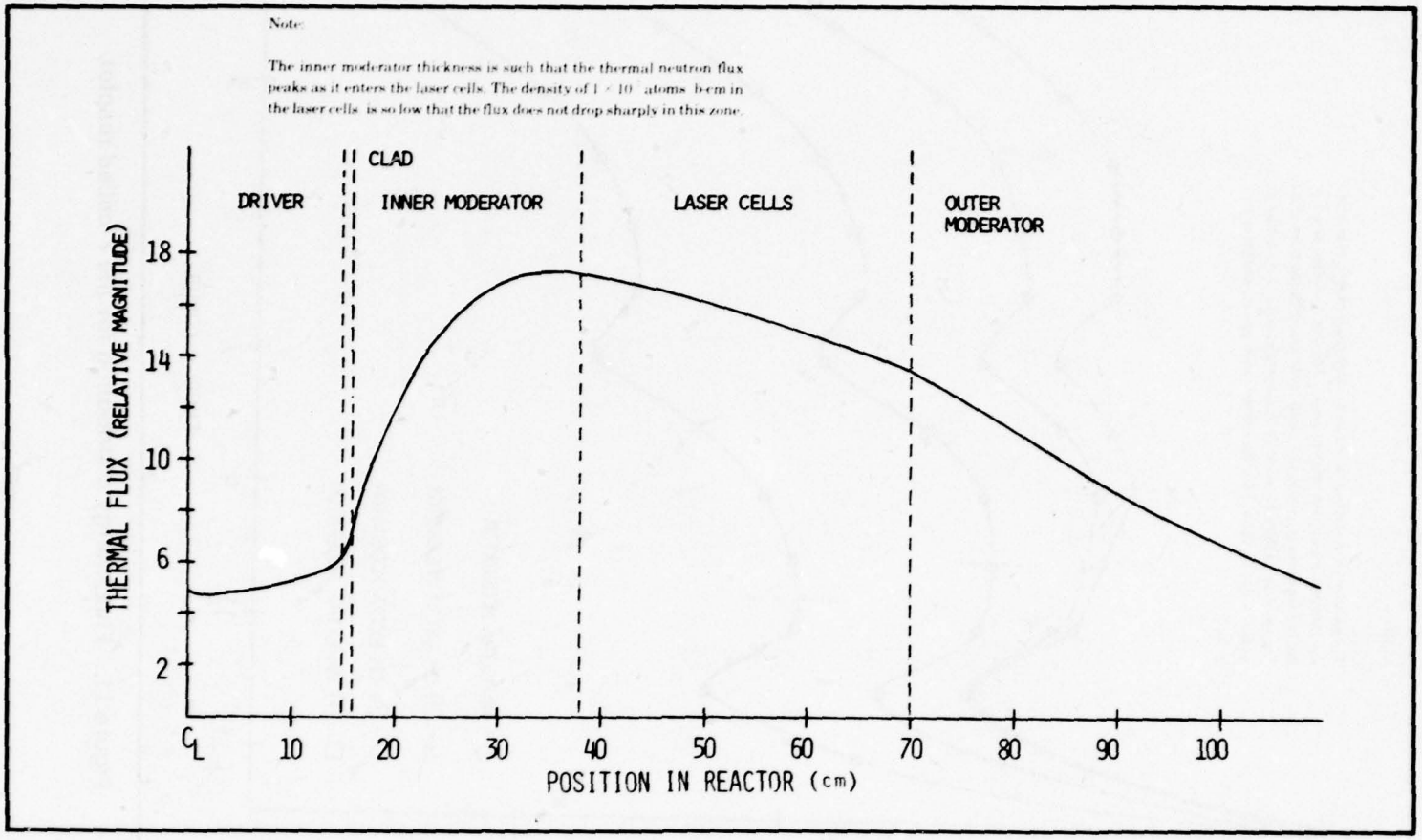

Figure 10. Spatial flux in 7-celled reactor for near optimal inner moderator.

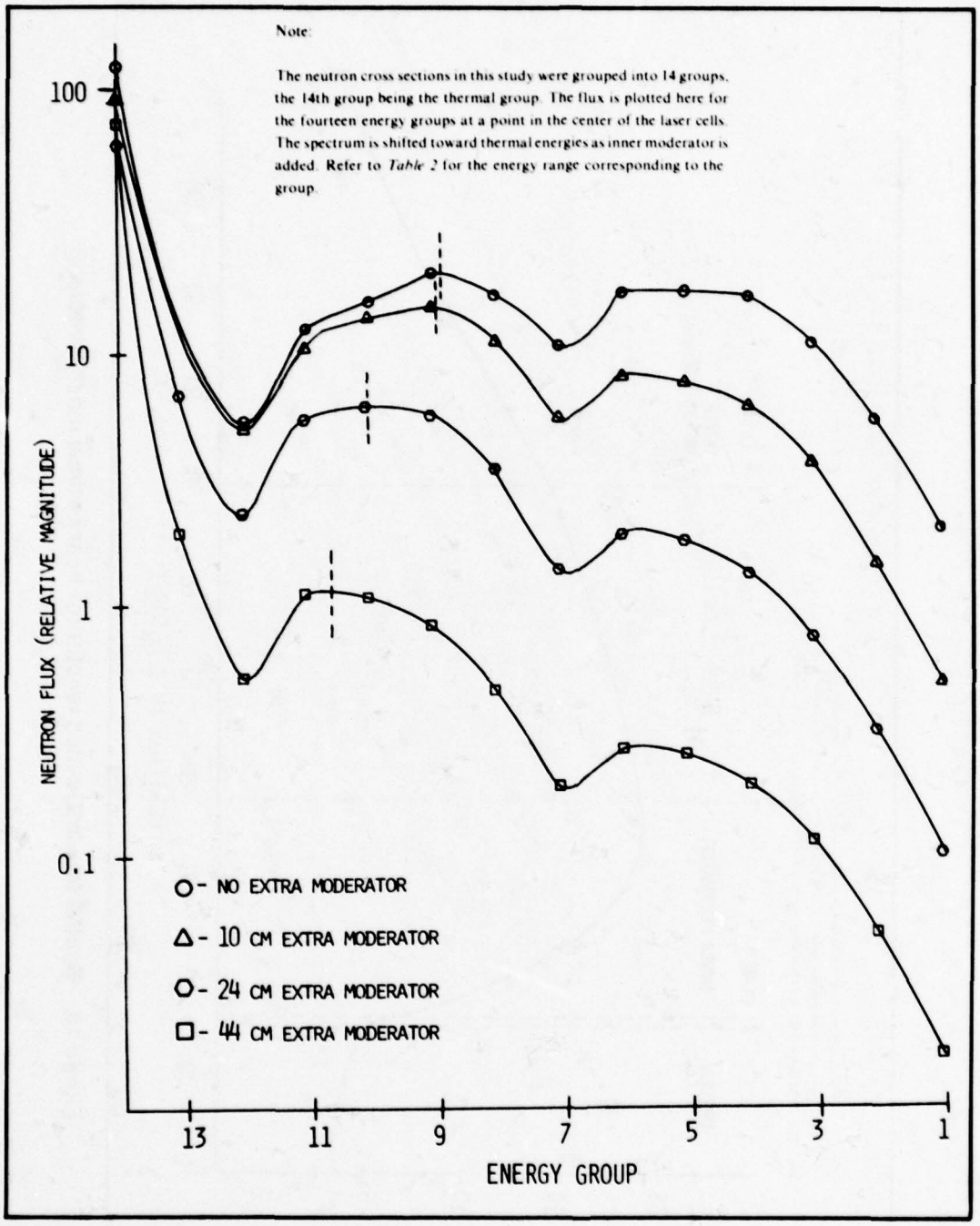

Figure 11. Flux energy distribution for the 7-celled reactor.

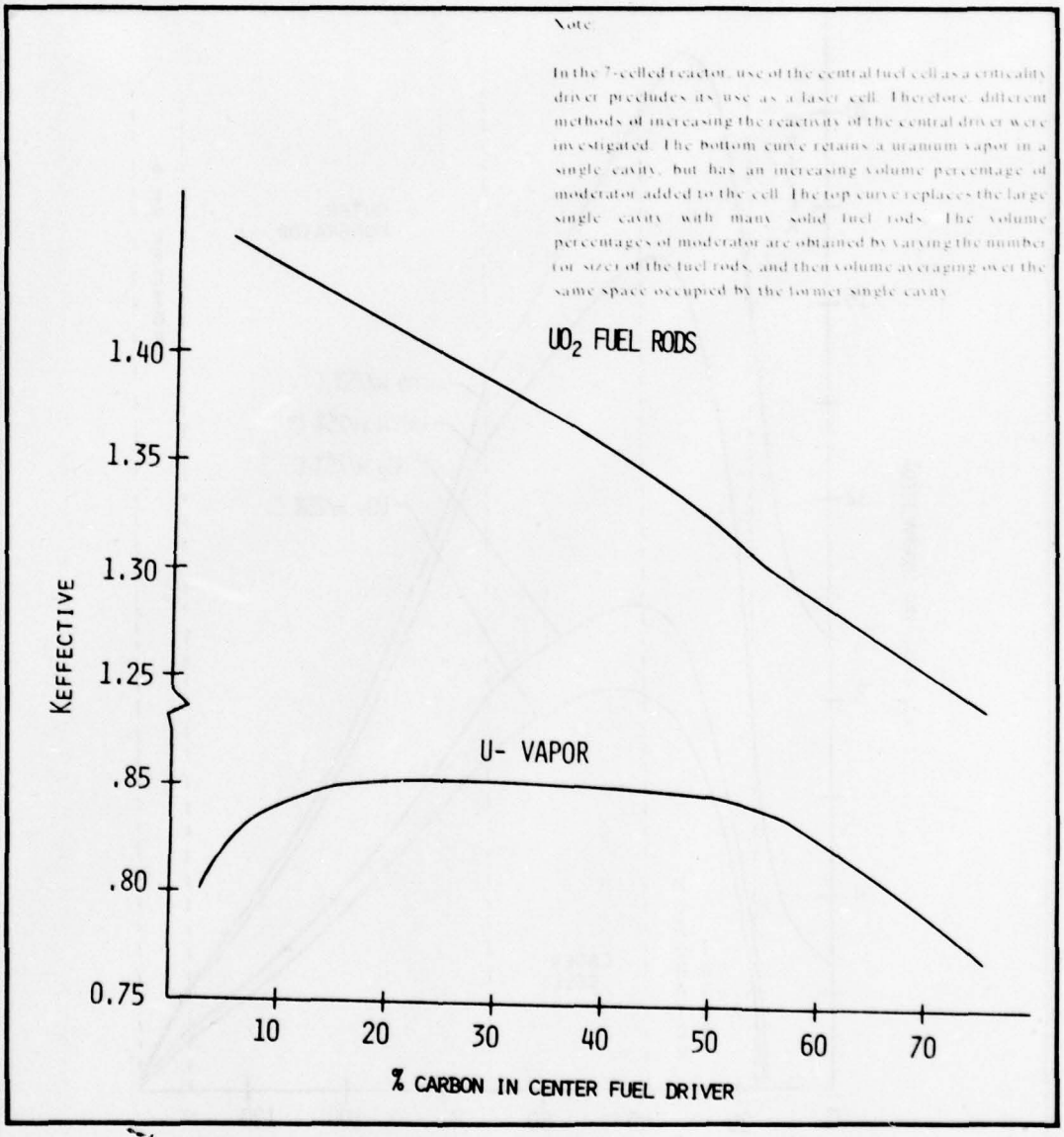

Figure 12. Different types of fuel in the central driver.

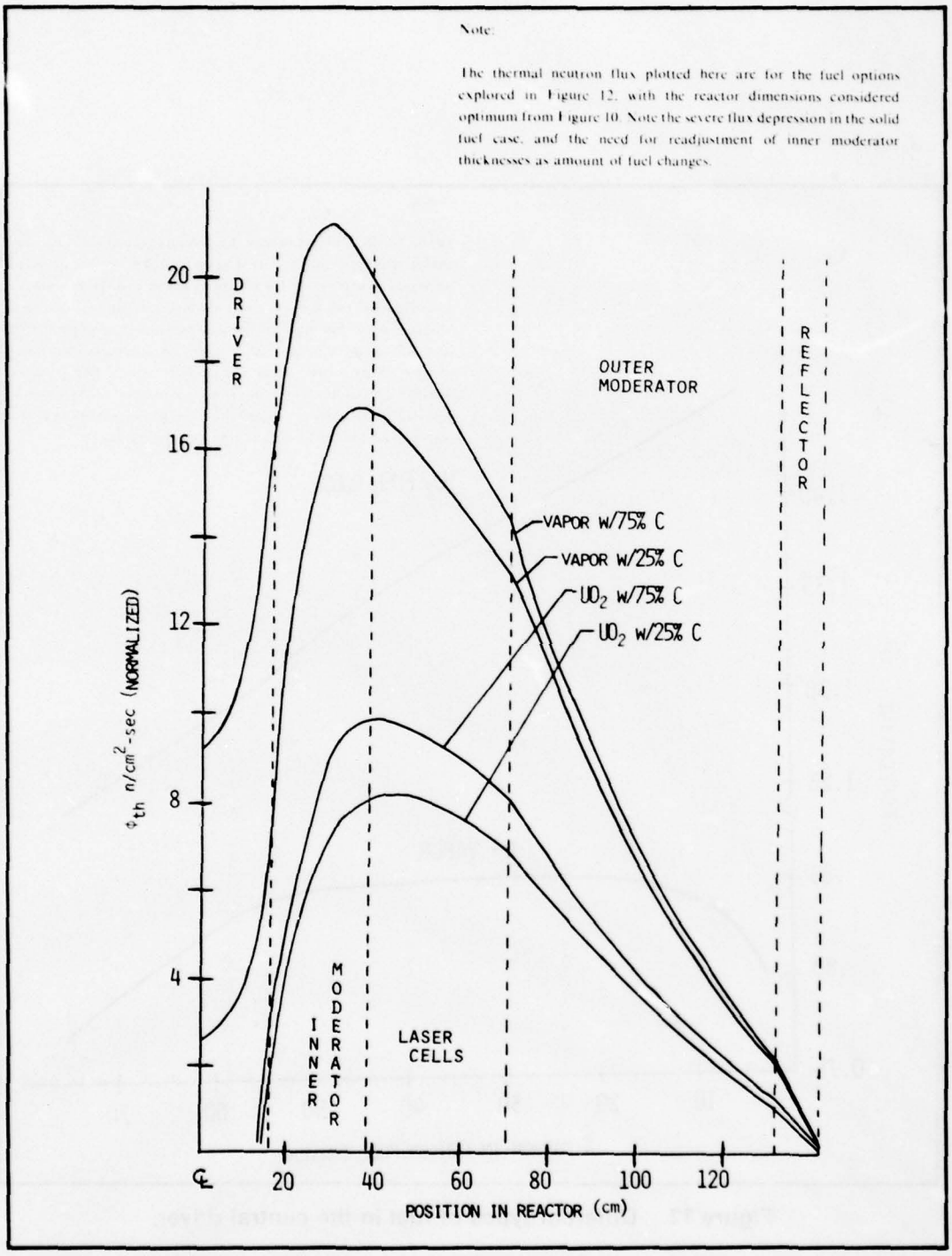

Figure 13. Thermal flux for varying density and percent moderator: 7-celled *reactor.*

inner moderator, the optimum thickness being about 12 cm for a single cell driver with 25 percent uranium vapor and 75 percent cabron. Solid fuel drivers yield a more flat flux shape across the laser cells, with the 25 percent moderator case resulting in a late peak and therefore more flat flux than the 75 percent moderator case. The shape of the thermal flux in a solid driver can be seen in *Figure 14*, demonstrating the severity of flux depression in a UO_2 criticality driver.

Uniformity of fuel cells would probably be a desirable feature in a reactor of this type, but retaining a vaporous driver will not allow the reactor to go critical with a laser density of 1×10^{-7} atoms/b-cm. Use of solid fuel drivers, in addition to lower thermal flux, would require a separate means of cooling, and, to maintain efficiency, would require an alternate means of extracting energy from the heat generated. The finalized characteristics of the 7-celled reactor are summarized in Table 3. The configuration using a large, single central cell with uranium vapor will be discussed further in section 6, where an investigation of varying the uranium density in the laser cells was performed. With a slightly higher density of fuel in the laser cells, the reactor can easily be made critical. Use of a solid fuel central driver was not explored further, the use of solid drivers positioned in the outer moderator yielding better thermal neutron flux shapes.

B. A1-U Plate Driven Reactor.

The seven-celled reactor discussed above did not achieve criticality unless solid fuel elements (thereby increasing fuel density) were employed. The use of solid fuel in the central driver did not yield desirable uniform flux shapes across laser cells. By placing solid aluminum-uranium (100 percent U-235 in this study) plating outside the laser cells, and by increasing the uranium vapor density in the central fuel (*Figure 4*), the laser cells can be maintained at a fuel density of 1×10^{-7} atoms/b-cm and the reactor can be made critical. In the interest of using common materials and reducing computational time, only two types of A1-U plate were investigated: ten and twenty percent by weight uranium, 100 percent U-235.

Figure 15 shows how keff varies, as the moderator thickness between the laser cells and A1-U plate is increased, for the two types of plate and for vapor or solid fuel in the central driver. Inner moderator thickness (between central driver and laser cells) is 22 cm graphite, as determined from section 5.A. All outermost moderator is 60 cm graphite, and all reflector is 10 cm Be. As seen in *Figure 15*, criticality is

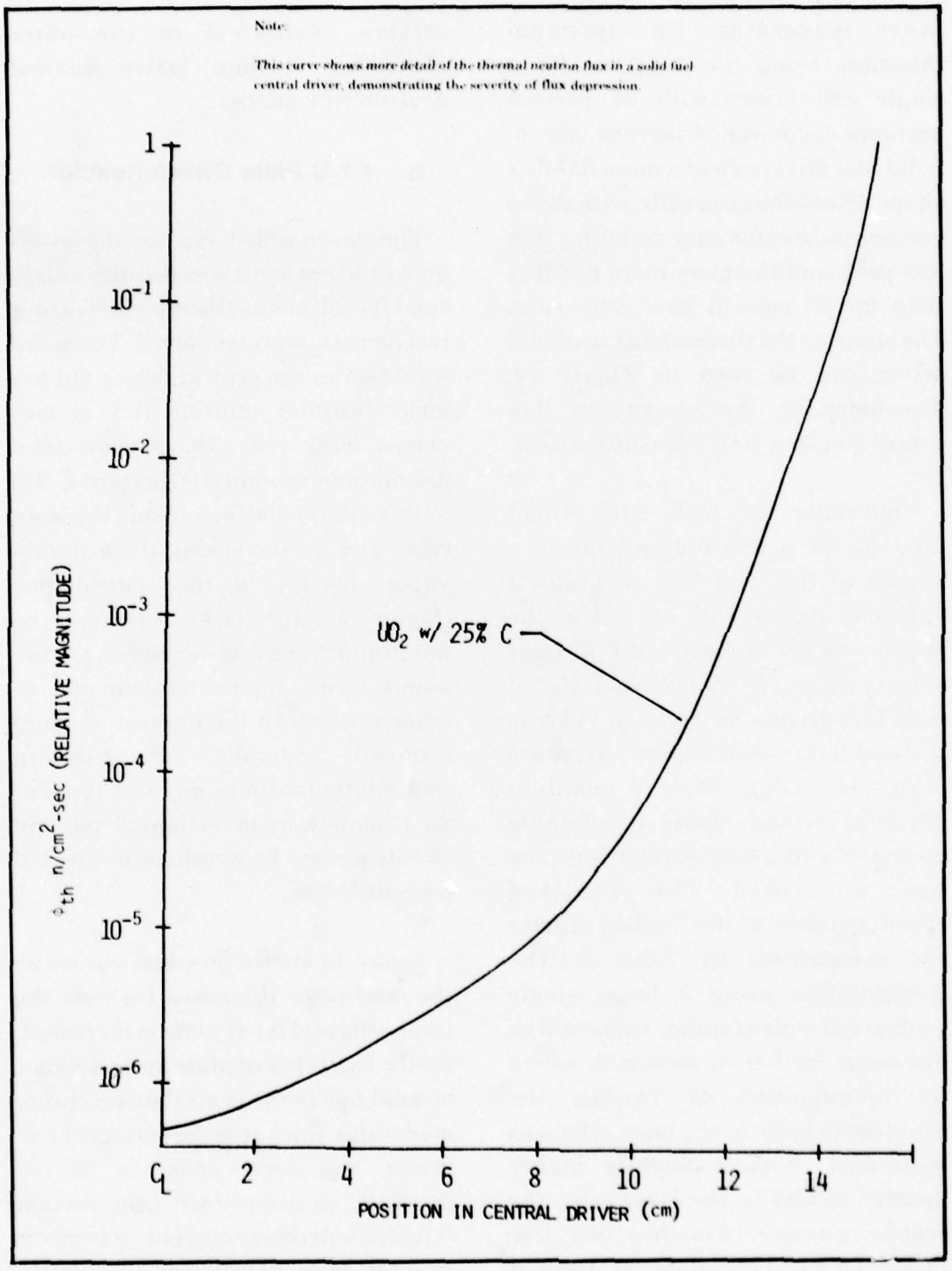

Figure 14. Thermal flux in the UO2 driver.

TABLE 3. SUMMARY OF 7-CELLED REACTOR.

DRIVER	INNER MOD.	LASER CELLS	OUTER MOD.	REFLECTOR	CRITICAL
32 cm DIA 10^{-4} $\frac{\text{atoms}}{\text{b-cm}}$ 25% C 75% U-235	22 cm Carbon	32 cm 10^{-7} $\frac{\text{atoms}}{\text{b-cm}}$ U-235 + Cu (+ BeO Clad)	60 cm Carbon	10 cm Beryllium	NO
32 cm DIA 25% C 75% UO_2	28 cm Carbon	32 cm 10^{-7} $\frac{\text{atoms}}{\text{b-cm}}$ U-235 + Cu (+ BeO Clad)	60 cm Carbon	10 cm Beryllium	YES

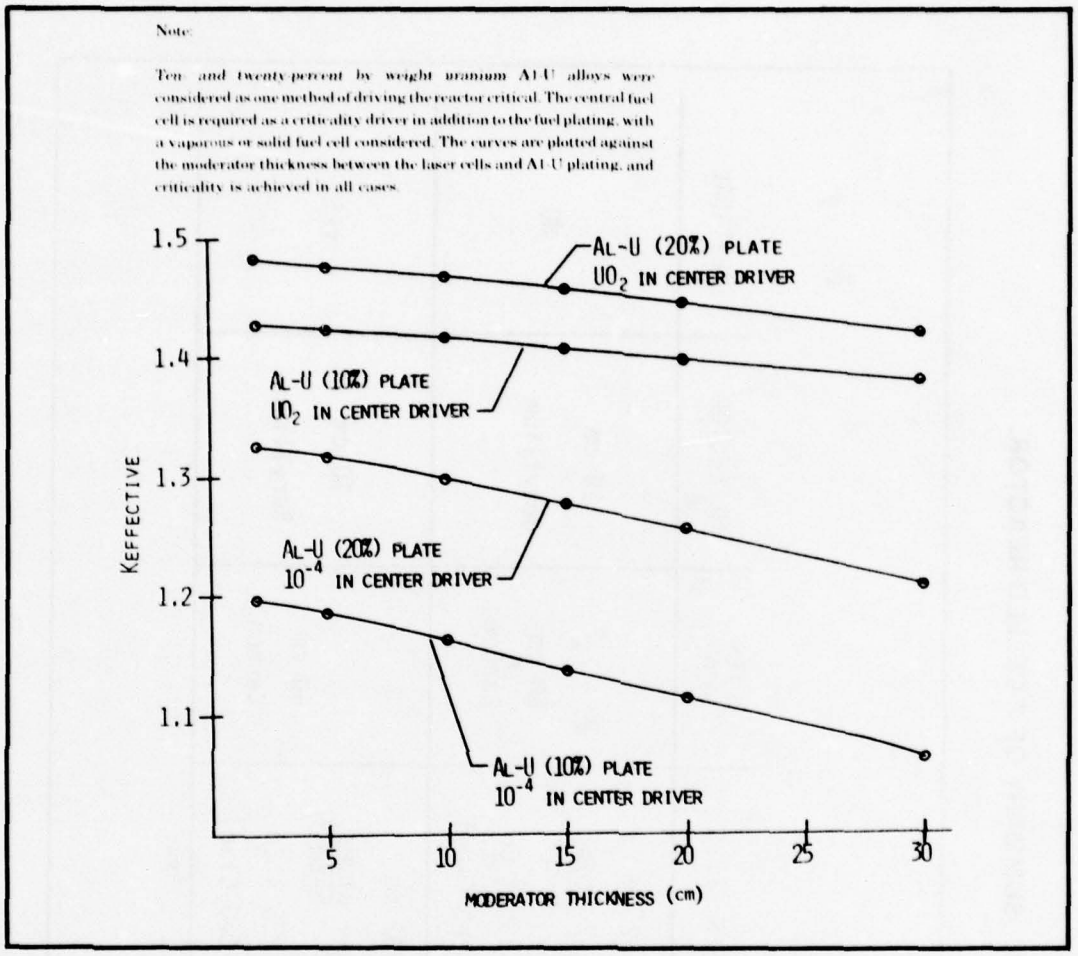

Figure 15. Keffective versus moderator thickness between laser cells and A1-U plating.

easily achieved in all cases, and, therefore, solid fuel elements in the central driver will not be discussed. Due to close coupling between the intense neutron sources of the central driver and A1-U driver, the reason for decreasing keff with increasing moderator thickness (contrary to, say, *Figure 8*) was not clear.

The thermal neutron flux across the reactor is depicted in *Figure 16*. The flux across the laser cells is very uniform as compared to the 7-celled reactor. Presumably due to the greater neutron source, the 20 percent by weight uranium case yields better shapes than the 10 percent case. The central driver has a density of 1×10^{-4}

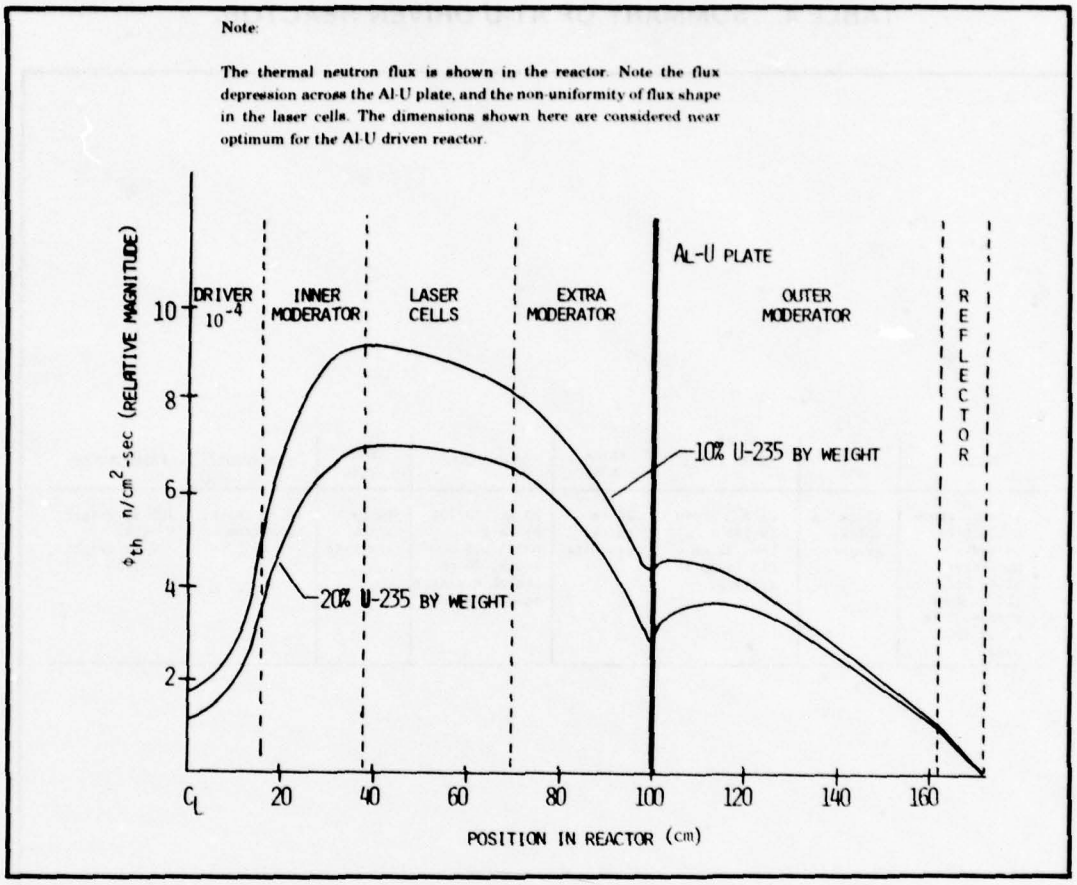

Figure 16. Spatial flux for A1-U driven reactor.

atom/b-cm, and 30 cm of graphite moderator between laser cells and A1-U plate. Experiments reported in Reference 40 were performed using thin sheets of metallic uranium (orally) to simulate the plasma, and reported the same self-shielding effects as *Figure 16* shows across the solid plate. With more numerous fissions in the A1-U plate, in contrast to when the laser cells are the outer fuel region, expected thermal neutron build-up occurs in the outermost moderator.

After further computations, the final dimensions for the A1-U driven reactor were chosen, and are presented in Table 4. Both types of A1-U plated reactors will have density investigations performed in section 6. There are

TABLE 4. SUMMARY OF A1-U DRIVEN REACTOR.

DRIVER	INNER MOD.	LASER CELLS	EXTRA MOD.	A1-U PLATE:	OUTER MOD.	REFLECTOR:	KEFFECTIVE:
1 $x10^{4}$ atoms U-235/b-cm no added moderator 32 cm DIA (15 cm fuel radius, 1 cm thick BeO clad)	22 cm thick, graphite	$1x10^{-7}$ atoms (U-235 + Cu)/ b-cm 32 cm DIA (same as driver)	20 cm thick, graphite	28 Al, 10/20% by weight U-235 0.5 cm thick, 20 cm length 6 plates equally spaced	60 cm thick graphite	10 cm thick, beryllium	10% by weight U--1.11 20% by weight U--1.25

no magic reasons for the choice of the A1-U plate dimensions or quantity. *Figure 4a* demonstrates a possible positioning of the plates, but since the zone was homogenized into a thin annulus for input to ANISN, the positioning has no effect. A1-U plating was considered a common type of fuel easily machineable, but fuel rods or pins could perform the same function in any number or spatial arrangement for a one-dimensional treatment. These many options should be investigated further with a two-dimensional neutron transport computer code. The results presented here are intended to help reduce the cost and time of performing two-dimensional computer code calculations.

C. Thirteen-Celled Reactor.

The A1-U driven reactor exhibits a more uniform flux shape across the reactor than does the 7-celled reactor, and can easily be made critical. A problem with design uniformity still exists with the A1-U driven reactor, however, in that different means of cooling must be supplied to the solid fuel plates, and some other means than laser light must be used to extract energy. Also, only six of the seven cells can be used for lasing. To retain uniformity of fuel cells but still maintain criticality, a 13-celled reactor (*Figure 5*) was investigated, where an extra ring of six fuel cells, identical to the laser cells, replaces the solid A1-U plates.

The thirteen fuel cells of this reactor have the same dimensions as given earlier. Laser cells have a U-235 (plus Cu) density of 1×10^{-7} atoms/b-cm and include the central and middle six cells. The outer six cells, or driver cells, have a U-235 density of 1×10^{-4} atoms/b-cm, with no additives (except BeO clad homogenization). The results presented here have values of keff of around 1.5, indicating the driver cells can be reduced in density.

Figures 17 through *20* show thermal flux shapes across the reactor for different inner and extra (between the outer laser cells and driver) moderator thicknesses. All outer moderator is 60 cm graphite, with 10 cm of Be reflector, as determined earlier. The self-shielding effect of the dense driver cells is clearly demonstrated, as is thermal neutron build-up in the outer moderator. The reactors of *Figures 17* and *18*, as well as *19* and *20*, where equal total amounts of moderator is present, have equal values of keffective. The moderator thicknesses examined in *Figures 17* and *18* did not yield good flux shapes across the outer laser cells. The moderator thicknesses of *Figure 19*, 40 cm inner and 22 cm extra, exhibit very uniform thermal flux across the outer laser cells, but the flux drops sharply in the inner moderator resulting in a relatively low magnitude of thermal flux in the central laser cell. Reversal of the thicknesses between inner and extra moderator worsened the flux shape, as seen in *Figure 20*. From *Figure 20*, however, one can see a peak in the flux at about 30 cm of extra moderator. *Figure 21* depicts the flux for the moderator thicknesses considered optimum, 22 cm inner and 30 cm extra. The shape of the thermal flux is uniform through the laser cells and does not drop sharply in the inner moderator, though the outer cells continue to have a slightly higher flux.

Note:

Figures 17-21 present the thermal neutron flux shape in the 13-celled reactor. Close neutron coupling between the many cells made plots of this kind valuable in investigating moderator thicknesses. Note the flux depression in the driver and the thermal neutron buildup in the outer moderator. The driver contains U-235 only, the laser cells contain uranium and copper, of which the central cell is now one. 1×10^{-4} and 1×10^{-5} atoms/b-cm are the densities in the driver and laser, respectively.

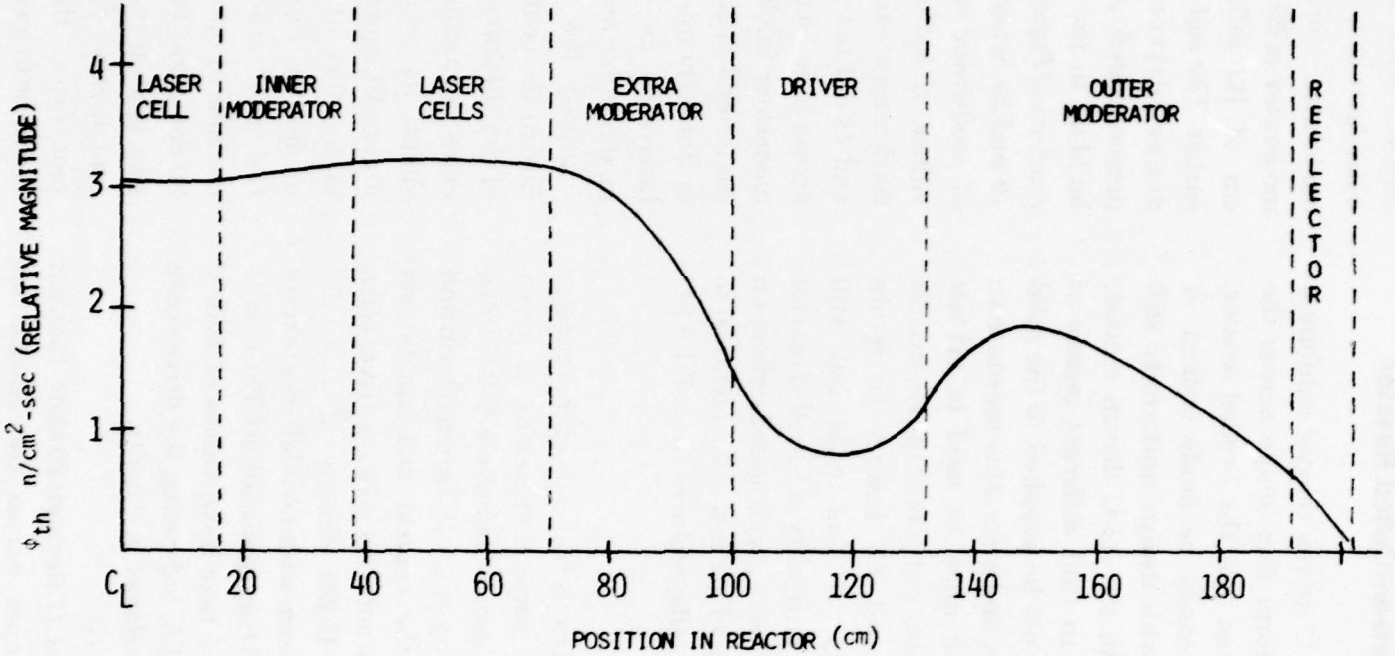

Figure 17. 13-Celled reactor thermal flux shape: 10 cm inner, 22 cm extra moderator.

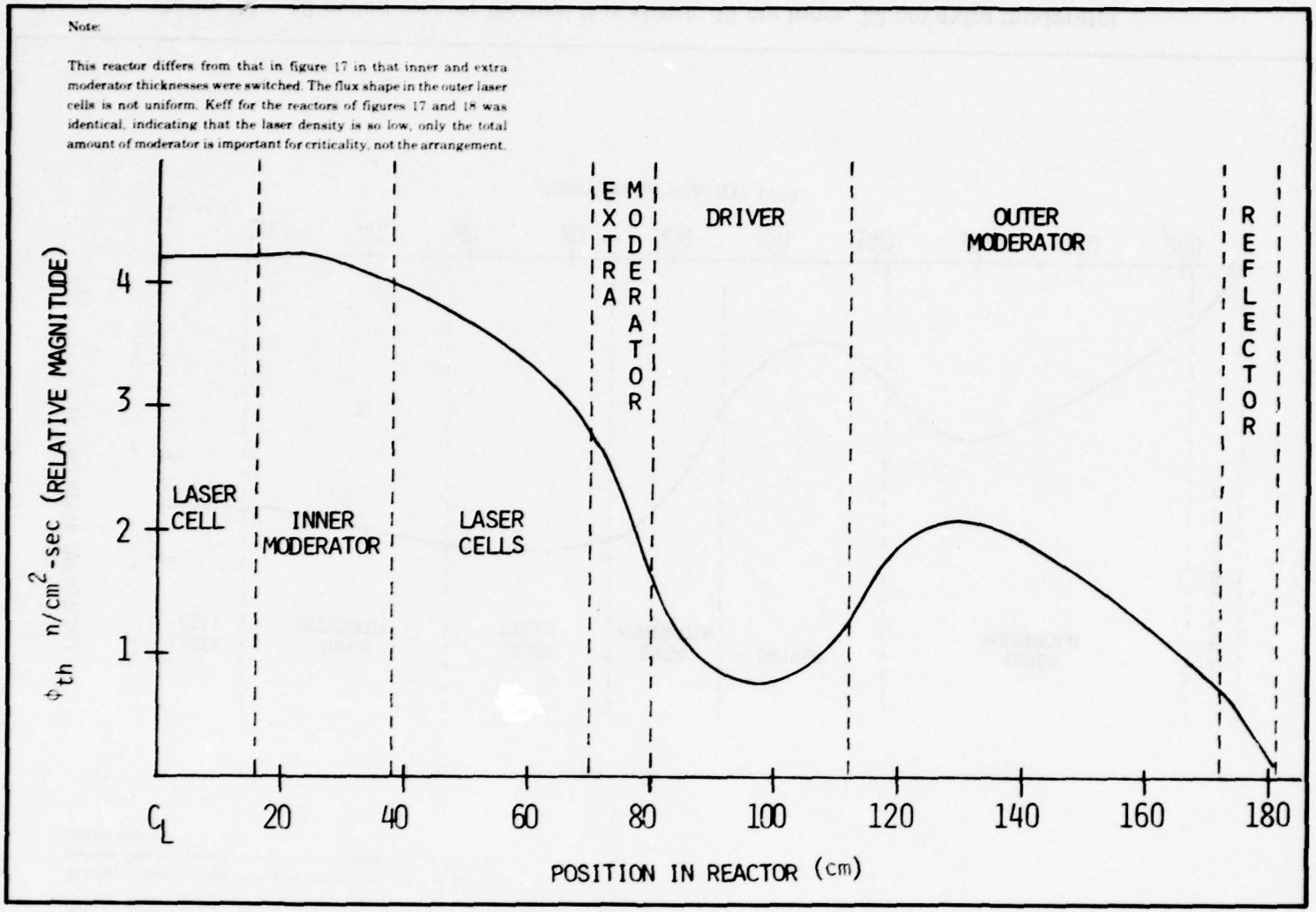

Figure 18. 13-celled reactor thermal flux shape: 22 cm inner, 10 cm extra moderator.

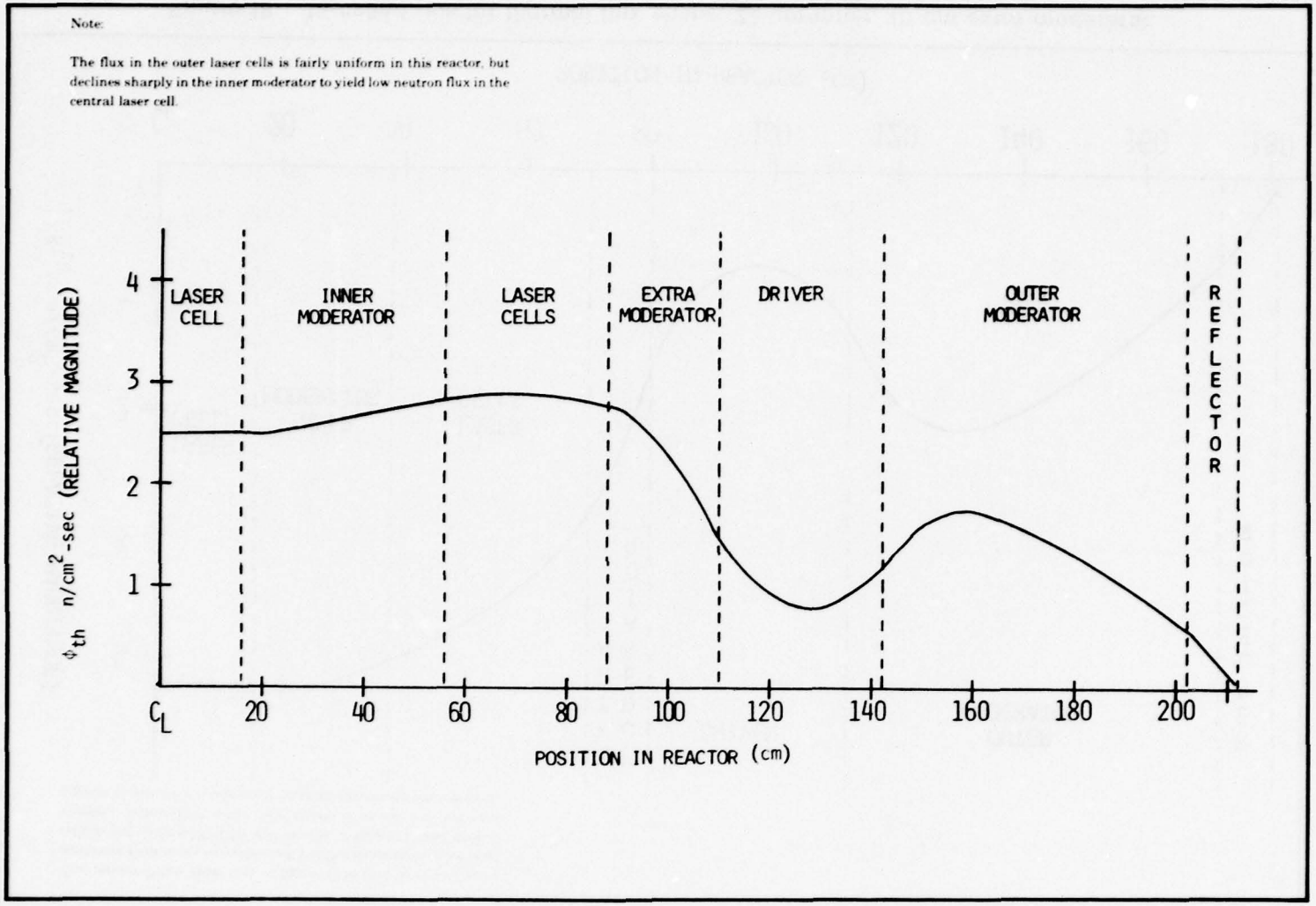

Figure 19. 13-celled reactor thermal flux shape: 40 cm inner, 22 cm extra moderator.

Note:

Reversing the dimensions of the inner and extra moderator has a negative effect on the flux shape in the outer laser cells with respect to figure 19. A peak is seen in the extra moderator, however, enabling a guess at the optimum extra moderator thickness. The total amount of moderator is the same for figures 19 and 20, and, again, the Keff was identical.

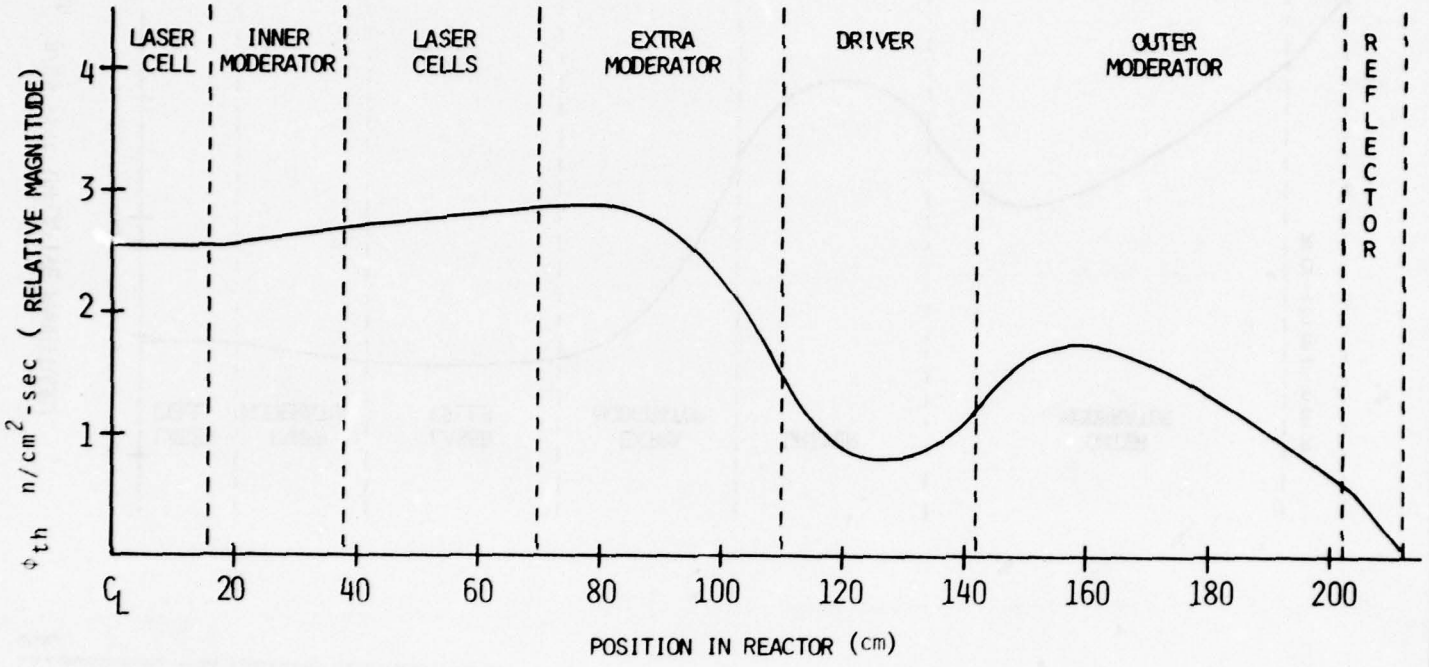

Figure 20. 13-celled reactor thermal flux shape: 22 cm inner, 40 cm extra moderator.

Note:

From the information obtained in figures 17-20, the dimensions in this reactor are considered optimum: 22 cm inner moderator, 30 cm extra moderator. Flux shapes are fairly uniform in the laser cells, and there is not a great dispairity in flux levels between the central and outer laser shells.

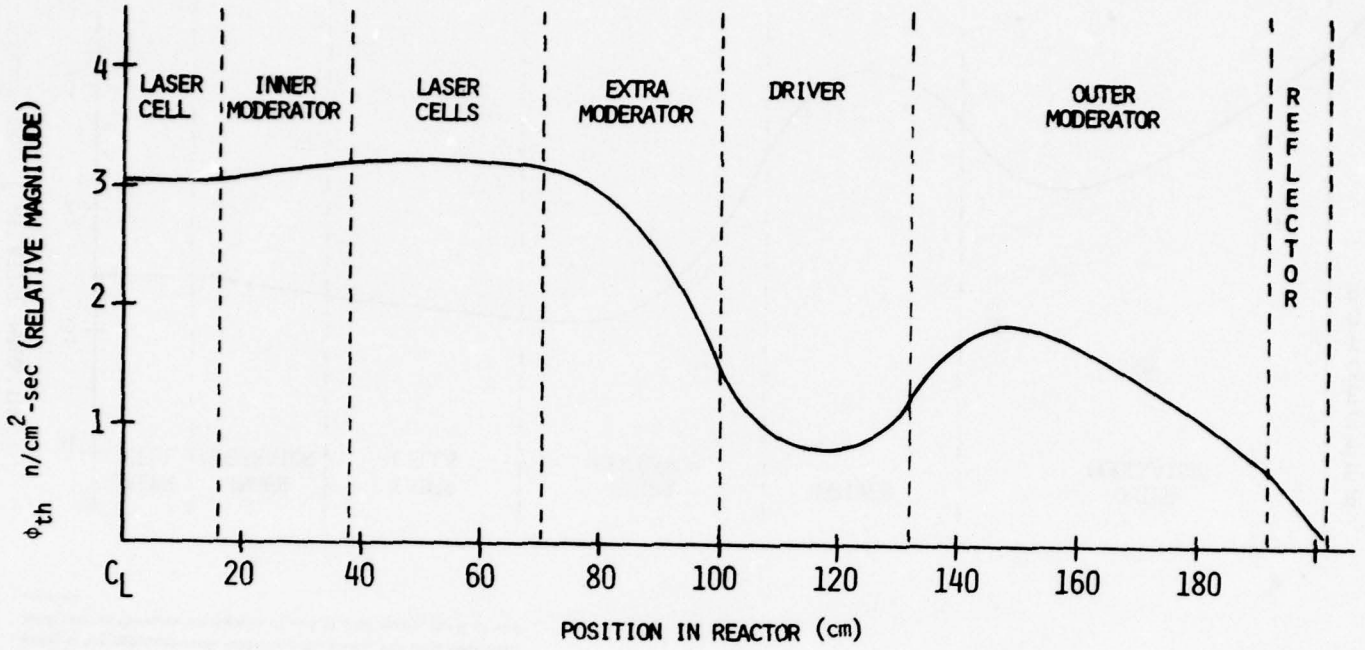

Figure 21. 13-celled reactor thermal flux shape: optimum moderator dimensions.

A summary of the 13-celled reactor chosen as best is given in Table 5. In section 6, the density required in the driver for the desired value of keff is given, as well as the effects of increasing the laser cell density.

6. FUEL DENSITY VARIATIONS IN LASER CELLS

Earlier it was explained about the importance of determining what uranium density can be used in a laser cell before light can no longer escape or is severely degraded. This determination also has an important bearing on fission density. Too low a density requirement negates the advantage of using uranium as an excimer metal, that being the laser pumping source via fissions. The results presented in the previous section were based upon a fuel density criteria, in laser cells, of 1×10^{7} atoms/b-cm. This section will investigate increasing the laser cell densities, and the subsequent decreasing of criticality driver fuel densities, maintaining a keff of 1.2 in the reactor.

As the density of the laser cells and driver cells approach equal value, the ratio of fissions in the laser cells to fissions in the total system increases. This is one measure of neutron efficiency, and related to the laser/reactor efficiency. In the results to be presented, copper was added to the driver cells at the same density as the U-235 fuel. At the value in which uranium density is equal in all fuel cells, all fuel cells are considered laser cells, irrespective of densities suitable to lasing. Densities greater than 1×10^{4} atoms/b-cm were not considered in the fuel cells, that being considered near maximum for maintaining (or confining) a plasma or vaporous state of uranium.

Figure 22 presents curves for the four reactor configurations maintained at a keff of 1.2. The 13-celled reactor and 20 percent by weight uranium A1-U driven reactor can be made critical at a laser cell density of 1×10^{7} atoms/b-cm. Discrepancies in values of keffective versus laser cell density, in this section as compared to section 5, is a result of having added copper to the driver cells (the driver cells of section 5 were pure U-235). As the density in the laser cells is increased, density in the driver cells correspondingly decreases. In the 7-celled reactor and A1-U driven reactors, the driver cell being affected is the center fuel cell only. In the 13-celled reactor, the driver cells include the outermost six cells only, the central cell being a laser cell. The 10 percent A1-U driven reactor and 7-celled reactor can not be made critical at a

TABLE 5. SUMMARY OF 13-CELLED REACTOR.

LASER CELLS	INNER MOD.	EXTRA MOD.	DRIVER CELLS	OUTER MOD.	REFLECTOR	KEFFECTIVE
$1x10^{-7}$ atoms (U-235 + Cu)/ b-cm 32 cm DIA (15 cm fuel radius, 1 cm BeO clad)	22 cm thick, graphite	30 cm thick, graphite	$1x10^{-4}$ atoms U-235/b-cm No added moderator/copper 32 cm DIA (same as laser cell) Six cells	60 cm thick, graphite	10 cm thick, beryllium	1.501

keffective of 1.2 with a density of 1×10^{-7} atoms/b-cm in the laser cells. At a fuel density of 1×10^{-4} atoms/b-cm in the driver cell, the 10 percent A1-U driven reactor requires a laser cell density of approximately 2.4×10^{-6} atoms/b-cm, and the 7-celled reactor requires a laser cell density of approximately 9.0×10^{-6} atoms/b-cm. Also shown on *Figure 22* is the density at which all fuel cells have the same density of uranium, and, therefore, all become laser cells. The 20 percent A1-U driven reactor has the lowest density, 2.05×10^{-6} atoms/b-cm, followed by the 10 percent A1-U driven reactor, $5.35\ 10^{-6}$, the 13-celled reactor, 8.2×10^{-6}, and the highest density is required by the 7-celled reactor, 1.25×10^{-5} atoms/b-cm (1.25×10^{19}) atoms/cm^3).

Figure 23 presents the results of the ratio of fission source in the laser cells to fission source in the total system as the laser cell fuel density increases. The abrupt jump to maximum ratios is a result of not considering all fuel cells

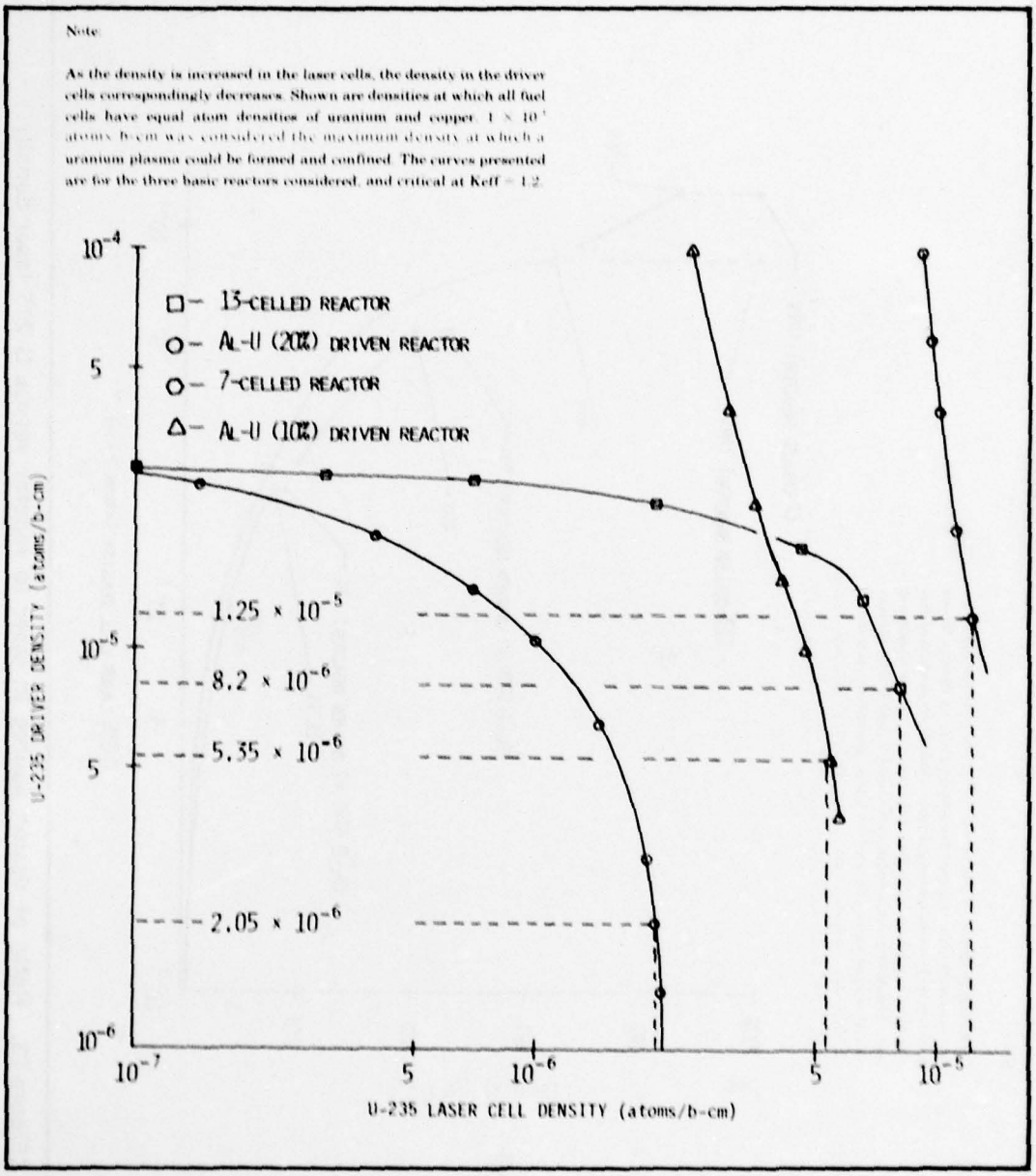

Figure 22. U-235 density in driver versus laser at keff = 1.2.

Note:

The number of fissions per sec per cm³ in the laser cells over that in the total reactor are plotted against the laser cells uranium density. Where the curves make an abrupt vertical jump is the density at which all fuel cells have equal atom densities, and, therefore, can be considered lasers. THe Al-U driven reactors cannot reach a ratio of 100% because the fuel plating cannot be used as lasers. Depending upon which uranium density laser light can be extracted, there are clear choices on reactor configurations.

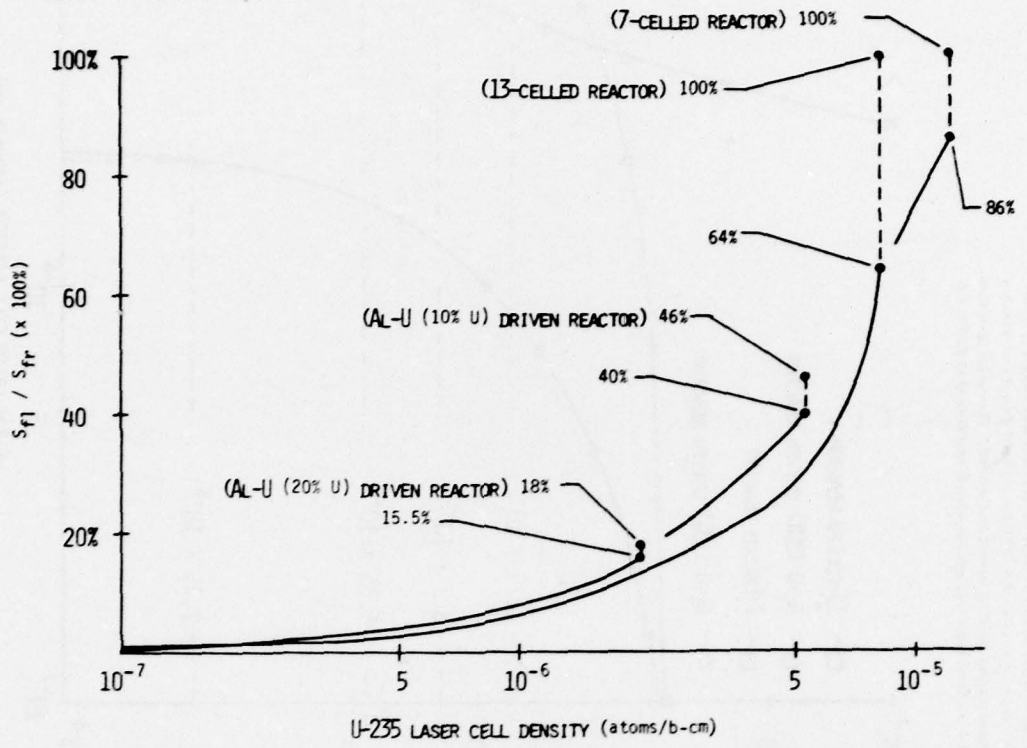

Figure 23. Ratio of fission source in laser to reactor versus U-235 laser density.

as laser cells until all cells have equal fuel densities. Both the 13-celled and 7-celled reactor achieve ratios of 1.0 because all fissioning fuel is in a laser cell at that density. The 13-celled reactor reaches a ratio of 1.0 at a lower density than the 7-celled reactor due to the greater amount of fuel contained with the additional six fuel cells. Although the A1-U driven reactors have a lower fuel density when all cells have equal density (*Figure 22*), the solid fuel driven reactors can not achieve a fission source ratio of 1.0. The A1-U plates can not be used as laser cells. The 20 percent A1-U driven reactor achieves a maximum ratio of 0.18, and the 10 percent reactor reaches 0.46.

Time did not permit a reexamination of optimum moderator dimensions at the higher laser cell densities. *Figures 24* through *26* present thermal neutron flux shapes across the reactors of previously determined dimensions at the fuel densities in which all fuel cells are laser cells. The figures indicate that some adjustment of moderator thicknesses would be required in order to maintain a high and uniform thermal flux across laser cells. Definite peaks and sharp decline of thermal flux is seen in the inner moderator of the 7-celled reactor (*Figure 24*) and 13-celled reactor (*Figure 26*). The 13-celled reactor exhibits poor flux shape in the outermost laser cells, indicating some internal reflection may be in order. Most uniform thermal flux shapes across laser cells occur in the A1-U driven reactors (*Figure 25*), probably due more to the lower fuel density in the fuel cells than any design advantage. The 7-celled reactor demonstrates the most severe self-shielding in fuel cells, also having the highest fuel density of the reactors.

7. CONCLUSIONS—SUMMARY OF REACTOR DESIGN

If experiment determines that uranium number density must be low to be compatible with lasing, solid fuel criticality drivers will have to be employed. These fuel elements should be positioned around the outside of the laser cells to yield uniform thermal neutron flux shapes in the laser cells. Poor use of fission population will result with this design, however. The 13-celled reactor could be used at extremely low densities, but has an even lower fission-use efficiency than solid fuel criticality driven reactors. At laser cell number densities of U-235 less than 1×10^{6} atoms/b-cm, a solid fuel driven reactor, having a fuel loading equivalent to 20 percent by weight uranium A1-U plating, would be best. At number densities between 1×10^{6} and 5×10^{6} atoms/b-cm, a solid fuel driven reactor with an equivalent fuel loading as the 10 percent case is optimum.

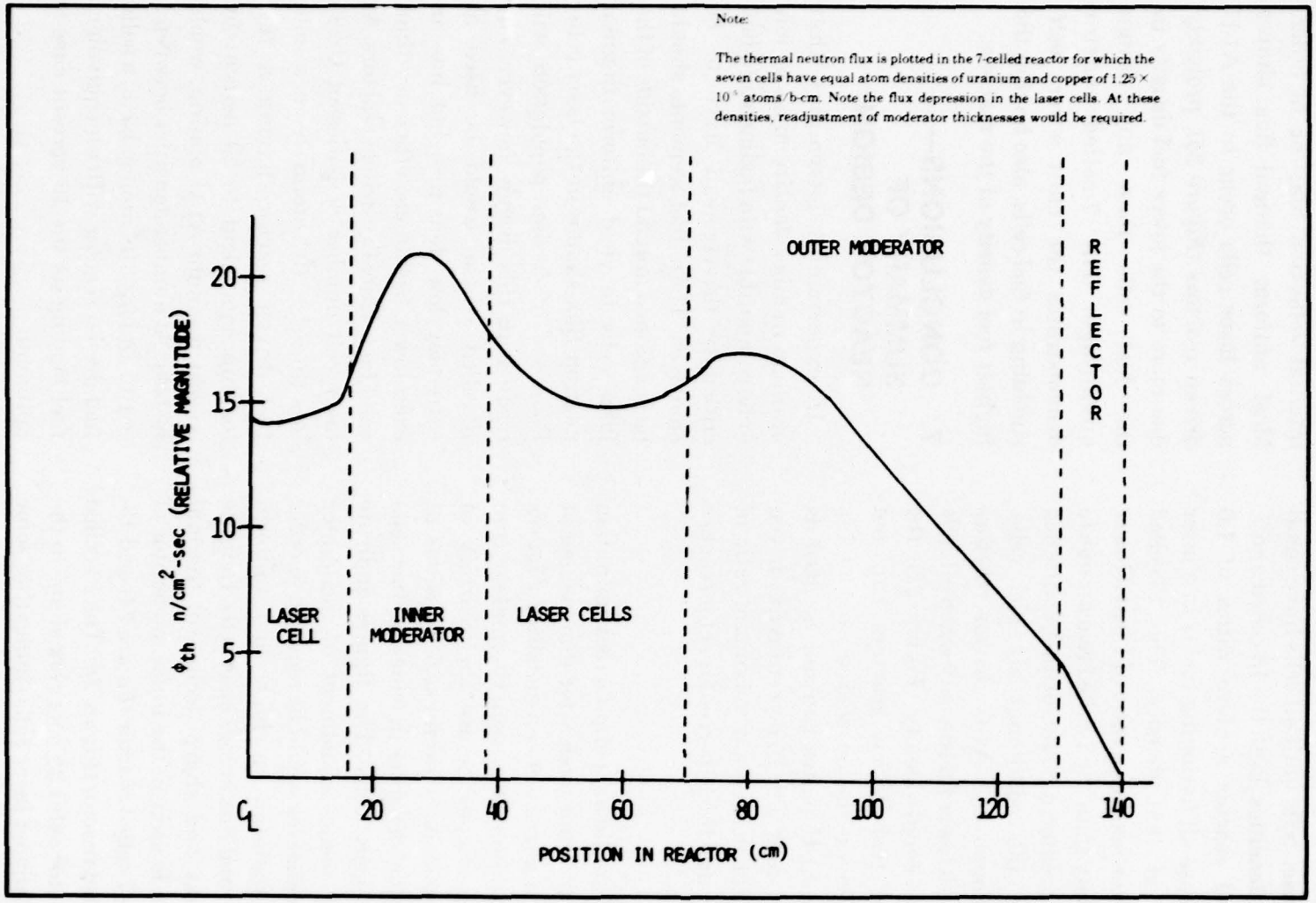

Figure 24. Thermal flux across 7-celled reactor: laser cells at same density.

Note:

As in figure 24, readjustment of moderator thicknesses would be required in the Al-U driven reactor in which all fuel cells have equal atom densities of uranium and copper of 5.35×10^{-4} atoms/b-cm. The density is still fairly low; thus no flux depression is evident.

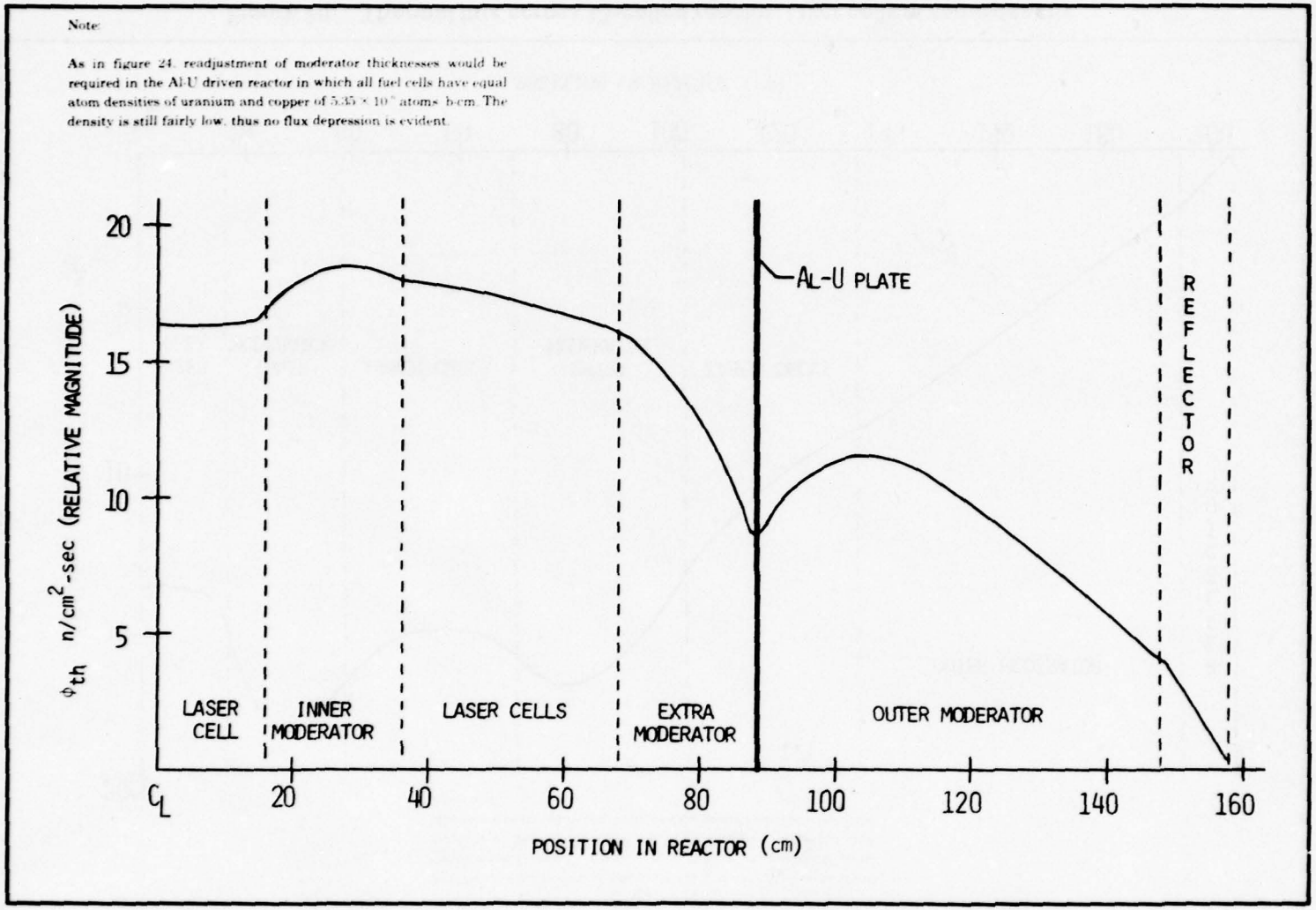

Figure 25. Thermal flux across A1-U driven reactor: laser cells at same density.

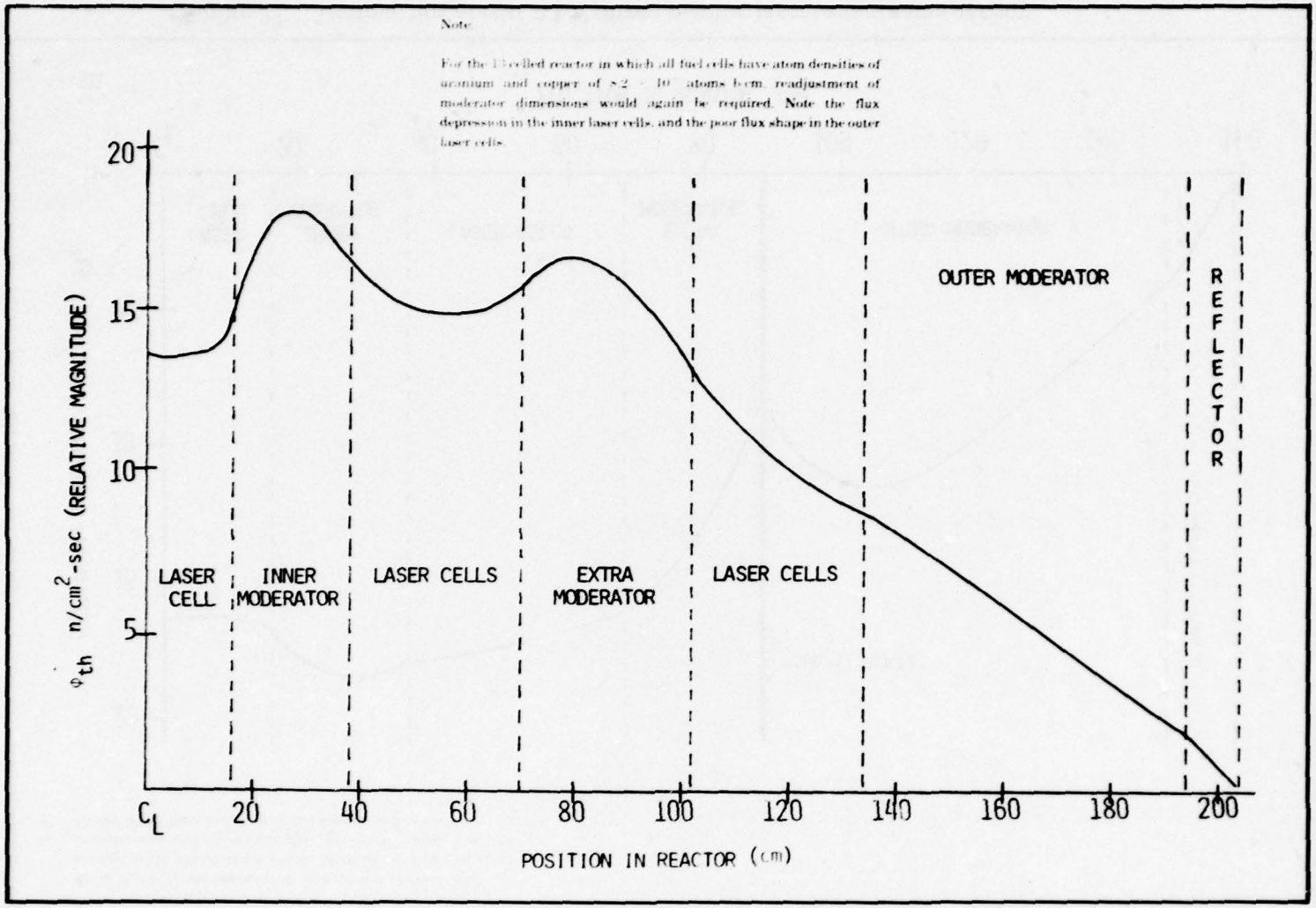

Figure 26. Thermal flux across 13-celled reactor: laser cells at same density.

The 13-celled reactor yields the highest fission-use efficiencies at laser cell number densities between 5×10^6 and 1.2×10^5 atoms/b-cm (with corresponding driver cell density depicted in *Figure 22*). At number densities greater than 1.2×10^5 atoms/b-cm, either the 13-celled or 7-celled reactor design can be utilized, both having a fission use efficiency of 100 percent. The 13-celled reactor offers more laser cells and, therefore, more laser power; the 7-celled reactor offers smaller dimensions, less weight, less complexity. The 10 percent Al-U driven reactor is optimum at number densities just over 1×10^6 atoms/b-cm, but the 13-celled reactor offers the advantage of lower number density in its driver cells as compared to the central cell of the solid fuel driven reactor. The plasma could be more easily confined, therefore, in the 13-celled reactor driver cells.

Table 6 presents a summary of the four main reactor configurations examined in this study.

8. RECOMMENDATIONS FOR FUTURE RESEARCH

Efforts to combine nuclear pumped lasers with plasma core reactors is an ambitious concept. The complexity of achieving plasma confinement is illustrated by the change of emphasis by major laboratories to UF_6 fueled reactors. The success of a uranium-excimer nuclear laser depends in large part on the success of confining a vapor dense enough to warrant the use of uranium as an excimer metal.

At present, it is not known if uranium will form an excimer with another metal. With regards to future research on laser characteristics, the following broad recommendations are made:

- Metal excimers (Tl-Hg, Tl-Zn, etc.) have not yet been made to lase. Proof of achieving sufficient gain to lase should be accomplished.

- Densities of uranium conducive to lasing must be determined. Possible forms of uranium fuel must be investigated, such as the use of uranium nitride (UN), which dissociates at lower temperatures than pure U-metal, yielding free U-metal and N_2[35].

- Attempts to form uranium excimers should be made. With its electronic configuration, uranium may or may not form an excimer with Hg, Zn, or Cd. With its outer $7s^2$ subshell, uranium slightly resembles the above metals, and may form excimers with Tl or In instead. A different metal from those mentioned in this study may

TABLE 6. REACTOR CONFIGURATIONS SUMMARY.

REACTOR	LASER FUEL DENSITY RANGE (atoms/b-cm)	ADVANTAGES	DISADVANTAGES
7-CELLED	$\geq 1.25 \times 10^{-5}$	Simplist design. Smallest reactor. High fission use efficiency.	Cannot be critical with a U-235 density of 1×10^{-7} in laser cells.
10% Al-U	$1 \times 10^{-6} < \text{U-235} < 5 \times 10^{-6}$	Uniform thermal neutron flux shapes.	Requires extra coolant loops. Requires refueling of Al-U plating. Low fission use efficiency. Cannot be critical with a U-235 density of 1×10^{-7} in laser cells.
20% Al-U	$< 1 \times 10^{-6}$	Most uniform thermal neutron flux shapes. Low density in central driver.	Requires extra coolant loops. Requires refueling of Al-U plating. Lowest fission use efficiency.
13-CELLED	$< 1 \times 10^{-6}$	Uniform fuel cells. Largest number of laser cells. High fission use efficiency. Low density in driver cells.	Poor thermal neutron flux shape in outer laser cells. Largest reactor size.

prove successful (witness the metal excimer Cd-Hg).

- This nuclear study, as an initial attempt, was very general and somewhat simplistic. More refined calculations should be made with more suitable cross-sections, especially including upscatter, and with a two-dimensional neutron transport code. Detailed modeling, for the effects on nuclear considerations, should be made of heat exchangers, fuel injection ports, fuel recirculation loops, pumps, pressure shells, coolant systems, and resonant cavity materials. More realistic reactor lengths (500 cm in this study) should be determined.

No pressure or temperature corrections to cross-sections in fuel and moderator were included in this study. High pressures and temperatures are to be encountered, and quantitive results presented here may be far from realistic. Qualitative results and trends, however, may assist in providing guidelines for future calculations.

APPENDIX A
SINGLE CAVITY ANNULAR REACTOR

APPENDIX A
SINGLE CAVITY ANNULAR REACTOR

An early reactor configuration considered in this study was one proposed by Miller in his patent application [14]. It consists of a large single cavity in the shape of an annulus, shown in *Figure A1*, with moderator at the core and reflector (moderator) blanketing it. A variation of this configuration employed a thin Be shell surrounding the fuel cavity, shown in *Figure A2*. Although this reactor could not be made critical except at high U-235 densities, it provided design data on optimal moderator and reflector thicknesses, materials, and cavity dimensions.

Initial investigations at a U-235 density of 1×10^{-7} atoms/b-cm proved this too low a density to obtain meaningful results. *Figure A3* depicts how keff varies as the fuel cavity thickness increases for different U-235 densities. At a density of 6×10^{-6} atoms U-235/b-cm, the reactor is still far from critical. In addition, upon re-examination of *Figure A3*, there appeared to be an optimum thickness of fuel zone, and the higher the density of U-235, the smaller was this optimum thickness. This effect was attributed to self-shielding of neutrons by the fuel. *Figure A4* shows a plot of neutron flux vs. energy group for a point in the center of the fuel cavity (energy intervals of the 14 groups are given in *Table 2* of the main text). The flux is shown for two densities, and both exhibit peaks in the epithermal energy region, at about 3.3 keV, substantiating the possibility of resonance absorption self-shielding in the fuel. In an attempt to correct the self-shielding effects, increasing moderation by increasing the central moderator size was investigated. As shown in *Figure A5*, a larger central moderator did decrease the epithermal peak and increase the thermal peak, but the result was not great enough to remove the reactor from an epithermal spectrum. Increasing the reactor length from 500 cm to 1000 cm increased the keff of the reactor, but did not change the self-shielding effect, as can be seen in *Figure A6*. *Figures A3* through *A6* are results for a U-235 density of 3×10^{-6} atoms/b-cm, unless otherwise noted, and with graphite as a central moderator. Replacing the graphite with beryllium increased the fuel thickness at which self-shielding first becomes evident. From *Figure A3*, the optimum fuel thickness at a U-235 density of 3×10^{-6} and carbon core was approximately 60 cm, whereas it was about 75 cm for an inner moderator of beryllium, as shown in *Figure A7*.

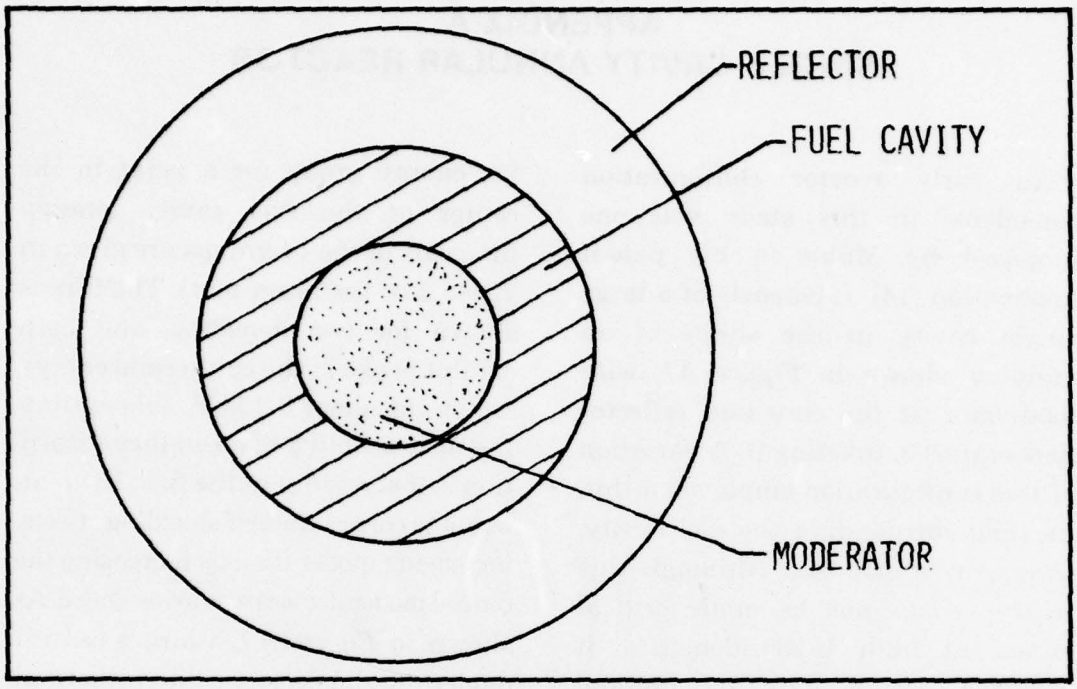

Figure A1. Single cavity annular reactor.

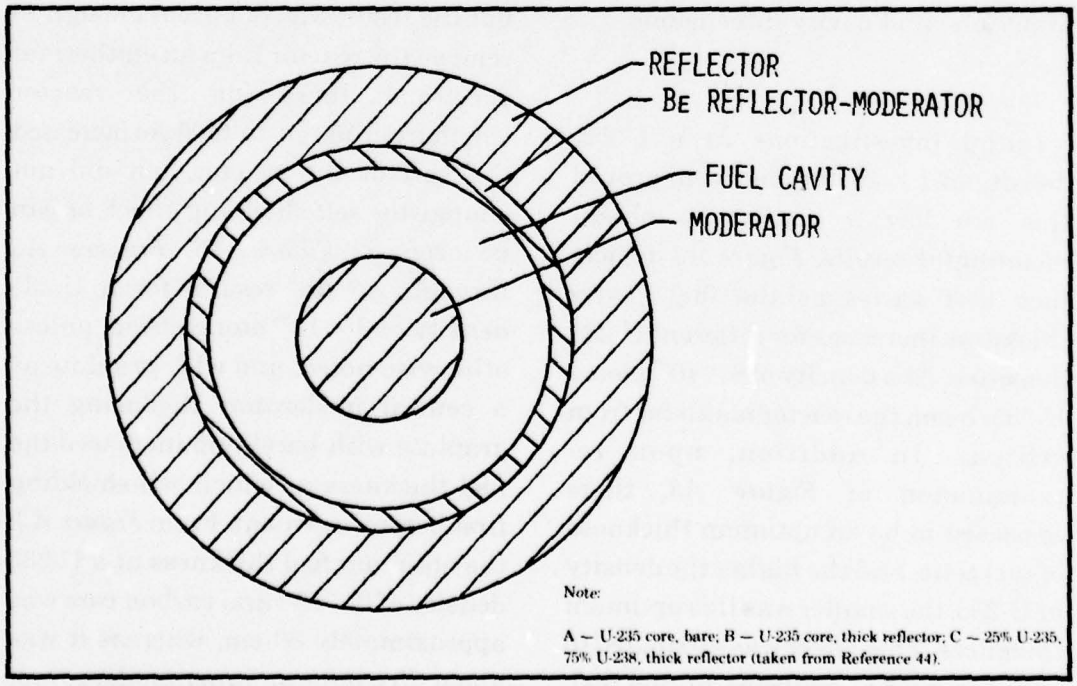

Figure A2. Annular reactor with inner Be shell.

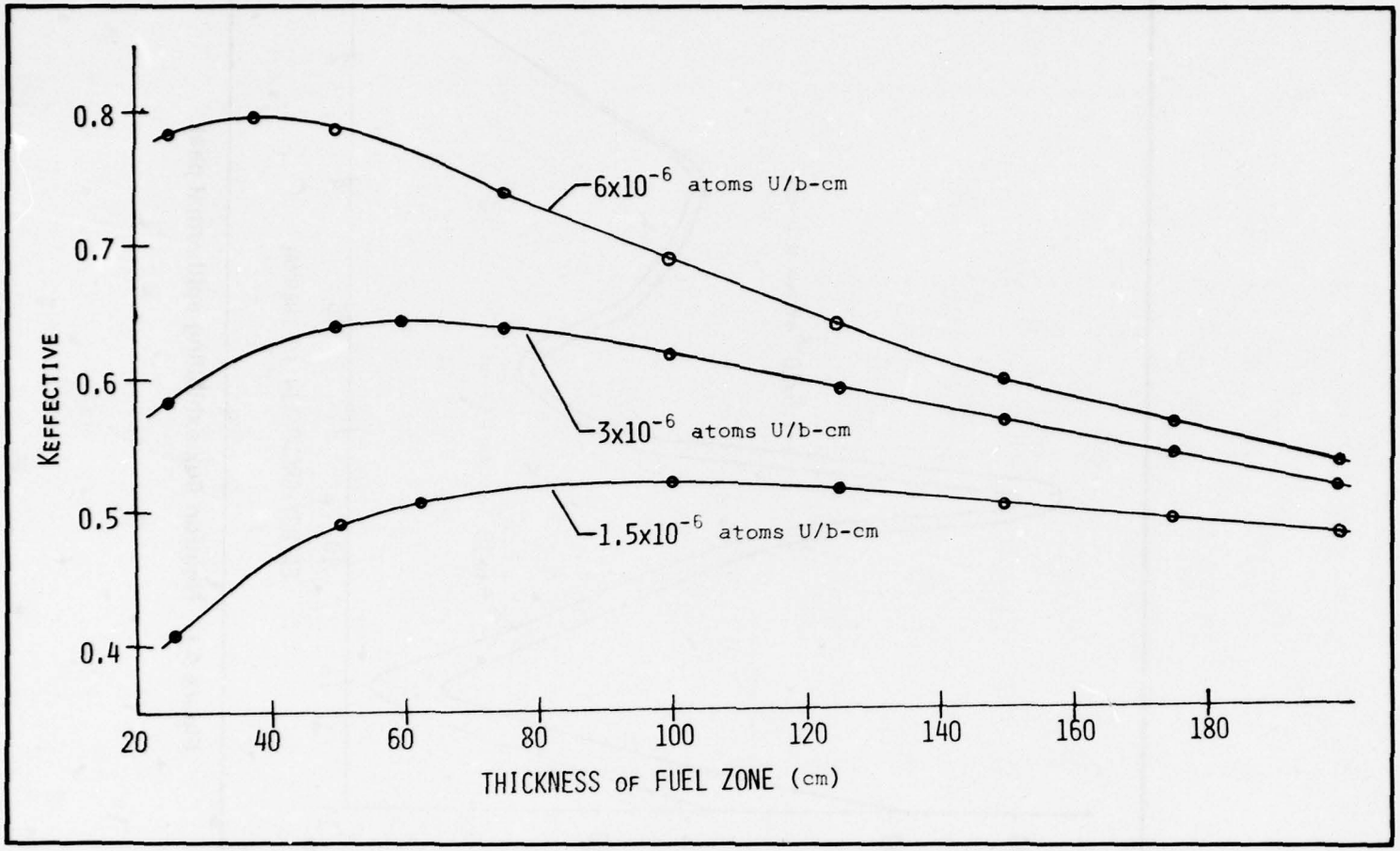

Figure A3. Self-shielding at different densities.

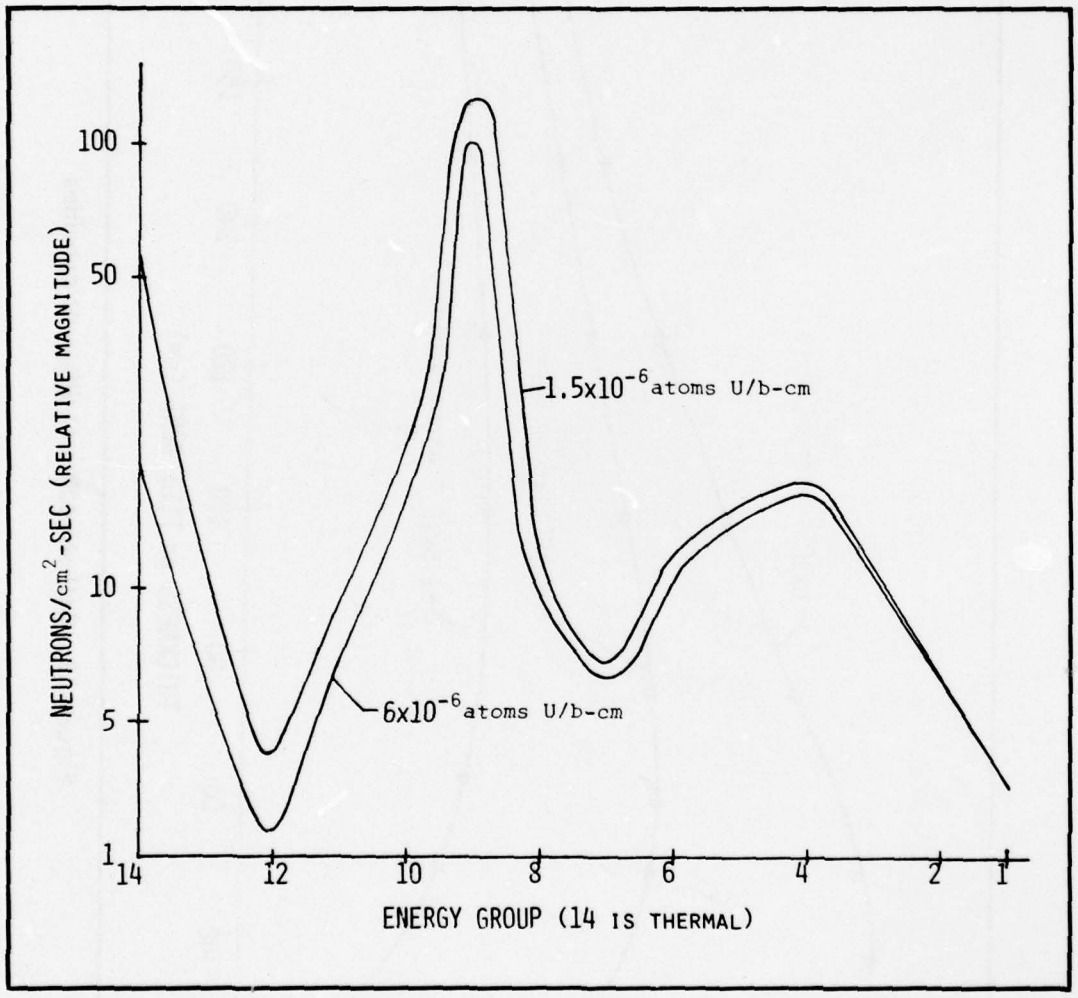

Figure A4. Neutron flux exhibiting epithermal peak.

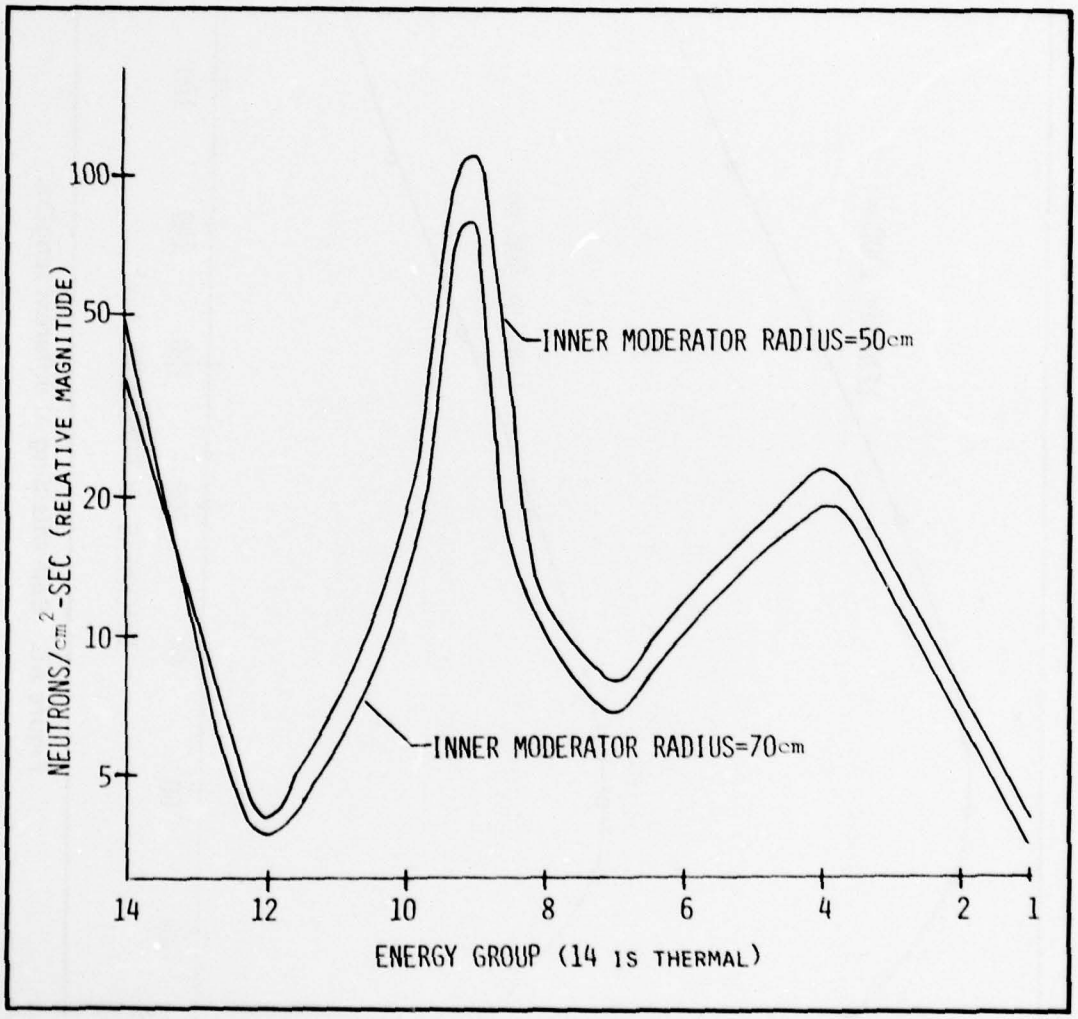

Figure A5. Epithermal flux for different moderator thicknesses.

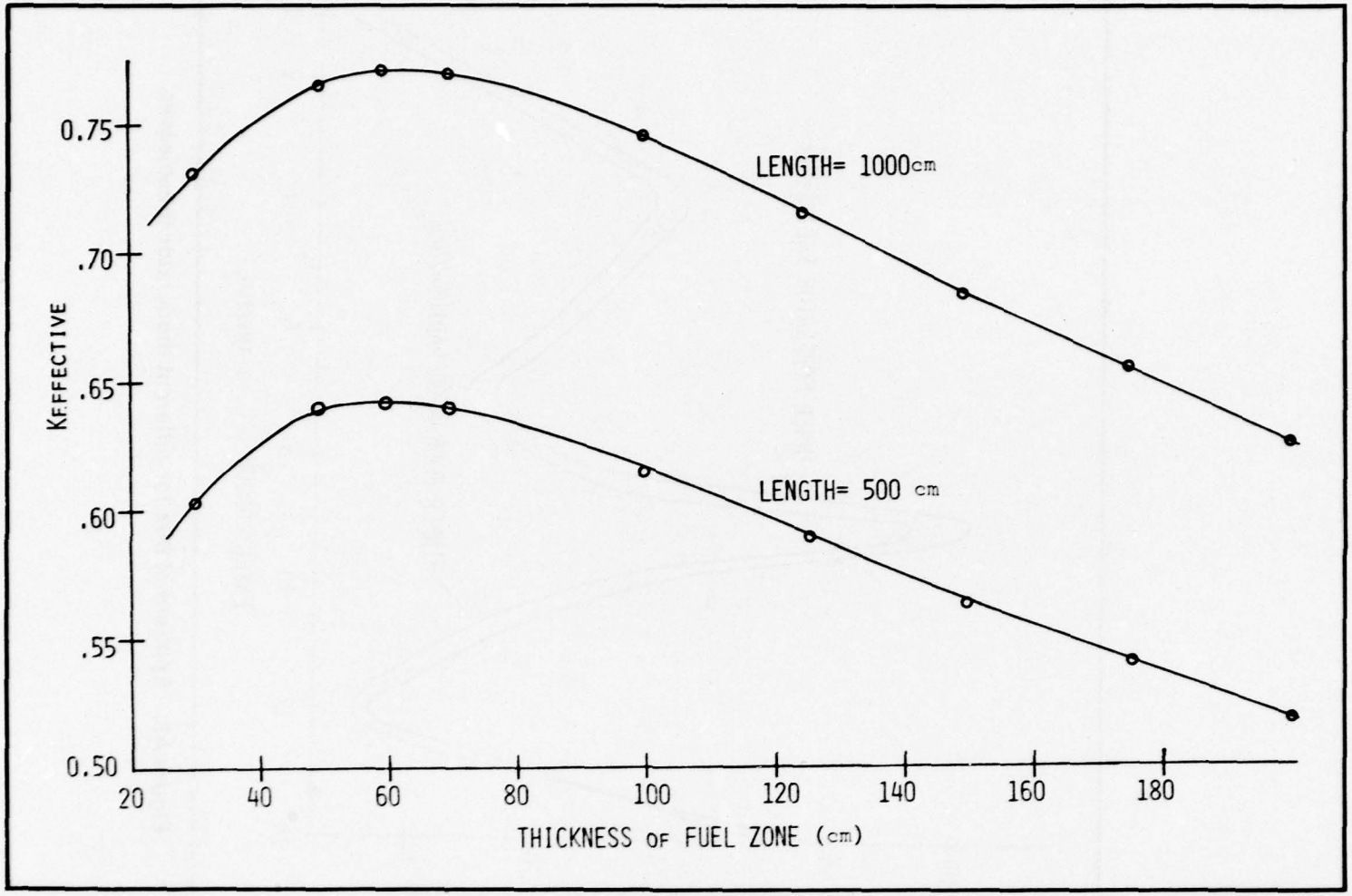

Figure A6. Self-shielding at different lengths.

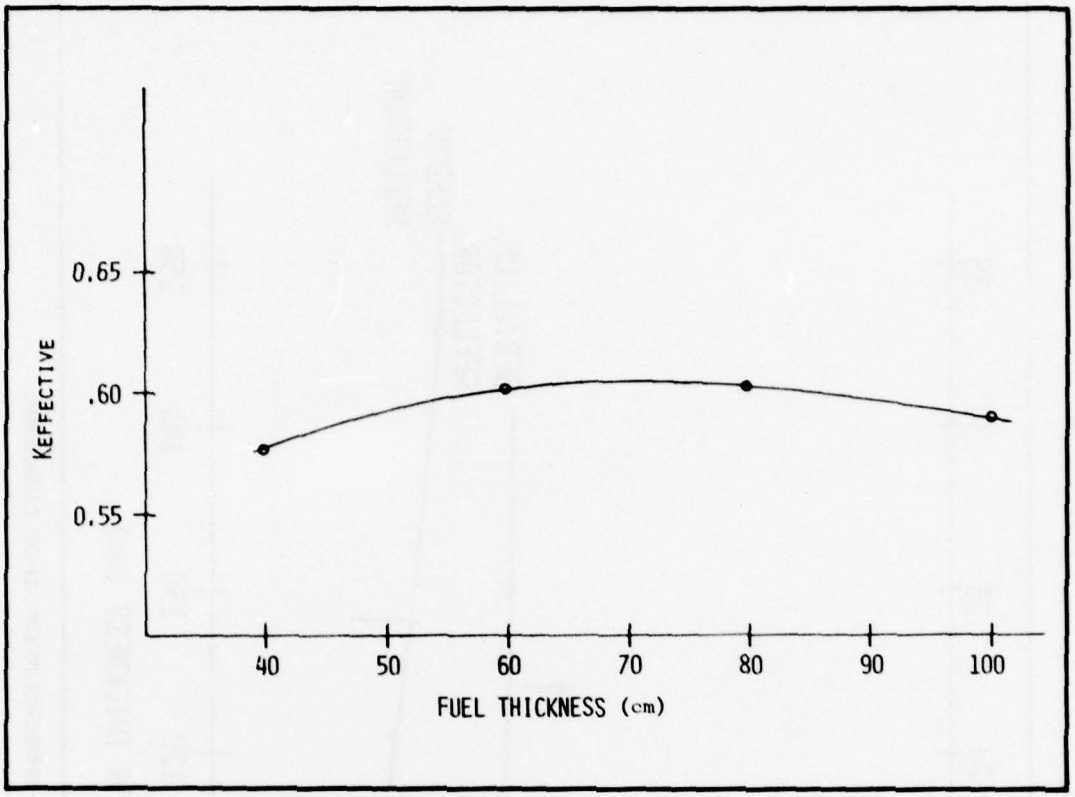

Figure A7. Self-shielding evident with beryllium as inner moderator and added shell.

Figure A8 depicts the effect of *increasing reflector thickness for* carbon and beryllium. Optimum thickness for carbon appears to be 100 cm or more, while that for the beryllium shell (with carbon on the outside) is about 10 cm. A beryllium shell inside the carbon reflector yields slightly higher results for keff, as can be seen in *Figure A9*. *Figure A10* depicts the results of increasing central moderator size, with and without a Be shell added. *Optimum inner moderator* thickness is approximately a 65 cm radius.

Because of self-shielding effects, the epithermal flux spectrum, and the difficulty of achieving criticality with this design, the single cavity annular reactor configuration was deemed inappropriate for a laser housing. Basic design data on reflector and moderator thicknesses was extracted, however, to lend a base to the three configurations discussed in the main text.

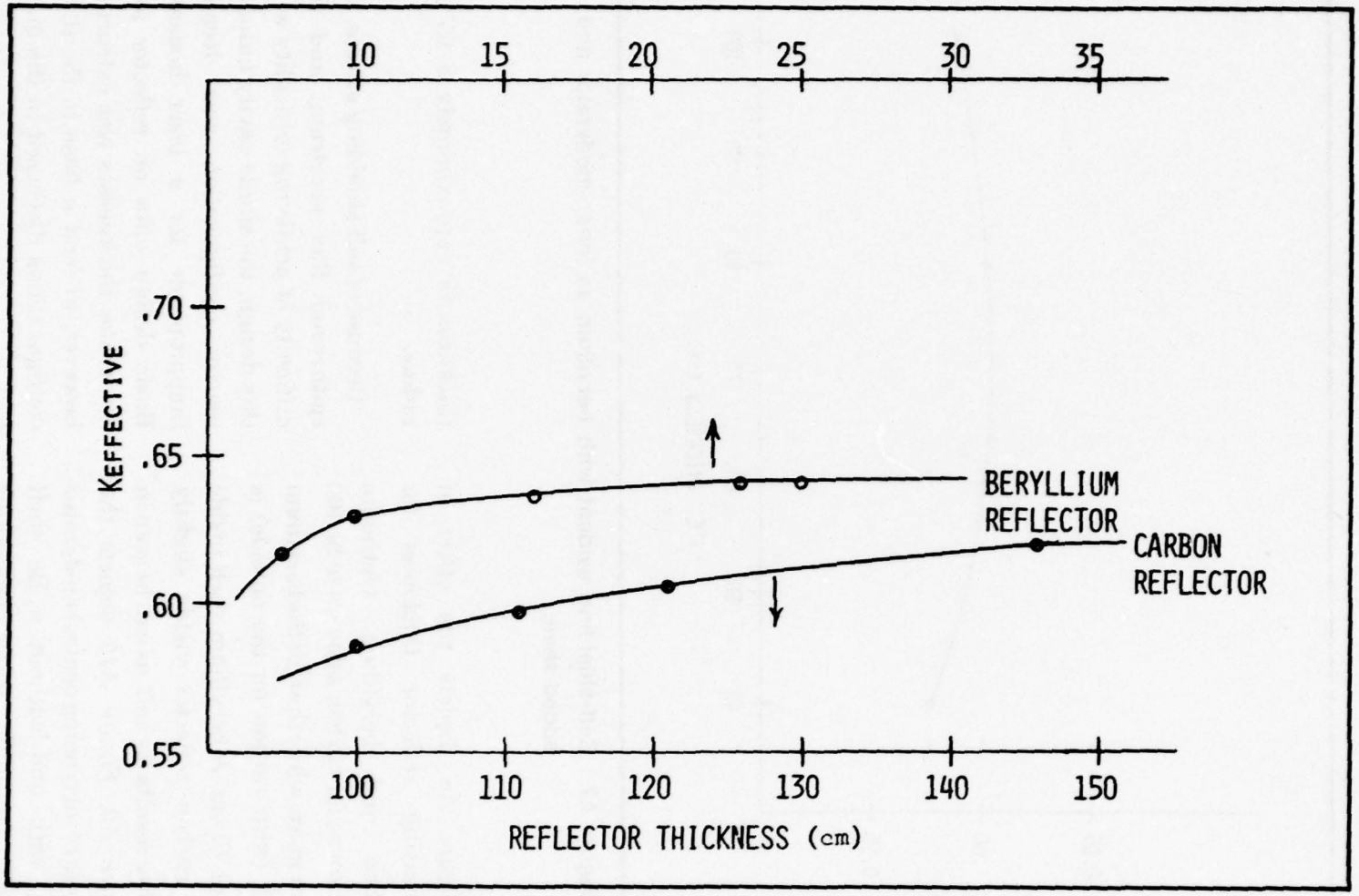

Figure A8. Effect of reflector material on criticality.

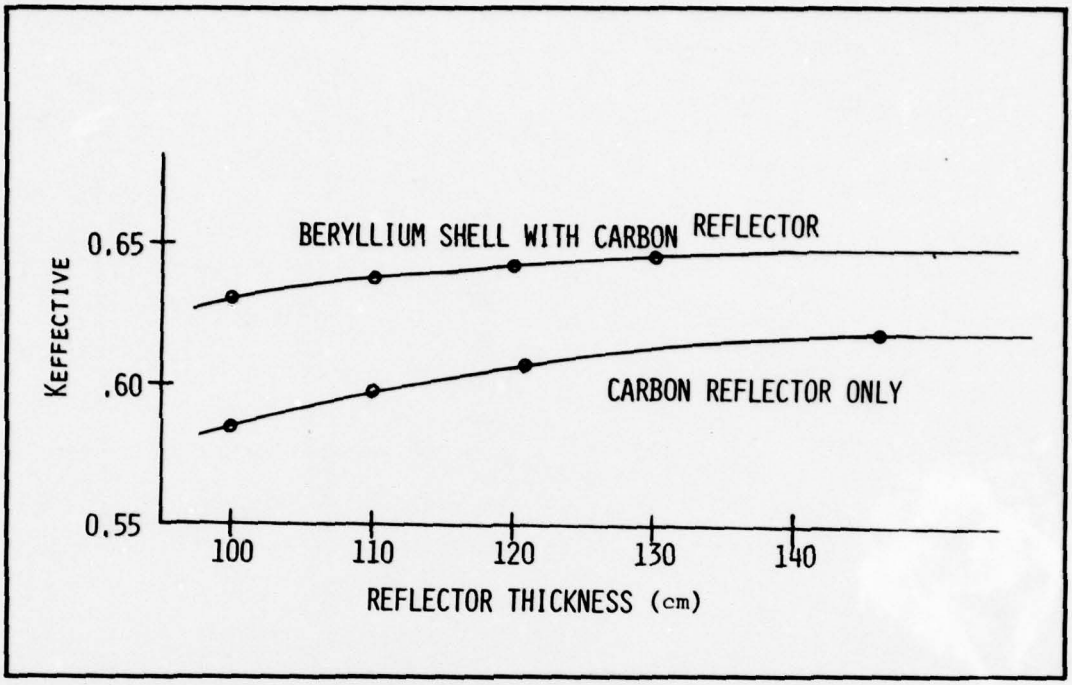

Figure A9. Improvement on criticality with beryllium shell.

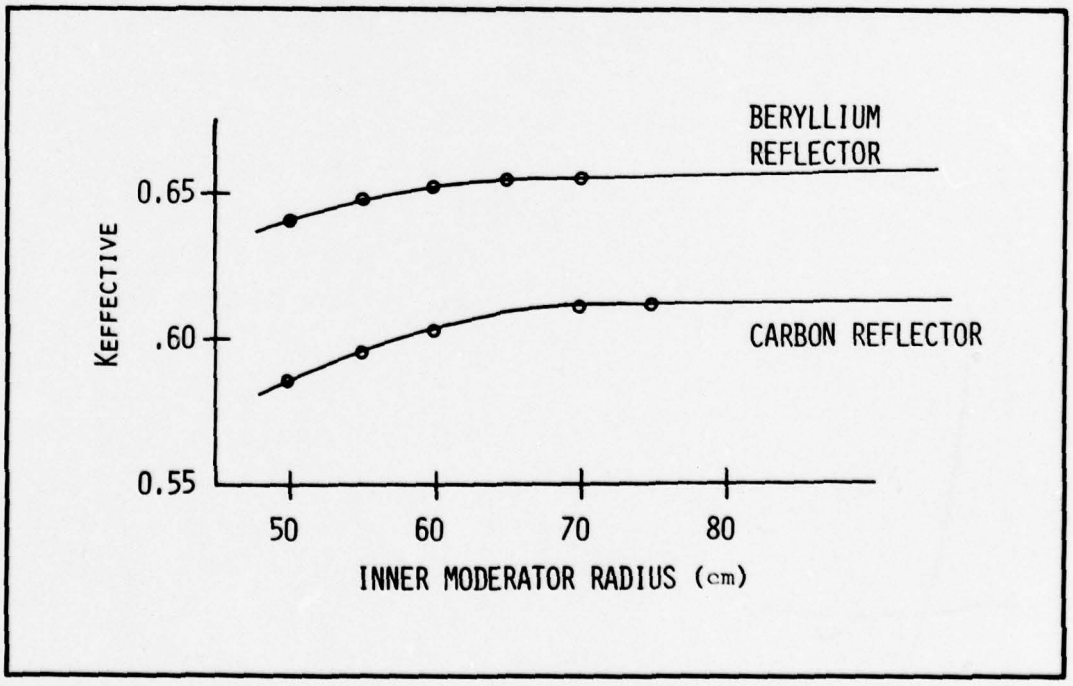

Figure A10. Effect of moderator thickness on criticality.

APPENDIX B
SINGLE CAVITY FAST REACTOR

APPENDIX B
SINGLE CAVITY FAST REACTOR

An early reactor configuration considered in this study was a single cavity reactor with reflector surrounding the outside, as shown in *Figure B1*. The neutron flux spectrum of such a reactor would be fast. A fast reactor is one in which there is very little moderator present to degrade the neutron spectrum to low energies. The single cavity reactor would be such a system in the absence of a central core of moderator. ANISN was not used to analyze this configuration.

A simple method to approach critical size calculations for a fast reactor is outlined by Glasstone and Sesonske. [46] The most satisfactory treatment of fast reactors is by multigroup methods, with neutron transport theory applied, because the neutron spectrum varies considerably with core composition, and cross-sections are highly dependent on neutron energy at high energies. *Figure B2* depicts typical neutron fluxes in a fast reactor. [46] Note the absence of a thermal neutron spectrum, due to the absence of neutron moderation.

The following treatment assumes a non-multiplying, "thick" reflector, and that, for a single neutron group, an asymptotic solution of the integral form of transport theory is given by*

$$\Psi B = \nu\Sigma_f \Psi \tan^{-1}(B/\Sigma_{tr}). \qquad (1)$$

It is assumed the spatial flux, $\phi(r)$, can be expressed as $\Psi F(r)$, where $F(r)$ is a factor dependent on position in the reactor only, and is the same for all neutron energies (this implies the neutron energy spectrum is the same at all positions in the core, not rigorously true near boundaries).

When extended to a multigroup treatment, the group fluxes (n groups) are given by,

$$\phi_1(r) = \Psi_1 F(r),$$

$$\phi_2(r) = \Psi_2 F(r),$$

$$\ldots \phi_n(r) = \Psi_n F(r),$$

and (1) becomes,

$$\Psi_g B = (\text{neutrons entering gth group}) \cdot \tan^{-1}(B/\Sigma^g_{tr})$$

or,

$$\Psi_g B = \left[\sum_{i=1}^{g} \Sigma_{ig}\Psi_i + \chi_g \sum_{g=1}^{n} (\nu\Sigma_f)_g \Psi_g\right] \cdot \tan^{-1}(B/\Sigma^g_{tr}), \qquad (2)$$

*Definition of symbols are given in *Table B-1*.

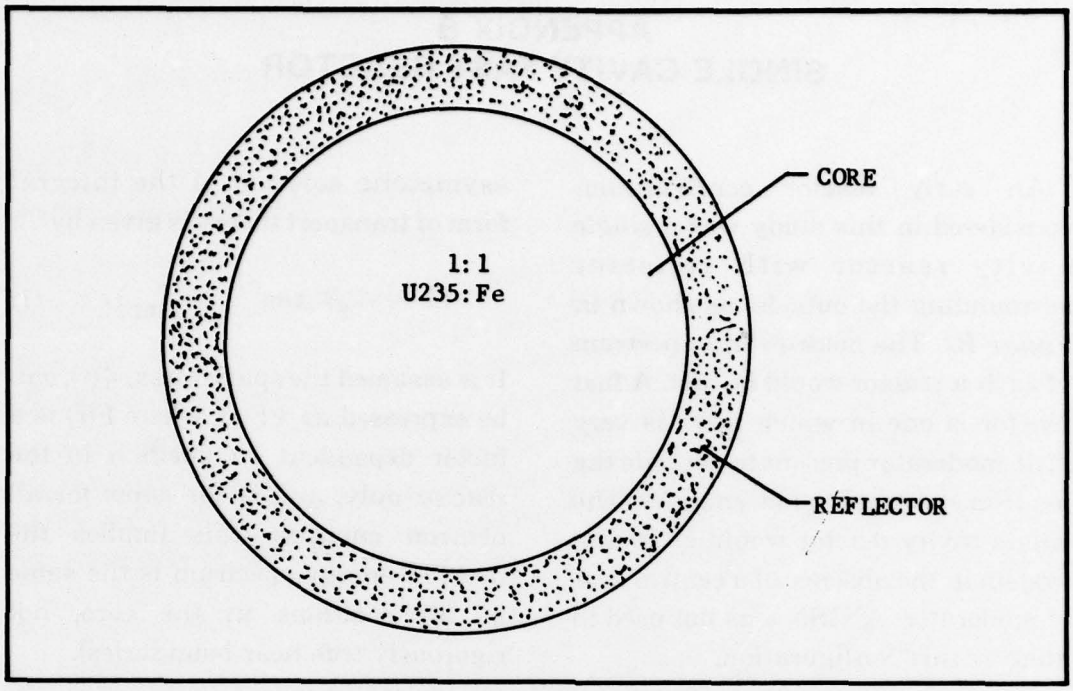

Figure B1. Single cavity reactor.

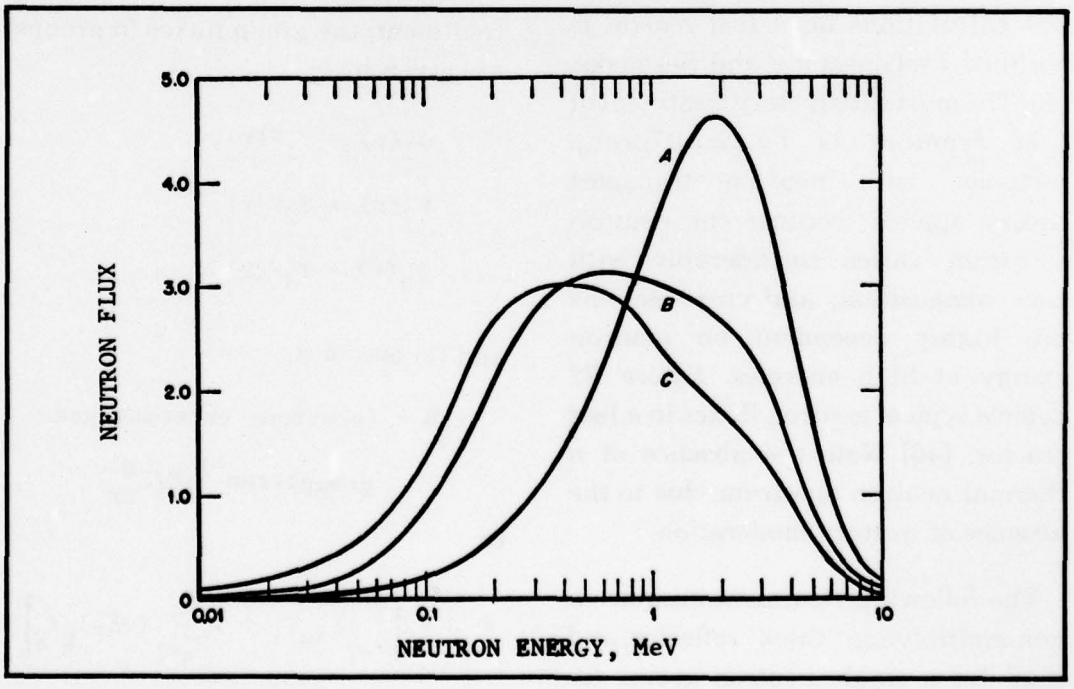

Figure B2. Fast-neutron spectra in three systems.

TABLE B1. DEFINITION OF SYMBOLS

B – buckling *	D_r – diffusion coefficient in the reflector
ν – the number neutrons liberated for every neutron absorbed in fission	L_r – thermal diffusion length in the reflector
Σ_f – macroscopic fission cross section	$N_{D,U}$ – number density of uranium (atoms/cm^3)
Σ_{tr} – macroscopic transport cross section	$N_{D,Fe}$ – number density of iron
Σ_a – macroscopic absorption cross section	σ_{tr} – microscopic transport cross section ($\Sigma = N\Sigma$)
Σ_{ig} – macroscopic cross section for scattering from the ith group to g	χ_g – fraction of neutrons appearing with energy of group g from all neutrons produced by fissions
R – radius of the core	$\phi(r)$ – neutron flux distribution in the core separated from boundaries
L – length of the core	ψ – magnitude of the neutron flux
δ – reflector savings	
D_C – diffusion coefficient in the core	

*See Appendix C for definition of nuclear terms

where χ_g is the fraction of neutrons appearing in group g from all neutrons produced by fissions ($\nu\Sigma_f\Psi$), and $\Sigma_{ig}\Psi_i$ is the neutron source from scattering in the ith group into group g.

It is customary to normalize the fission source to 1,

$$\sum_{g=1}^{n} (\nu\Sigma_f)_g \Psi_g \equiv 1 ,$$

and scattering events that remain in group g are separated,

$$\sum_{i=1}^{g} \Sigma_{ig}\Psi_i = \sum_{i=1}^{g-1} \Sigma_{ig}\Psi_i + \Sigma_{gg}\Psi_g$$

Equation (2) can now be written as

$$\Psi_g = \frac{\left[\sum_{i=1}^{g-1} \Sigma_{ig}\Psi_i + \chi_g\right].\tan^{-1}(B/\Sigma^g_{tr})}{B - \Sigma_{gg}\tan^{-1}(B/\Sigma^g_{tr})} \qquad (3)$$

and,

$$\Sigma_{gg} = \Sigma_{total} - \Sigma_a - \Sigma_{g\to g+1} - \Sigma_{g\to g+2} - \ldots \Sigma_{g\to n} .$$

In fast reactors, $\Sigma_t \simeq \Sigma_{tr}$ because most core material has high mass (if this is not the case, substitute Σ_t for Σ_{tr} in Equations (1), (2), and (3)).

With the critical value for buckling, B, known, and if the group cross-sections are known, the Ψ_g's can be computed from Equation (3). If the reactor is critical, then, from definition,

$$\sum_{g=1}^{n} (\nu\Sigma_f)_g \Psi_g = 1 . \qquad (4)$$

If Equation (4) is greater than 1.0, the number density of fissionable fuel is too high, and if Equation (4) is less than 1.0, the number density is too low.

To determine the critical buckling, the approximation for a partially reflected cylindrical thermal reactor was used:

$$B^2 = [2.405/(R+\delta)]^2 + [\pi/L]^2 . \qquad (5)$$

Here, δ is the reflector savings, which, for a "thick" reflector is

$$\delta = (D_c/D_r)L_r$$

where D_c is the diffusion coefficient in the core, L_r is the thermal diffusion length in the reflector, and D_r is the diffusion coefficient in the reflector. Recommended value to use in the core in a multigroup treatment is the value of the group with the highest flux

(usually group 3 in this work: a ten group treatment was used, as discussed below). In the absence of like group data for a graphite reflector, epithermal values were used. From [43], $D_r = 1.016$ cm and $L_r = 51.8$ cm for graphite. Using the relation,

$$D_c = 1/3\Sigma^c_{tr}$$

$$= [3(N_{D,u}\sigma_{tr,u}+N_{D,F_e}\sigma_{tr,F_e})]^{-1}$$

and obtaining values of σ_{tr} in group 3 from *Table B1*, one obtains an expression for reflector savings:

$$\delta \simeq (17)/[(5.1)N_{D,u}+(5.5)N_{D,F_e}]$$

Once a number density is chosen, δ can be calculated; and once a radius and length are chosen, buckling can be calculated from Equation (5). This provides a rather crude estimate of the buckling, but one that is quickly and simply determined. Use of this gross estimate of buckling will at least allow qualitative results to be obtained.

Ten groups were used for the fast reactor calculations. Cross-sections, shown in *Table B2*, were obtained from [44], with data for iron being substituted for copper, and 100 percent U-235 assumed. Calculations were performed on a Hewlett-Packard 9810A programmable calculator.

The procedure used was to calculate an initial buckling for a specific reactor radius and length with Equation (5), solve Equation (3) for the group fluxes, and then perform the summation (Equation (4)). Values of Equation (4) were determined for a number of values of buckling and plotted, as shown in *Figure B3*. Using this iterative procedure, the critical buckling could be determined and used in Equation (5) to determine the critical length of the reactor. This was repeated for each U-235 number density investigated.

Figure B4 depicts the length of the reactor required for criticality vs. number density of U-235. The core radius was 50 cm. It can be seen that at the low number densities predicted necessary for the uranium-excimer system, this reactor configuration becomes an untenable size, even for this very crude treatment of the fast reactor system.

TABLE B2. TEN GROUP DATA FOR FAST REACTOR ANALYSIS.

GROUP CHARACTERISTICS

u = lethargy
E_i = energy at lower group boundary
X_i = fraction of the total neutrons originating with energy in the ith group

Group No.	1	2	3	4	5	6	7	8	9	10
u	0-1.5	1.5-2	2-3	3-4	4-5	5-6	6-7	7-11	8-16	Thermal
E_i (Mev)	2.231	1.353	0.498	0.183	0.0674	0.0248	9.12×10^{-3}	1.67×10^{-4}	1.125×10^{-6}	—
X_i	0.3266	0.227	0.303	0.107	0.0283	0.0065	0.0022	0.0	0.0	0.0

MICROSCOPIC CROSS SECTIONS (BARNS)

σtr = transport cross section
$\sigma i \to i$ = transfer cross section for scattering from any group i into the same group
$\sigma i \to i+n$ = transfer cross section for scattering from group i into a higher lethargy group, $i + n$, where n = 1, 2, etc.

Group	$\nu\sigma f$	σtr	$\sigma i \to i$	$\sigma i \to i+1$	$\sigma i \to i+2$	$\sigma i \to i+3$	$\sigma i \to i+4$
URANIUM-235							
1	3.646	4.50	1.096	0.773	0.880	0.260	0.100
2	3.290	4.52	1.474	1.173	0.350	0.100	0.050
3	3.041	5.10	3.129	0.467	0,120	0.030	0.010
4	3.338	7.50	5.699	0.199	0.035	0.015	—
5	4.079	9.50	7.391	0.0632	—	—	—
6	5.535	12.0	9.075	—	—	—	—
7	7.872	13.13	8.810	—	—	—	—
8	22.14	25.5	12.0	—	—	—	—
9	105.8	75.5	11.0	—	—	—	—
10	787.2	396.3	11.3	—	—	—	—
IRON							
1	—	2.0	0.950	0.428	0.44	0.13	0.05
2	—	2.0	1.353	0.494	0.12	0.03	—
3	—	2.4	2.186	0.170	0.03	0.01	—
4	—	3.0	2.889	0.106	—	—	—
5	—	3.0	2.886	0.106	—	—	—
6	—	3.0	2.888	0.100	—	—	—
7	—	4.0	3.850	0.133	—	—	—
8	—	7.5	7.408	0.0469	—	—	—
9	—	11.0	10.717	0.0134	—	—	—
10	—	13.0	11.300	—	—	—	—

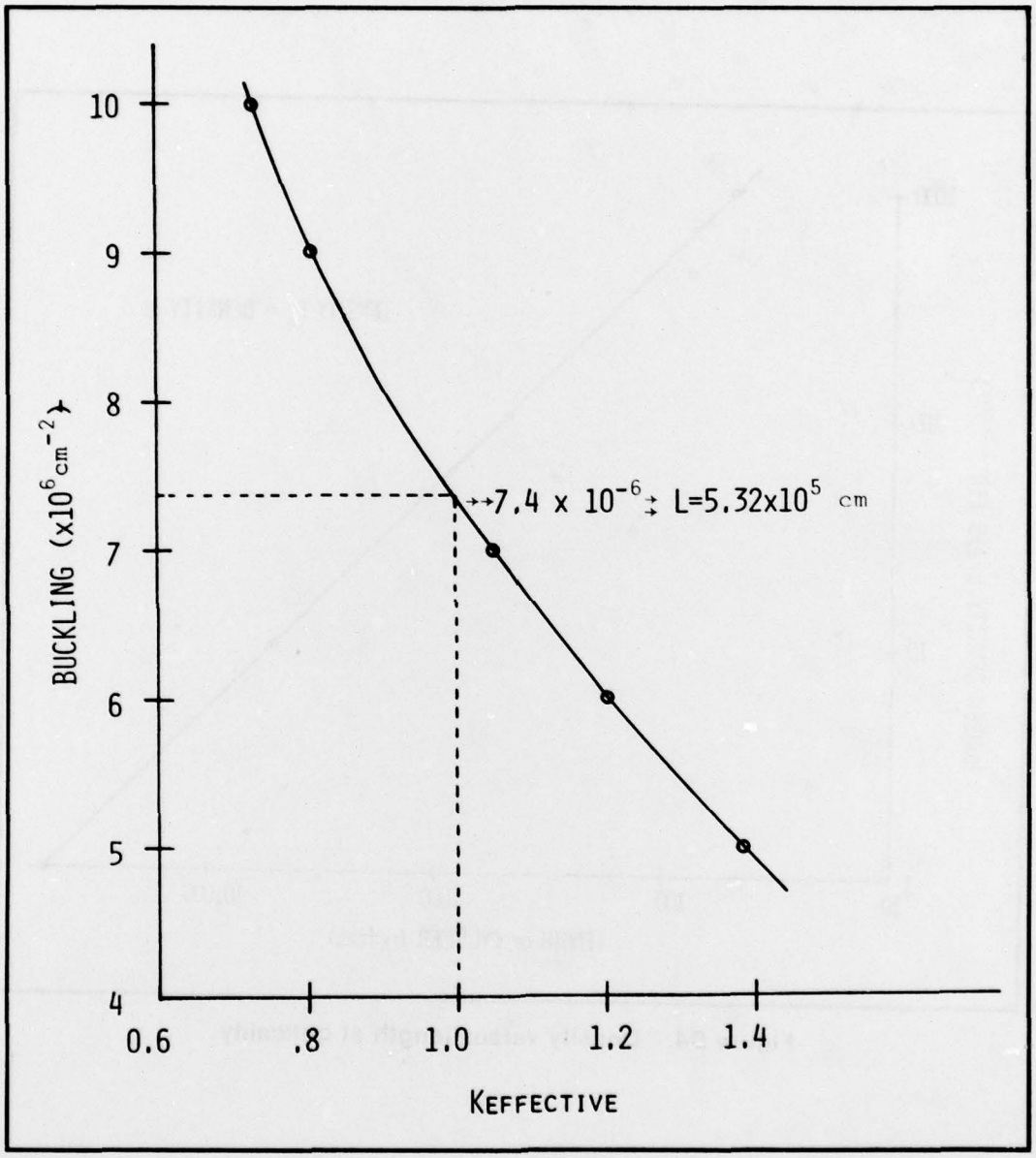

Figure B3. Buckling versus Keff at 10^{18} atoms U/cm³.

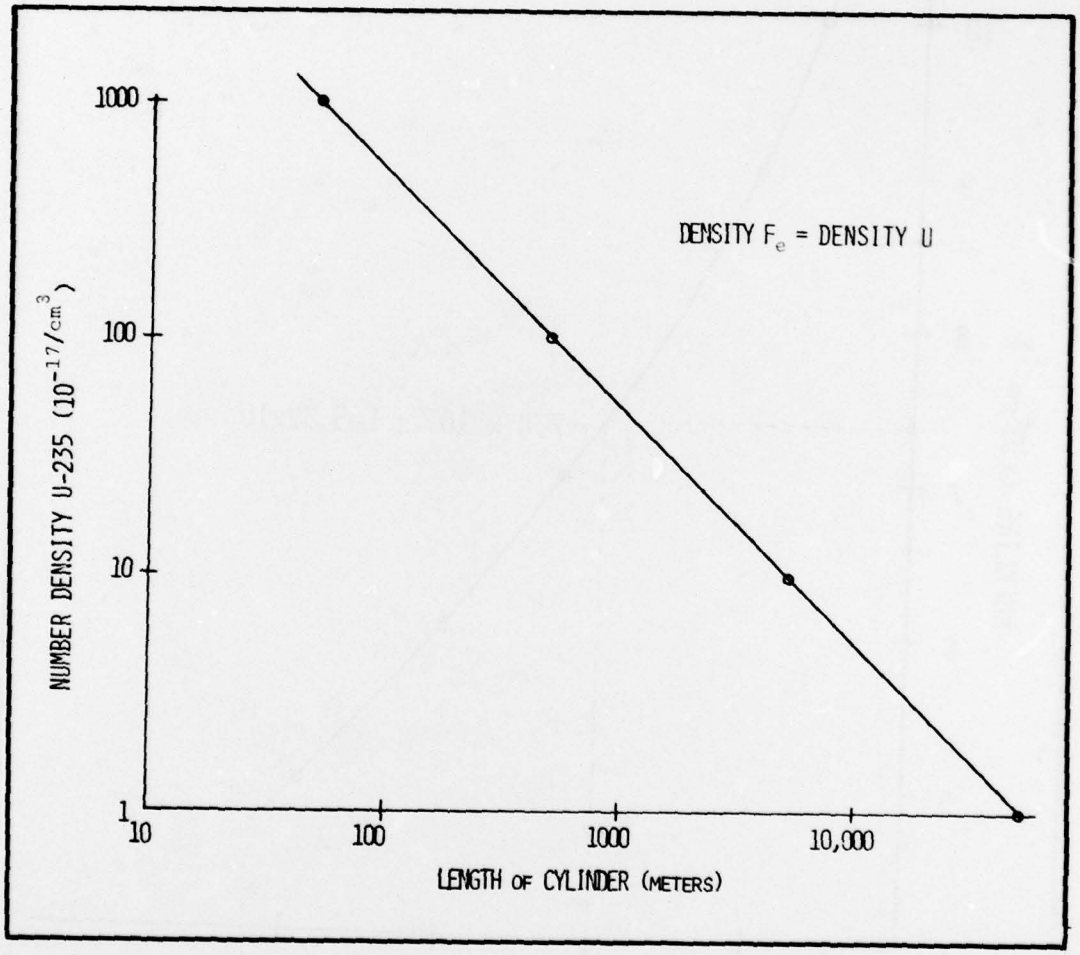

Figure B4. Density versus length at criticality.

APPENDIX C
DESCRIPTION OF NUCLEAR TERMS

APPENDIX C
DESCRIPTION OF NUCLEAR TERMS

BARN (b): $1b = 1 \times 10^{-24}\ cm^2$.

BUCKLING (B^2): In a multigroup numerical analysis of nuclear reactors, the reactor equation is represented by a series of equations of the form

$$\nabla^2\phi + B^2\phi = 0 .$$

In developing the reactor equation, various terms describing the material properties of the reactor core were grouped into B^2. This is called the material buckling, and its magnitude bears an inverse relation to the size a core must have to be critical. When the reactor equation is solved for a particular geometry, B^2 becomes an eigenvalue solution and a function only of the geometric size of the core. When the reactor is critical the harmonics die out and only the principal eigenvalue remains, called the geometric buckling. Material buckling and geometric buckling are equal when the reactor is critical. Buckling, then, is a measure of the size of a critical core. If a cylindrical geometry is being analyzed, the reactor equations can be solved with radial geometry in detail, and a buckling correction to the length of the core can be added to account for error in not considering the axial geometry.

CRITICAL: One neutron is used in the fissioning of a nucleus, with many neutrons released. If one of the released neutrons causes one other fission, a chain reaction is created and the reactor is critical. If, over an average of many fissions, there is less than one-to-one correlation the reactor is subcritical and cannot sustain a chain reaction at that power level. If there is greater than a one-to-one correlation the reactor is supercritical and the power level will rise.

KEFFECTIVE (keff): The multiplication factor for an infinite core size is expressed as a product of four factors, called the four-factor equation:

$$k_\infty = \epsilon p f \eta .$$

The four-factor equation describes the neutron life cycle. In the equation, ϵ is the fast fission factor (ratio of all fast neutrons to the number of fast neutrons from fission), P the resonance escape probability (ratio of neutrons thermalized to the total of all fast neutrons), f the thermal utilization factor (ratio of neutrons absorbed in the fuel to all neutrons absorbed in the core), and η the thermal fission factor (number of fast neutrons produced per thermal neutron absorbed in fuel). If k_∞

is equal to 1.0, leakage and absorption are just balanced against fissions, so that one neutron absorbed in fission will result in one other neutron that will induce fission. For a real core, the multiplication factor must account for leakage of neutrons, buildup of fission fragments, consumption of fissionable nuclei, and changes in temperature and pressure in the core [49]. The real core multiplication factor is keff and is larger than k_∞ to account for the finite size of the core. If keff is equal to 1.0, the reactor is critical. If keff is less than 1.0 the reactor is subcritical, and a keff greater than 1.0 defines a supercritical reactor.

MODERATOR: The fission cross-section of nuclei is highest for neutrons of thermal energy. Fission events emit neutrons across a wide energy spectrum, the average of which is 2 MeV. A moderator is a material of light atomic weight which is used to slow down neutrons to increase the likelihood of fission.

POISON: A material of high absorption cross-section that removes neutrons from the chain reaction without inducing fission.

REFLECTOR: A material of light atomic weight with a high albedo, i.e. a high probability of scattering neutrons back into the core. A moderator material is often used as a reflector.

SELF-SHIELDING: Includes resonance absorption in this study.

A. Resonance absorption — A large number of resonances are present in uranium which leads to parasitic absorption of neutrons, removing them from the chain reaction. If a neutron remains in the fuel lump or region too long it may be scattered into an energy range containing a large resonance and become absorbed. Once born, if a neutron can escape the fuel the moderator can slow the neutron to thermal energies, past the medium energy range where resonances are predominant, before the neutron re-enters the fuel.

B. Self-shielding — A flux of thermal neutrons that are incident on a large lump of uranium experiences much absorption near the surface of the lump, and the deeper into the lump the more are absorbed. This depletion of *thermal* neutrons reduces the thermal neutron flux in the center of the lump, which decreases the neutron utilization of the fuel.

REFERENCES

1. McArthur, D. A., and P. B. Tollefsrud, Appl. Phys. Letters, 26, 187 (1975).

2. Helmick, H. H., J. L. Fuller, and R. T. Schneider, Appl. Phys. Letters *26*, 327 (1975).

3. DeYoung, R. J., W. E. Wells, G. H. Miley, and J. T. Verdeyen, Appl. Phys. Letters *28*, 519 (1976).

4. Jalufka, N. W., R. J. DeYoung, F. Hohl, and M. D. Williams, Appl. Phys. Letters *29*, 188 (1976).

5. DeYoung, R. J., N. W. Jalufka, and F. Hohl, Appl. Phys. Letters 30, 19 (1977).

6. Akerman, M. A., G. H. Miley, and D. A. McArthur, Appl. Phys. Letters *30*, 409 (1977).

7. Thom, K., and R. T. Schneider, AIAA Journal *10*, 400 (1972).

8. McArthur, D. A., T. R. Schmidt, J., S. Philbin, and P. B. Tollefsrud, SAND 76-0585, SANDIA Laboratories, September 1977.

9. Miller, T. G., USAMIRADCOM, US Army High Energy Laser Laboratory, Redstone Arsenal, Alabama, 1977.

10. Schneider, R. T., and K. Thom, Nuc. Tech. *27*, 34 (1975).

11. Thom, K., and F. C. Schwenk, Paper No. 77-513, AIAA Conference on the Future of Aerospace Power Systems, March 1977.

12. Rodgers, R. J., T. S. Latham, and N. L. Krascella, NASA CR-145048, by United Technologies Research Center, September 1976.

13. Schneider, R. T., K. Thom, and H. H. Helmick, Paper No. 75-015, International Astronautical Federation 26th Congress, September 1975.

14. DeYoung, R. J., Ja H. Lee and W. T. Pinkston, *Nuclear Pumped Lasers II*, Dept. of Physics and Astronomy, Vanderbilt University, NASA Grant No. NSG 1232 (August 1975-August 1977).

15. Miller, T. G., *The Uranium Excimer Laser*, Patent Appl. Pending, US Army Missile Research and Development Command, Redstone Arsenal, Alabama 35809, 3 June 1977.

16. Bennett, Jr., W. R., Appl. Phys. Letters *31*, 667 (1977).

17. Jacob, J. H. and J. A. Mangano, Appl. Phys. Letters *28*, 724 (1976).

18. Tam, A. C., G. Moe, B. R. Bulos and W. Happer, Opt. Commun. 16, 376 (1976).

19. Drummond, D. and L. A. Schlie, J. *Chem. Phys. 65*, 3454 (1976).

20. Santaram, C. and J. G. Winans, *Phys. Rev. 136*, A57 (1964).

21. Santaram, C. and J. G. Winans, *J. Molec. Spectrosc. 16*, 309 (1965).

22. Santaram, C., V. K. Vaidyan and J. G. Winans, *J. Phys. B 4*, 133 (1971).

23. Werner, C. W., E. V. George, P. W. Hoff and C. K. Rhodes, *IEEE J. Quant. Elect. QE-13*, 769 (1977).

24. Schiff, L. I., *Quantum Mechanics 3rd Ed.*, McGraw-Hill Book Co., New York, 1968 (p. 426-428).

25. Leighton, R. B., *Principles of Modern Physics*, McGraw-Hill Book Co., New York, 1959 (249-253).

26. Enge, H. A., M. R. Wehr and J. A. Richards, *Introduction to Atomic Physics*, Addison-Wesley Pub. Co., Reading, Mass., 1972 (p. 427-432).

27. Eisberg, R. and R. Resnick, *Quantum Physics*, John Wiley & Sons, New York, 1974 (p. 357-365).

28. Thom, K., J. *Spacecraft 9*, 633 (1972).

29. Helmick, H. H., G. A. Jarvis, J. S. Kendall and T. S. Latham, Preliminary Study of Plasma Nuclear Reactor Feasibility, Los Alamos Scientific Laboratory Rpt. LA-5679 (August 1974).

30. McLafferty, G. H. and H. E. Bauer, *Studies of Specific Nuclear Light Bulb and Open-Cycle Vortex-Stabilized Gaseous Nuclear Rocket Engines*, United Aircraft Research Laboratories Rpt. F-910093-37 (September 1967).

31. Rodgers, R. J., T. S. Latham and N. L. Krascella, *Investigation of Applications for High-Power, Self-Critical Fissioning Uranium Plasma-Reactors*, NASA CR-145048, by United Technologies Research Center (September 1976).

32. Rodgers, R. J., T. S. Latham, H. E. Bauer and J. W. Clark, *Analytical Studies of Nuclear Light Bulb Engine Radiant Heat Transfer and Performance Characteristics*, United Aircraft Research Laboratories Rpt. K-910900-10 September 1971).

33. Latham, T. S., F. R. Biancardi and R. J. Rodgers, *Applications of Plasma Core Reactors to Terrestrial Energy Systems*, AIAA Paper No. 74-1074, AIAA/SAE 10th Propulsion Conference (October 1974).

34. Thom, K. and R. T. Schneider, *IEEE Trans. Plas. Sci. PS-5*, 259 (1977).

35. Pawlick, E. V. and W. M. Phillips, *J. Spacecraft 14*, 518 (1977).

36. Estabrook, W. C., D. R. Koenig and W. Z. Prickett, *Comparative Assessment of Out-Of-Core Nuclear Thermionic Power*

Systems, NASA TM-33-749 (November 1977).

37. Schneider, R. T. and K. Thom, *Nucl. Technol. 27*, 35 (1975).

38. John S. Kendall, Program Manager, Plasma Core Reactor Research, United Technologies Research Center, private communication, November 1977.

39. Bauer, H. E., R. J. Rodgers and T. S. Latham, *Analytical Studies of Start-Up and Dynamic Response Characteristics of the Nuclear Light Bulb Engine*, United Aircraft Research Laboratories Rpt. J-910900-5, also NASA CR-111097, (September 1970).

40. Kunze, J. F. and P. L. Chase, *Critical Experiments on a Modular Cavity Reactor*, Idaho Nuclear Corporation Rpt. IN-1376, also NASA CR-72681, (May 1970).

41. Mills, C. B., *Nucl. Sci. and Engr. 13*, 301 (1962).

42. Etherington, H., *Nuclear Engineering Handbook*, McGraw-Hill Book Co., New York, 1958 (p. 12-69).

43. Engle, Jr., W. W., *A User's Manual for ANISN, a One-Dimensional Discrete Ordinates Transport Code with Anisotropic Scattering*, K-1693, Oak Ridge National Laboratories (March 1967).

44. Latham, T. S., *Nuclear Studies of the Nuclear Light Bulb Rocket Engine*, NASA CR-1315, by United Aircraft Corporation (April 1969).

45. Latham, T. S., *Nuclear Criticality Studies of Specific Nuclear Light Bulb and Open-Cycle Gaseous Nuclear Rocket Engines*, United Aircraft Research Laboratories Rpt. F-910375-2 (September 1967).

46. Glasstone, S. and A. Sesonske, *Nuclear Reactor Engineering*, Van Nostrand Reinhold Co., New York, 1967 (p. 209-221).

47. Foster, A. R. and R. L. Wright, Jr., *Basic Nuclear Engineering*, Allyn and Bacon, Inc., Boston, 1973 (p. 207-211).

NOTE ADDED IN PROOF: An excellent publication has been released since this report was written that will be of interest to any party engaged in nuclear laser research: E. W. McDaniel, et. al., "Compilation of Data Relevant to Nuclear Pumped Lasers," US Army Missile Command Technical Report H-78-1, Vol. III and IV, December 1978. For copies write T. G. Roberts, address in the distribution list.

DISTRIBUTION

	No. of Copies
Defense Documentation Center Cameron Station Alexandria, Virginia 22314	12
US Army Materiel Systems Analysis Activity ATTN: DRXSY-MP	1
Aberdeen Proving Ground, Maryland 21005	1
Director Ballistic Missile Defense Advanced Technology Center ATTN: ATC, Mr. J. D. Carlson	1
ATC-O, Mr. W. Davies	1
Mr. G. Sanmann	1
Mr. J. Hagefstration	1
ATC-T, Dr. E. Wilkinson	1
ATC-R, Mr. D. Schenk P. O. Box 1500 Huntsville, Alabama 35807	1
Defense Advanced Research Projects Agency 1400 Wilson Boulevard ATTN: Director, Laser Division Arlington, Virginia 22209	1
Los Alamos Scientific Laboratory P. O. Box 1663 ATTN: MS 560, Dr. W. L. Talbert	1
MS 550, Dr. K. Boyer Los Alamos, New Mexico 87544	1

	No. of Copies
IIT Research Institute ATTN: GACIAC 10 West 35th Street Chicago, Illinois 60616	1
Joint Institute for Laboratory Astrophysics University of Colorado ATTN: J. W. Gallagher Boulder, Colorado 80302	1
US Army Research Office ATTN: *Dr. R. Lontz* P. O. Box 12211 Research Triangle Park, North Carolina 27709	1
Science Applications Incorporated 2109 Clinton Avenue W ATTN: H. Smith Huntsville, Alabama 35805	2
Systems Development Corporation 4810 Bradford Boulevard NW ATTN: Bonnie McDaniel Huntsville, Alabama 35805	10
United Technologies Research Center M. S. 16 ATTN: J. S. Kendall East Hartford, Connecticutt 06108	1

DISTRIBUTION (Concluded)

	No. of Copies
ATTN: DRCPM-HEL, COL D. H. Lueders	1
-HEL-T, Dr. C. J. Albers	1
DRSMI-LP, Mr. Voigt	1
DRSMI-T(R&D), Dr. J. Kobler	1
-H, Dr. J. Hallowes	1
-HS, Dr. T. Honeycutt	1
Dr. T. G. Roberts	1
Dr. T. G. Miller	10
-NS	1
-TBD	3
-TI (R&D) Record Set)	1
-TI (R&D) Reference Copy)	1
DRSMI-C, COL K. L. Chesak	1
-CG, Mr. A. Norman	1
-CGB, Mr. K. Evans	1
-CGB, Lt. D. Womack (Additional Distribution)	100

☆ U.S. GOVERNMENT PRINTING OFFICE: 1979—640-287/115 REGION NO.4